TAMPEREEN TEKNILLINEN YLIOPISTO
TAMPERE UNIVERSITY OF TECHNOLOGY

Kaarlo Paakinaho

Processing Derived Control of Hydrolytic Degradation and Generation of Shape-Memory in Lactide Copolymers

Julkaisu 1144 • Publication 1144

Tampere 2013

Tampereen teknillinen yliopisto. Julkaisu 1144
Tampere University of Technology. Publication 1144

Kaarlo Paakinaho

Processing Derived Control of Hydrolytic Degradation and Generation of Shape-Memory in Lactide Copolymers

Thesis for the degree of Doctor of Science in Technology to be presented with due permission for public examination and criticism in Rakennustalo Building, Auditorium RG202, at Tampere University of Technology, on the 9th of August 2013, at 12 noon.

Tampereen teknillinen yliopisto - Tampere University of Technology
Tampere 2013

ISBN 978-952-15-3100-2 (printed)
ISBN 978-952-15-3114-9 (PDF)
ISSN 1459-2045

Abstract

Polylactide and lactide copolymer implants are advantageous in the sense that they are absorbed out of the body, after fulfilling their function as a temporary support for the damaged tissue. For a predictable performance in the physiological environment, the key factors affecting the hydrolytic degradation and their relationship to the manufacturing process should be well known and controlled. Prior to a significant hydrolytic degradation, the physiological environment affects the thermal properties of lactide-based polymers. This phenomenon can be exploited with orientation-based polymer processing methods in order to develop actively moving polymers.

The main aims of this thesis was to study the effects of melt-extrusion on the thermal degradation of lactide copolymers, the effects of melt-processing on the hydrolytic degradation at the physiological temperature and the generation of a water-induced shape-memory on lactide copolymer using orientation-based polymer processing. The main focus in the degradation study was the generation of lactide monomer in the extrusion process and the hydrolysis-catalysing effect of the lactide monomer on poly(L/D-lactide) 96L/4D and poly(L-lactide-co-glycolide) 85L/15G. The study of the generated water-induced shape-memory for amorphous poly(D,L-lactide) focused on demonstrating the properties, mechanism and efficacy of the shape-memory.

Results showed that during melt-extrusion the polymers degraded due to high shear stress and high melt temperatures. The degradation in the melt generated lactide monomer into the polymer, which significantly affected the hydrolytic degradation *in vitro*. The degradation rate was directly proportional to the lactide concentration of the polymer and even small quantities of lactide monomer (0.05-0.20 wt-%) were found to affect the retention of mechanical properties *in vitro* at 37 °C. Mass loss, crystallinity and dimensional stability were also found to be affected.

The orientation-programming process generated an oriented temporary structure for poly(D,L-lactide) that was able to transform its shape at 37 °C in an aqueous environment without any external energy and to further adapt to a predefined stress level as a result of stress generation or relaxation. In an aqueous environment at the physiological temperature, the shape-memory is activated by the plasticizing effect of water molecules diffused into the oriented polymer matrix causing a directed relaxation of oriented and preloaded polymer chains. Although the shape-transformation was slow, the efficacy of the shape-memory was demonstrated with shape-memory nails in a pull-out test in which the pull-out force of the nails increased 360 % during a seven day test period *in vitro* at 37 °C. The results clearly show that functionality in terms of shape-memory can be generated in suitable bioabsorbable polymers without tailoring the polymer chain structure, and thus shortening the time from the development of the technology to its utilization in medical devices.

Acknowledgements

The work presented in this thesis was carried out at Tampere University of Technology, Department of Biomedical Engineering (since 1st of January 2013 Department of Electronics and Communications Engineering).

I express my gratitude to my supervisor, Professor Minna Kellomäki Dr Tech. for her guidance and support throughout the research.

I am very grateful to Harri Heino M.Sc. for the hands-on guidance to processing of biodegradable polymers, and Professor Emeritus Pertti Törmälä Ph.D., M.D. Sci.h.c. for giving the guidance and vision in medical device technology development processes.

I would like thank all the co-authors for their contributions to my research, especially Seppo Syrjälä Ph.D. for the guidance and expertise in the rheological analysis and Adjunct Professor Terttu Hukka Dr. for the expertise and efforts in the Fourier Transformation infrared spectroscopic analysis.

The financial support from Tekes – the Finnish Funding Agency for Technology and Innovation, the Graduate School of the Processing of Polymers and Polymer-based Multimaterials (POPROK), the European Union (EU), the Eemil Aaltonen Foundation, Jenny and Antti Wihuri Foundation and the City of Tampere (Science Foundation) is greatly appreciated.

I wish to express my thanks to the people who are working or have worked at the biomaterials laboratory of the Department of Electronics and Communications Engineering (former Department of Biomedical Engineering) and at the Bioretec Ltd. for their contributions to my work.

I express my deep gratitude to Henna for the unwavering support and love in the present and the upcoming future.

Finally, there are no words great enough to describe my gratitude to my mother and father, Kaija and Jussi Paakinaho, for the support and contributions during my doctoral studies.

Tampere, June 2013
Kaarlo Paakinaho

Table of Contents

List of original publications

I Paakinaho, K., Ellä, V., Syrjälä, S., Kellomäki, M. 2009. Melt spinning of poly(L/D)lactide 96/4: Effects of molecular weight and melt processing on hydrolytic degradation. Polymer Degradation and Stability 94 3, pp. 438-442.

II Paakinaho, K., Heino, H., Väisänen, J., Törmälä, T., Kellomäki, M. 2011. Effects of lactide monomer on the hydrolytic degradation of poly(lactide-co-glycolide) 85L/15G. Journal of the Mechanical Behavior of biomedical Materials 4 7, pp. 1283-1290

III Paakinaho, K., Heino, H., Pelto, M., Hannula, M., Törmälä, P., Kellomäki, M. 2012. Programmed water-induced shape-memory of bioabsorbable poly(D,L-lactide): activation and properties in physiological temperature. Journal of Material Science: Materials in Medicine 23, pp. 613-621

IV Paakinaho, K., Hukka, T.I., Kastinen, T., Kellomäki, M. 2013. Demonstrating the Mechanism and Efficacy of Water-Induced Shape-Memory and the Influence of Water on the Thermal Properties of Oriented Poly(D,L-lactide), manuscript accepted for publication in Journal of Applied Polymer Science

Author's contribution

I The author designed the experimental part and shared with the co-authors the experimental work. He interpreted the results and wrote the manuscript as corresponding author. All the authors commented on the experimental part, and read and approved the manuscript.

II The author designed the experimental part with Harri Heino, analysed and interpreted the results presented in the publication and wrote the manuscript as corresponding author. All the authors commented on the experimental part, and read and approved the manuscript.

III The author designed the experimental part and the processing and testing systems with Harri Heino. The author executed and interpreted all the analyses and wrote the manuscript as the corresponding author. All the authors commented on the experimental part, and read and approved the manuscript.

IV The author designed the experimental part and wrote the manuscript as the corresponding author. In the analyses he collaborated with T. Hukka, who was responsible for the FTIR analysis and the interpretation and reporting of the FTIR results. All the authors commented on the experimental part, and read and approved the manuscript.

Abbreviations

λ	The elongation ratio
γ	Shear rate
GC	Gas chromatography
GPC	Gel permeation chromatography
D	Outer screw diameter
DSC	Differential scanning calorimetry
FTIR	Fourier transformation infrared spectroscopy
H	Screw flight depth
IM-PGA	Injection moulded polyglycolide
IM-PLLA	Injection moulded poly(L-lactide)
i.v.	inherent viscosity
I.v.	intrinsic viscosity
k	Bolzmann constant (1.38066×10^{-23} J/K)
MDSC	Modulated differential scanning calorimetry
M_w	Weight average molecular weight
M_n	Number average molecular weight
N	The number of chain segments between the netpoints in a cross-linked polymer, Screw revolution speed (rpm)
PDLLA	Poly(D,L-lactide)
$PDLLA_{OP}$	Orientation programmed poly(D,L-lactide)
PDLA	Poly(D-lactide)
PDI	Polydispersity
PGA	Polyglycolide
PLGA	Poly(lactide-co-glycolide)
PLLA	Poly(L-lactide)
P(L/D)LA	Poly(L/D-lactide), copolymer of L- and D-lactide
P(L/DL)LA	Poly(L/DL-lactide), copolymer of L- and DL-lactide
S	Entropy
SEM	Scanning electron microscopy
SR-PGA	Self-reinforced polyglycolide
SR-PLLA	Self-reinforced poly(L-lactide)
SR-P(L/DL)LA	Self-reinforced poly(L/DL-lactide)
T	Temperature
T_g	Glass transition temperature
T_g-onset	Extrapolated onset glass transition temperature
T_g-wet	Glass transition temperature polymer-water complex
T_m	Melting temperature
T_{trans}	Transition temperature for the shape-recovery
U	Free energy for the deformation of a standard volume
W	The probability of a polymer chain conformation

1. Introduction

The use of bioabsorbable polymers as implant materials in medical applications, where only a temporary support for the healing of the tissue is required, offers an advantage over non-degradable materials because the need for an implant removal operation is avoided. The purpose of the bioabsorbable implant is to fix the damaged tissue up to the point where the natural healing of the tissue has advanced to a sufficient level for the tissue to carry loads from the surrounding environment. The implant then gradually absorbs out of the body via the natural metabolic pathways. The most commonly used bioabsorbable polymers in medical applications are polylactide and lactide copolymers that are hydrolytically-degradable, thermoplastic polymers. These polymers are used in various applications such as in the fields of orthopaedic and craniomaxillofacial surgery for use as sutures, pins, screws and plates.

The time needed for the fixing or the supporting of damaged tissue and the mechanical load falling upon the device depends on the tissue type and its location. The challenge related to lactide based polymers, when compared to non-absorbable metallic devices, is a lack of knowledge as to which implant manufacturing-dependent factors become significant and in what magnitude in affecting the device's performance in the physiological environment. Although the raw materials are purified and of high quality, the melt-processed implant might still fail because of unexpectedly short strength retention times that might be related to the low quality of the melt processing. The wide tolerances in the degradation times of lactide-based polymers, due to melt-processing related factors, may affect the application of optimal materials for the implants.

The development of new and advanced surgical techniques requires materials that have active properties such as the ability to transform their shape upon a specific stimulus. Thus, polymers with shape-memory properties are becoming one of the most promising material groups under development for use in clinical applications. A significant advantage of the shape-memory property is that medical devices can be inserted into the body through a small incision and transformed to their final shape inside the body. Typically, polymers with shape-memory properties are highly tailored and they have mostly not yet been thoroughly proven to be suitable for clinical use.

This thesis presents how melt-processing-related factors, especially degradation in the melt, affect the hydrolytic degradation behaviour of lactide copolymers *in vitro* at the physiological temperature. The presented results serve as a basis that enables the hydrolytic degradation behaviour to be predicted and the high quality in lactide-based medical devices to be maintained. The thesis also describes how shape-memory properties can be generated into a lactide copolymer using advanced processing methods. The properties of this new combination of active properties as well as the molecular mechanism that enables the shape-memory effect will also be discussed.

2. Review of the literature

2.1. Polylactide and lactide copolymers

The chemistry behind polylactide and lactide copolymers is based on the polymerization of lactic acid (2-hydroxy propanoic acid) into high molecular weight polymer chains that have ester bonds that are capable of cleaving under conditions where water is present. The lactic acid molecule has two possible stereoisomers, L- and D-isomer, of which the L-isomer is present in mammalian biological systems. Several different polymerization methods such as polycondensation can be used to achieve the polymerization of lactic acid, but ring-opening polymerization is the most commonly used method. With the ring-opening polymerisation method, it is possible to accurately modify and control the polymer's chemistry and those properties that are depended on the polymer chain's structure. In this synthesis method, lactic acid is first polymerized by polycondensation into a low molecular weight polymer that is then thermally cleaved into cyclic lactide dimers. In the actual polymerization step, the cyclic dimers are polymerized using the ring-opening method. Because of the two stereo isomers of lactic acid, the lactide dimer can exist in three different forms: L,L-lactide, D,D-lactide and D,L-lactide. The general principle in the ring-opening polymerization of polylactide is presented in Figure 1. (Södergård and Stolt. 2002, Gupta and Kumar. 2007, Jacobsen et al. 2000, Kricheldorf. 2001, Ajioka et al. 1998, Hyon et al. 1997, Bendix. 1998, Kricheldorf and Lee. 1995)

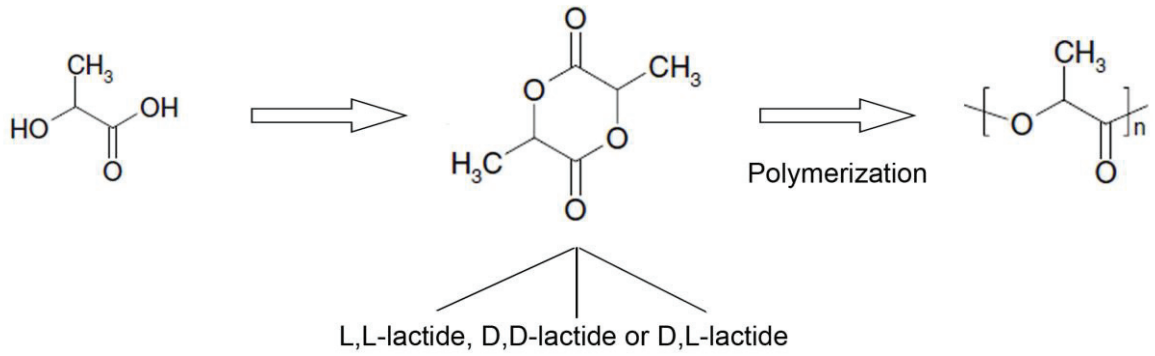

Figure 1. Schematic presentation of the synthesis of polylactide using ring-opening polymerization

The homopolymer poly(L-lactide) (PLLA), synthesized from pure L-lactide, is a semicrystalline, hard and brittle polymer. It is hydrolytically degraded into L-lactic acid, a natural metabolic by-product, due to a nonspecific scission of its ester bonds. In the human

body, the lactic acid produced is metabolized through the citric acid cycle into carbon dioxide (CO_2) and water (H_2O). The glass transition temperature (T_g) of PLLA is in the range of 55 – 65 °C and the melting point is about 180 °C. PLLA has good strength retention and can be processed into many different forms such as fibres, rods and plates. The melt-processed and rapidly quenched PLLA shows amorphous-like behaviour, but is re-crystallized when reheated, especially at temperatures between 100 to 118 °C. (Perego et al. 1996, Södergård and Stolt. 2002, Gupta and Kumar. 2007, Maurus and Kaeding. 2004, Jamshidi et al. 1988)

An effective method for varying the properties such as degradation time and thermal and mechanical properties of a polymer over a broad range is the copolymerization of suitable comonomers. The structural variation and characterization of copolymers compared to a homopolymer involves the structure of the comonomer, the molar ratio of both monomers and the sequence of the monomers in the polymer chain. By introducing D-lactide into the lacide-polymer chain using copolymerization, the degree of crystallization and the brittleness resulting from the crystallization tendency compared to PLLA can be significantly decreased. In addition, the T_g is also lowered with the increasing D-unit due to the intrinsically lower stiffness of the polylactide chains at lower tacticities. With a 50L:50D ratio, the T_g is in the range of 50 – 55 °C. Poly(L/D-lactide)s in which the L/D-ratio is smaller than 87.5/12.5 are intrinsically amorphous and do not crystallize even if annealed. The change in the morphology from semicrystalline towards amorphous due to the addition of the D-units typically lowers the initial mechanical properties of the copolymer and accelerates the hydrolytic degradation with increasing D-unit content. (Joziasse et al. 1996, Kellomäki et al. 2003, Södergård and Stolt. 2002, Gupta and Kumar. 2007, Kricheldorf. 2001, Reed and Gilding. 1981,Vert and Chabot. 1981)

In addition to lactide stereocopolymers, the mechanical properties and the degradation rate of polymers can be adjusted by the copolymerization of glycolide or ε-caprolactone comonomers (Vert and Chabot. 1981, Reed and Gilding. 1981, Malin et al. 1996). Because the non-polar methyl group is not present in the polymer, pure polyglycolide (PGA) is stated to be more hydrophilic than PLLA (Reed and Gilding. 1981). The addition of glycolide to the PLLA polymer backbone increases the hydrophilicity of the polymer and thus causes more rapid hydrolytic degradation compared to PLLA. The crystallinity of an L-lactide-based polymer is significantly influenced by the copolymerization with glycolide. With copolymers based on L-lactide and glycolide, both of which are semicrystalline as homopolymers (PLLA and PGA), the morphology is amorphous with a glycolide content of between 25-70 %. In the case of poly(D,L-lactide) (PDLLA), which is an amorphous polymer, the addition of glycolide has to be over 70 % to change the morphology from amorphous to semicrystalline. Because of the lower T_g of the PGA homopolymer (36 °C), it is possible to adjust the T_g of copolymers based on L-lactide and glycolide in the range of 54-44 °C, when the glycolide content is in the range of 25-70 %. (Törmälä and Pohjonen. 1995, Reed and Gilding. 1981, Vert and Chabot. 1981)

Elastic properties can be greatly influenced by copolymerizing ε-caprolactone with L-lactide. Although ε-caprolactone is considered to be more hydrophobic than lactide, the effect of copolymer morphology has been reported to be a more significant factor in hydrolytic degradation (Malin et al. 1996). The chemical structures of lactide and glycolide homopolymers and their copolymers are present in Figure 2.

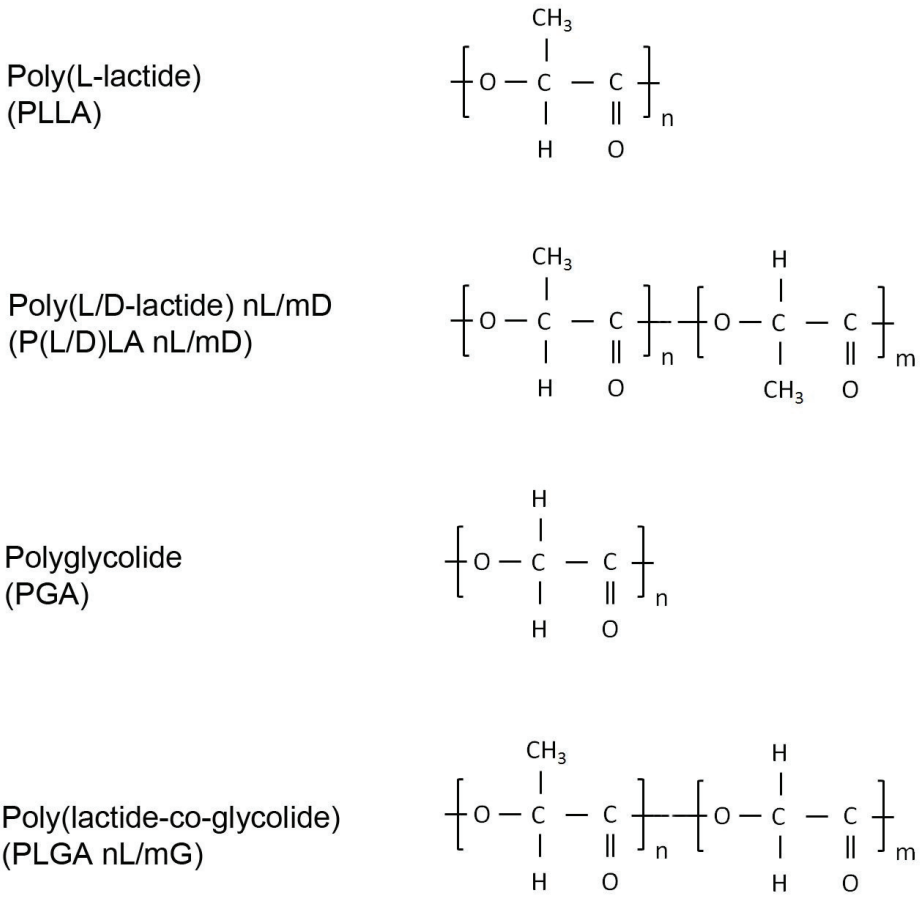

Figure 2. Chemical structures of lactide and glycolide homopolymers and their copolymers

2.2. Melt-extrusion and orientation of lactide-based polymers

2.2.1. Melt-extrusion

In medical applications, the materials implanted into the human body have to perform predictably and should not contain or release harmful substances into the body (Rokkanen. 2001, Törmälä and Pohjonen. 1995). By processing the polymers in the melt and possibly using secondary processing steps based on heating and deforming or reforming the polymer, the use of any substances that could be harmful to the body can be avoided. For continuous

melt processing, extrusion is the most important technique for lactide-based polymers. In the melt-extrusion process, raw material granules are fed through a hopper into a heated barrel with one or two rotating screws that carry the granules towards a forming die or spinneret. The polymer is melted and mixed in order to manufacture a solid continuous profile. The polymer that is extruded out of the forming die is cooled so that it solidifies into the generated shape. For hydrolytically degradable polymers, initial drying and the use of an inert gas in the extrusion process are necessary in order to minimize chain cleavage in the melt. (Lim et al. 2008, Kellomäki and Törmälä. 2003, von Oepen and Michaeli. 1992)

In melt processing, the long residence time and the high processing temperatures have been described as the main drawbacks of the method (Breitenbach. 2002). Because of their sensitive thermal stability, this is especially important for polylactides (Lim et al. 2008, Weir et al. 2004, Wachsen et al. 1997, von Oepen and Michaeli. 1992). Factors that affect thermal stability are typically moisture, low molecular weight compounds, e.g. monomers and oligomers, and residual catalytic metals (Gogolewski and Mainil-Varlet. 1997). Cam et al. reported the drastic influence of residual metals on the thermal stability of PLLA compared to the influence of moisture or residual monomers (Cam and Marucci. 1997). The residual catalytic metals accelerate inter- and intra-molecular transesterification reactions at temperatures above 240 °C. The most obvious mechanism for the thermal degradation due to these metals is the backbiting of the polymer chain. This has led to an attempt to protect the ends of the polymer chains in order to increase thermal stability. Fan et al. demonstrated that by protecting the hydroxyl group end of PLLA using acetic anhydride, the thermal degradation process may slow down in the beginning, but carboxyl ends generated by the random scission of the polymer chains reduces the influence of any end-protection (Fan et al. 2004). Wachsen et al. reported a method to stabilize the degradation in the melt by the addition of 2-hydroxy-2,4,6-cycloheptatrienone (Tropolone) that deactivates the tin catalyst by the formation of a stable complex (Wachsen et al. 1997). A simple way to enhance the thermal stability of polylactide is the enantiomeric blending of the L- and D- forms (PLLA and PDLA) of polylactides at a ratio of 1:1. The increase in the thermal stability of the L/D-blend was discussed by Tsuji et al. and is thought to be the result of a higher molecular interaction between the PLLA and PDLA that decreases the molecular mobility and thus enhances the thermal stability of the polymer blend (Tsuji and Fukui. 2003).

The rheological properties of the polymer have a profound effect on its behaviour in the melt especially when exposed to the conditions required for specific extrusion processes e.g. when the polymer is forced through very small channels in the melt-spinning process. Studies executed with a conical plate rheometer for PLLA with a molecular weight of 159 500 g/mol have shown that with low residence times the molecular weight is virtually invariant to the changes in shear rate. However, with increasing residence times, the effects of both shear rate and melt temperature on degradation are increased. With very small moisture contents (0.043 %) the molecular weight reduction increases only slightly in the temperature range of 190 to

230 °C, but even small increases in the moisture content significantly amplifies the influence of the temperature on the degradation process. (von Oepen and Michaeli. 1992)

2.2.2. Melt-spinning of lactide-based polymers

Because no harmful solvents are needed in the melt-spinning process and it is possible to achieve high production rates, the process is a safe and economical method to produce fibres from a lactide-based polymer (Pirhonen and Ellä. 2008). Fibre spinning from the melt has been studied with pure PLLA (Fambri et al. 1997, Eling et al. 1982, Schmack et al. 1999, Yuan et al. 2001, Pegoretti et al. 1997) as well as with different lactide copolymers with different L/D-ratios (Andriano et al. 1994, Mikkonen et al. 2009, Ellä et al. 2007, Cicero et al. 2002a, Cicero et al. 2002b, Schmack et al. 2004, Kellomäki and Törmälä. 2003), copolymers of lactide and glycolide (Juuti et al. 2012) and from copolymers of lactide and ε-caprolactone (Penning et al. 1993). Although the twin screw extruder is generally considered to be more suitable especially for thermally sensitive polymers and has been used for the melt-spinning of lactide-based polymers (Huttunen et al. 2006), the melt-spinning processes reported for lactide-based polymers are most commonly executed with a single screw extruder (Kellomäki and Törmälä. 2003, Huttunen et al. 2008, Fambri et al. 1997, Schmack et al. 1999, Yuan et al. 2001, Pegoretti et al. 1997, Andriano et al. 1994, Mikkonen et al. 2009, Ellä et al. 2007, Cicero et al. 2002b, Kellomäki et al. 2000a, Kellomäki et al. 2000b). This is possibly due to the easier understanding of the melt-extrusion process of the single screw extrusion in which the material transport is a drag-type mass transport with friction drag in the solids-conveying zone and viscous drag in the melt-conveying zone (Rauwendaal. 2001).

The melt-spinning of polymer fibres is basically a two-step process: the first step being the melt-extrusion and the second step the fibre drawing process. The two processes can be executed separately, but typically the fibre drawing is done continuously after the melt-spinning. The molten polymer is then rapidly cooled down so that it can be drawn off from the spinneret. The cooled and possible slightly pre-drawn fibre (as-spun fibre) is heated and drawn in the second step of the process resulting in an oriented morphology in the polymer that significantly affects the tensile properties with the increasing draw ratio (Penning et al. 1993).

The oriented structure in the fibres is based on a skin-covered fibrillated structure that is constructed of alternating amorphous and crystalline phases in the oriented polymer matrix (Cicero et al. 2002b). The oriented polymer matrix in a lactide-based polymer, as possibly with other polymers as well, increases the modulus and strength of the polymer, but decreases the elongation at break (Cicero et al. 2002a, Andriano et al. 1994). According to Cicero et al., the modulus of P(L/D)LA 98L/2D increased from ~3 MPa to 10 MPa as the draw ratio changed from 2 to 7 and the microfibrils generated in the polymer fibre became more regular and aligned (Cicero et al. 2002b). The maximum tensile strength (~400 MPa) for melt-spun

lactide copolymer fibres reported both by Andriano et al. and Cicero et al. was obtained with a draw ratio between six and seven (Cicero et al. 2002b, Andriano et al. 1994).

Due to the good mechanical properties and ductile behaviour of the polymer fibres, they are not only used as sutures (Reed and Gilding. 1981), but also refined further into different structures for use in numerous medical applications e.g. in the form of braids (Mikkonen et al. 2009), knits (Kellomäki and Törmälä. 2003, Honkanen et al. 2003, Kellomäki et al. 2000a, Kellomäki et al. 2000b) and non-woven structures (Ellä et al. 2007). The refined fibrillar structures, in which the fibre diameter and the mechanical properties have been optimized according to the application, have been successfully used for example in vascular graft regeneration (Tschoeke et al. 2009) and in the bioreconstructive joint arthroplasty of small joints (Honkanen et al. 2003).

2.2.3. Orientation-based reinforcing of biodegradable polymers

The superior mechanical properties of the polymer fibres used in biodegradable sutures were expanded into larger bulky devices such as rods and plates by the mechanical deformation of a non-reinforced polymer (Törmälä et al. 1987, Törmälä and Pohjonen. 1995, Vainionpää et al. 1987, Shikinami and Okuno. 1999, Bendix. 1998, Furukawa et al. 2000). The processing methods for the deformation referred to as self-reinforcing (Törmälä and Pohjonen. 1995, Törmälä. 1992, Törmälä et al. 1987, Vainionpää et al. 1987) and forging (Shikinami and Okuno. 1999, Furukawa et al. 2000) were based on different means of generating an oriented anisotropic form to the originally isotropic and brittle polymeric materials. The generation of anisotropic polymer morphology increases the polymer's mechanical strength and toughness in a similar way to the melt-spun and drawn fibres. The self-reinforced oriented anisotropic structure within a biodegradable polymer can be created by sintering the polymer fibres or by the mechanical deformation of an isotropic polymer (Törmälä and Pohjonen. 1995, Törmälä. 1992), whereas the forging technique is based on compression moulding at a very specific temperature (Shikinami and Okuno. 1999).

The sintering of the fibres is a straight-forward method that takes advantage of the mechanical properties of biodegradable fibres. During the sintering of the polymer fibres, the elements that are controlled are temperature, time and compaction pressure. According to Hine et al., a homogenous product that retains a high portion of the original fibre properties while achieving reasonable strength can be achieved by delicately controlling the compaction temperature in order to only melt the fibre surfaces (Hine et al. 1993). The first reported bioabsorbable polymers used in the technology development were based on the absorbable suture materials polyglactin 910 (Törmälä et al. 1987), a commercial glycolide-lactide-copolymer used in the Vicryl® suture, and polyglycolide (PGA) (Vainionpää et al. 1987), a polymer used in the Dexon® suture. Törmälä et al. reported the sintering of PLLA or PGA fibres at temperatures of 5-25 °C below the melting temperature (T_m) of the fibres under

elevated pressure in order to generate high initial bending strength and shear strength for these biodegradable composite materials (Törmälä and Pohjonen. 1995, Törmälä. 1992). The results of the mechanical properties for the sintered composites are presented in Table 1.

Compared to the sintering of polymer fibres to a fibrillated composite structure, the mechanical deformation of a non-oriented polymeric material has been found to be a more effective way to create a self-reinforced structure for biodegradable polymers. The deformation can be accomplished using different methods, e.g. free-drawing, die drawing or rolling at temperatures between the T_g and the T_m (Törmälä and Pohjonen. 1995). The common feature associated with all self-reinforcing methods is that a highly oriented and fibrillated structure is generated in the polymers. Furthermore, it is possible to generate the oriented and reinforced structure for both semicrystalline and amorphous polymers. The element that gives increased mechanical properties to deformed biodegradable polymers is the oriented polymer chains, which in the case of a semicrystalline polymer can form microstructures, e.g. fibrils or extended chain crystals (Törmälä and Pohjonen. 1995). The forging technique, which is based on compression moulding, does not generate a fibrillated structure, but instead generates a complex crystal orientation to the polymer (Shikinami and Okuno. 1999). These molecular reinforcements are stiff and strong in the orientation direction and thus generate high strength and modulus for the macroscopic composite in the orientation direction. The mechanical properties of free drawn PGA and die drawn PLLA are high compared to non-oriented PGA and PLLA manufactured by injection moulding and this clearly shows that the orientation process significantly increases the initial mechanical properties (Törmälä. 1992). For amorphous polymers that do not have a strong crystal-phase as a reinforcing component, the initial strength value for both non-oriented and oriented polymers are generally considered lower than with semicrystalline polymers, but the effect of orientation is still important for amorphous polymers (Törmälä and Pohjonen. 1995, Törmälä et al. 1998). The mechanical properties for both the self-reinforced, forged and non-oriented lactide and glycolide-based polymers are presented in Table 1.

Table 1. Example results of the mechanical properties of oriented and non-oriented lactide- and glycolide-based polymers reported by (Törmälä and Pohjonen. 1995)*, (Törmälä. 1992)** and (Shikinami and Okuno. 1999)***

	Deformation Method	Bending Modulus [GPa]	Bending Strength [MPa]	Shear Strenght [MPa]	
SR-PGA	Sintering	10-14	290-430	-	*
SR-PLLA	Sintering	5-8	260-300	-	*
SR-PGA	Drawing	18	415	298	**
SR-PLLA	Drawing	10	300	220	**
SR-P(L/DL)LA	Drawing	-	160	115	*
Forged-PLLA	Compression	7	260	93	***
IM-PGA	-	7	218	95	**
IM-PLLA	-	3	119	68	**

SR = Self-reinforced
IM = Injection moulded

The outcome of an orientation process that generates a self-reinforced structure depends on the morphology of the polymer as well as the orientation parameters. Within the stereocopolymers of L- and D-lactide, the D-units increase the molecular disorder in the polymer chains. This leads to a decrease in the intrinsic stiffness of the polymer chains and the crystallinity that both significantly affect the possible increase in the initial mechanical properties compared to non-oriented polymers. The processing conditions in the orientation process, e.g. drawing temperature and draw ratio, have a profound effect on the generation of mechanical properties measured as bending and shear strength. Kellomäki et al. reported that the highest processing-based variation in mechanical properties is with semicrystalline PLLA, which has a high crystallinity and thus a high number of possible components that enable the reinforcement to be obtained in the orientation process (Kellomäki et al. 2003). For PLLA, a higher orientation is obtained at higher orientation temperatures due to the development of the microfibrillar structure, but also due to the increased crystallinity of the amorphous phase (Wong et al. 2008). The maximum obtainable bending strength, shear strength and bending modulus are dependent on the crystal phase within the lactide copolymers. At the same time, the possible variability of the mechanical properties is decreased as the morphology of the lactide copolymer is changed from semicrystalline towards amorphous morphology. (Kellomäki et al. 2003, Törmälä et al. 1998, Joziasse et al. 1996)

2.3. Hydrolytic degradation of lactide copolymers

Hydrolysis of lactide-based polymers can be generally regarded as a reverse polycondensation reaction that leads to molecular fragmentation. Typically in medical applications, the environment where the biodegradable device should perform is basically an aqueous environment at a temperature of 37 °C, and the hydrolytic degradation is considered as a beneficial function. The hydrolysis process of the lactide-based polymers can be affected by various factors such as the chemical structure of the polymer, molecular weight and its distribution, purity, morphology, shape of the specimen and the history of the polymer, as well as the conditions under which the hydrolysis is conducted. (Williams. 1982, Kellomäki et al. 2003, Gupta and Kumar. 2007, Södergård and Stolt. 2002, Nakamura et al. 1989, Reed and Gilding. 1981, Vert and Chabot. 1981, Andriano et al. 1994, Landes et al. 2006b, Hyon et al. 1998)

Although the high molecular weight lactide-based polymers are insoluble to water, they cannot resist the diffusion of a small amount of water into the polymer matrix in an aqueous environment. The hydrolytic degradation begins with the scission of the ester bonds in the polymer chains by the diffused water molecules followed by the loss of the mechanical properties of the polymer and finally the initiation of the mass loss. The initial hydrolytic degradation, described as bulk erosion, occurs homogenously throughout the matrix of the solid polymer due to the faster diffusion rate of water into the polymer matrix than the hydrolysis rate of the ester bonds of the polymer. (Reed and Gilding. 1981, Södergård and Stolt. 2002)

The hydrolytic scission of the ester bonds in lactide-based polymers is considered to follow a random scission, but according to Shih the degradation-mediated increase of acidic chain-ends causes the ester bond-scission to be faster in the chain-ends than in the internal bonds (Shih. 1995). Such a phenomenon is due to the short distance between the carbonyl and the alkoxyl groups in the polylactide main chain making the cleavage of the ester bonds non-random in acidic conditions. According to van Nostrum et al., the chain-end responsible for this backbiting mechanism is the hydroxyl-terminated chain-end within oligomers based on lactic acid (Van Nostrum et al. 2004). The balance and rate between the random scission and the chain-end scission can be significantly influenced, especially with lactide oligomers, by protecting the chain-ends with acetylation that limits the chain-end scission and pushes the balance towards the slow, random scission. The hydrolytic degradation mechanisms for the random scission and chain-end scission are presented in Figure 3.

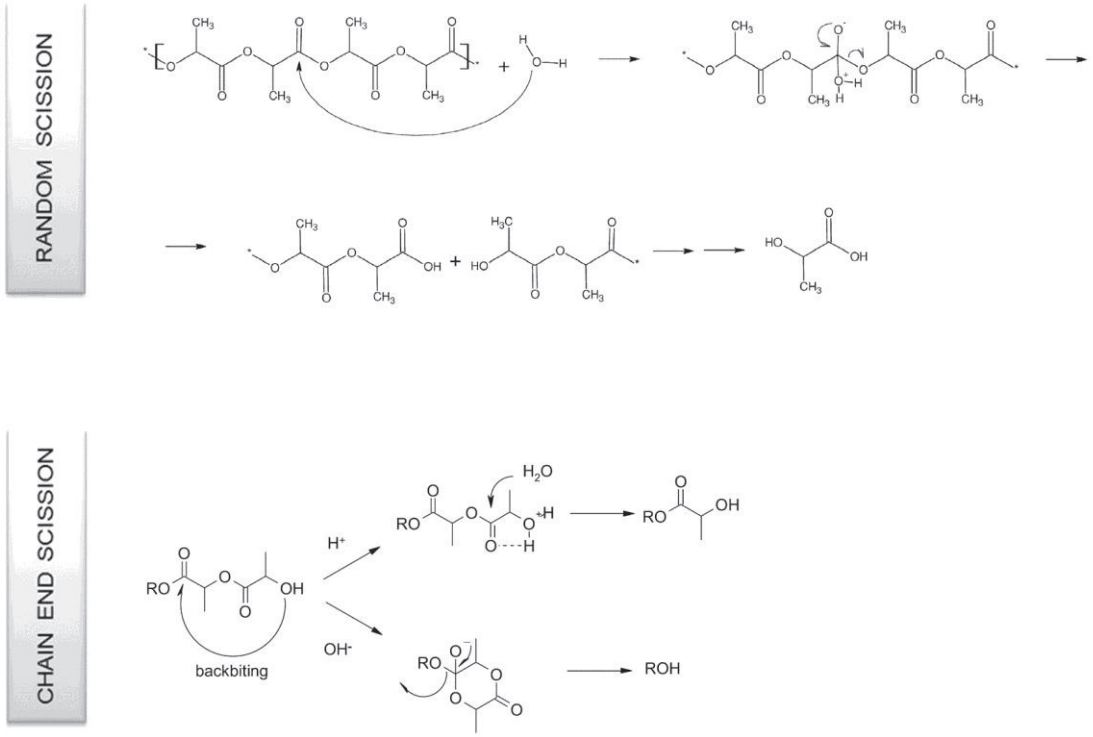

Figure 3. Hydrolytic degradation of polylactide by the random scission of the main chain ester bonds and the degradation of oligo(lactic acid) by chain-end scission (modified from Edlund and Albertsson. 2003, Van Nostrum et al. 2004)

2.3.1. Effects of morphology and the autocatalytic effect on the hydrolytic degradation

Because the diffusion of water is less restricted to the amorphous phase due to the lack of ordered crystallites, the initial morphology has a significant effect on the hydrolytic degradation rate. Another factor, reported by Tsuji et al.,within PLLA is that with high initial crystallinity the density of the hydrophilic terminal hydroxyl and carbonyl groups in the amorphous phase is increased due to their exclusion from the crystallites (Tsuji and Ikada. 2000). This further increases the penetration of water into the amorphous phase and thus accelerates the degradation rate. The hydrolysis of the amorphous regions of the polymer causes increased chain mobility within the polymer chains that tie the crystal blocks together by entanglement. This ultimately leads to a point where the remaining chain segment mobility and free space enable the reorganization of the polymer chains to crystals. The phenomena can be macroscopically seen as the whitening of the specimen caused by the degradation-induced molecular reorganization with the simultaneous decrease in mechanical strength and molecular weight (Niemelä. 2005).

With amorphous lactide copolymers, e.g. PDLLA and PLGA, the degradation for blocky specimens (15 mm x 10 mm x 2 mm) has been proposed to occur faster in the centre of the specimen than at the surface due to a shell formation that inhibits the diffusion of the acidic degradation products catalysing the hydrolytic degradation out of the polymer matrix (Li et al. 1990b, Li et al. 1990c, Li and McCarthy. 1999). According to Li et al., this type of autocatalysis is typical for lactide copolymers with amorphous morphology despite their intrinsic morphological nature. In their opinion, the autocatalysis occurs even with semicrystalline, lactide-based polymers that are initially amorphous due to quenching from the molten state, e.g. PLLA (Li et al. 1990a).

For lactide copolymers, stereoregularity plays a key role in the nature of the autocatalysis. The degradation-mediated structural changes for intrinsically semicrystalline lactide copolymers, e.g. P(L/G)LA 75L/25G, are characterized by the crystallization of the degradation products that occurs under the formed shell. The intrinsically amorphous lactide copolymers, e.g. P(DL/G)LA 75DL/25G or PDLLA, generate a viscous liquid in the core part of the specimen (Li et al. 1990c, Li and Vert. 1994). The autocatalytic effect of the terminal carboxyl groups has also been shown to occur in thin specimens, which do not generate a surrounding shell (Tsuji. 2002). According to Tsuji, the catalytic effect of the degradation products on films with a maximum thickness of 150 μm depends on the tacticity of the polymer as well as the molecular interaction between the polymer chains (Tsuji. 2002). Because of the molecular interactions between the L- and D-stereoisomers of lactic acid, the autocatalytic effect could be controlled by the stereocopolymerization of L-lactide and D-lactide and by their enantiomeric blending (Tsuji. 2002).

Despite the inherent morphology of the polymers, the degradation-driven shell formation that enhances the autocatalytic effect has been reported to be absent from the degradation process of oriented lactide copolymers. A non-heterogenous degradation and the absence of the shell has been reported by Kellomäki et al. with thin fibrillated plates (thickness 0.4 mm) comprised of P(L/DL)LA 70L/30DL and P(L/D)LA 96L/4D (Kellomäki et al. 2000a), by Niiranen et al. with self-reinforced P(L/DL) 70L/30DL (Niiranen et al. 2004) and by Niemelä with self-reinforced P(L/D)LA 96L/4D (Niemelä. 2005). In the orientation process that generates the fibrous polymeric structure, the mechanical deformation given to the polymer simultaneously generates microscopic longitudinal channels or capillaries between the reinforcing fibrils. These may affect the nature of degradation because the channels may absorb fluids into the polymer and further lead the catalysing degradation products effectively out from the oriented polymer matrix (Kellomäki et al. 2000a, Niiranen et al. 2004). The diffusion of the degradation products can be enhanced further by the addition of rigid ceramic particles into the polymer matrix that actively generate pores in the polymer during the orientation process and facilitates the extraction of the macromolecules to the surrounding medium (Niemelä. 2005).

2.3.2. Effects of the polymer purity on the hydrolytic degradation

The purity of lactide copolymers has been reported as a significant factor that influences hydrolytic degradation behaviour (Kellomäki et al. 2003, Hyon et al. 1998, Nakamura et al. 1989). In the polymerization process, it is possible that both the residues of the used catalytic metals and non-polymerized residual monomers can occur in the final polymer, if the polymer has not been carefully purified e.g. by precipitation to ethanol (Schwach et al. 2002). The catalytic metals, e.g. tin or zinc, have different effects on hydrolytic degradation. Compared to tin-based catalysts, the residues of zinc-based catalysts leads to a higher water uptake and thus may affect the degradation and the thermal properties in an aqueous environment as water is the driving force behind the hydrolytic degradation (Schwach et al. 2002, Siemann. 1985). The residual lactide monomer in the polymer matrix, whether intrinsically present or produced during the processing, affects the hydrolytic degradation rate by accelerating the diffusion of water into the polymer matrix and acting as a catalyst for the hydrolysis (Hyon et al. 1998, Vert and Chabot. 1981). The presence of residual lactide monomer in the raw material has been shown to have a significant effect on the hydrolytic degradation rate for different lactide copolymers, e.g. P(L/D)LA 96L/4D (Kellomäki et al. 2003), PDLLA (Hyon et al. 1998) and PLGA (Nakamura et al. 1989).

Because the lactide monomer is a small molecule, it can diffuse out of the lactide copolymer matrix in an aqueous environment. The rate and final amount of diffused monomer can depend on the crystallinity of the polymer as well as on whether the monomer is left in the polymer matrix during the polymerization process or is mixed as powder to a purified polymer. Most of the added and mixed lactide monomer can be readily extracted (one week) from the polymer matrix after immersion, but due to its distribution in the polymer some of it still remains and significantly accelerates the hydrolytic degradation. According to Hyon et al., the key factor in the lactide monomer's catalytic effect on the hydrolysis is its distribution in the polymer matrix (Hyon et al. 1998). The added monomer powder is dispersed as microphase-separated into small domains, whereas the non-polymerized lactide monomer molecules may be molecularly and homogenously distributed in the polymer matrix. The morphological structure has an effect on the extraction rate of the lactide monomer in an aqueous environment, but the extraction still occurs in both amorphous and semicrystalline lactide copolymers (Hyon et al. 1998, Cordewener et al. 1995). Cordewener et al. reported that the residual monomer content in as-polymerized P(L/D)LA 96L/4D rods decreased from 1.8 wt-% to 0.4 wt-% *in vivo* in rats as well as *in vitro* at 37 °C and no detectable amount of lactide monomer could be measured after two weeks (Cordewener et al. 1995).

The accelerated molecular degradation has a significant effect on the strength retention of the lactide copolymers in the aqueous environment. Reported by Hyon et al., the tensile strength of PDLLA samples with a lactide monomer content of between 5-15 wt-% decreased from 45 to 50 % in three weeks *in vitro* at 37 °C, whereas the tensile strength of the pure PDLLA without lactide monomer was not affected by the hydrolysis (Hyon et al. 1998). The initial

strength, however, is not affected by the purity of the polymer as presented by Kellomäki et al. with self-reinforced P(L/D)LA 96L/4D rods that contained either 0.13 wt-% or 4 wt-% of residual monomer (Kellomäki et al. 2003). With samples containing 4 wt-% of residual monomer, the loss of mechanical properties were reported to initiate immediately at the beginning of the hydrolytic exposure, and after 11 weeks the decrease in mechanical properties measured as bending strength was 50 % of its initial value, whereas the polymer with 0.13 wt-% of residual monomer maintained its initial strength for up to 24 weeks. Saikku-Bäckström et al. also reported 24-week strength retention measured as shear strength both *in vitro* at 37 °C and in an *in vivo* study in rabbits with self-reinforced P(L/D)LA 96L/4D rods that had the measured residual monomer content of 0.16 wt-% (Saikku-Bäckström et al. 1999).

Because of the hydrolytic degradation of the polymer chains, small molecular movements are possible and can be typically seen as increased crystallinity with semicrystalline lactide-based polymers (Zong et al. 1999, Landes et al. 2006b, Suuronen et al. 1998a, Niiranen et al. 2004, Niemelä. 2005, Tsuji and Ikada. 2000, Cordewener et al. 1995). As the diffusion of water is easier in the amorphous phase than it is in the crystalline phase, the crystallisable polymer chains in the amorphous phase are more affected by degradation than the polymers chains in the crystals. The degradation in the amorphous phase facilitates the crystallization because a considerable amount of material can be crystallized due to the increased molecular movement driven by the advancing degradation (Zong et al. 1999). This will lead to a low molecular weight, but higher crystallinity within the polymer. The degradation in the amorphous phase in the early stage of the degradation may cause the polymer chains, which are tying the polymer crystal together, to relax to energetically more favourable conformations. This phenomenon may simultaneously pull the crystal lamellae closer to each other thus lowering the lamellae thickness (Zong et al. 1999).

2.4. Hydrolytic degradation *in vivo* and clinical performance of lactide-based polymers

Because of their hydrolytic degradation nature, lactide-based polymers are used in various medical application in the form of pins, rods or tacks (Ajioka et al. 1998, Rokkanen et al. 1985, Nordström et al. 2002, Majola et al. 1992), screws (Manninen. 1993, Suuronen. 1991, Majola. 1991), plates (Suuronen et al. 1992b, Suuronen et al. 1992a, Peltoniemi et al. 1999), arrows for meniscal repair (Jani et al. 2004) or various textile structures e.g. scaffolds for small joint regeneration (Waris et al. 2008, Honkanen et al. 2003) and bone regeneration (Kellomäki et al. 2000b). The *in vivo* studies with self-reinforced PLLA screws in rabbit femora have shown that in the short-term the PLLA generates only mild foreign-body reaction with no accumulation of inflammatory cells. The reported reactions in the body have been similar to metallic surgical implants, and in the long-term the biocompatibility of PLLA

is equally good as with the standard metallic screws routinely used in surgical procedures (Viljanen et al. 1997, Pihlajamäki et al. 2006a). Viljanen et al. have shown the efficacy of self-reinforced PLLA in bone union in rabbit femur cancellous bone osteotomies. Solid body union at three-week follow-up was seen with 84 % with the self-reinforced PLLA group and with 76 % in the metallic implant group (Viljanen et al. 1997).

According to Pihlajamäki et al., the biodegradable polymeric implants are best suited for applications such as small fragmented fractures or osteotomies, but also for the fixation of ligamentous structures in the shoulder and the knee (Pihlajamäki et al. 2006a). PLLA degrades slowly *in vivo* and, for example, in a study conducted with 2 mm self-reinforced pins, no signs of degradation could be seen in the implantation site during the entire 52-week follow-up period (Pihlajamäki et al. 2006b). After the implantation, the self-reinforced PLLA and metallic implants evoked an osteostimulatory response in the neighbouring cancellous bone tissue (Viljanen et al. 2001, Pihlajamäki et al. 1994, Pihlajamäki et al. 2006b). This result, however, is more likely to be related to a non-specific bone front growth between the implant and the bone tissue and in longer follow-up times (51 weeks) the intensive bone remodelling seen as an osteostimulatory effect fades away (Pihlajamäki et al. 2006a).

Bergsma et al. have reported adverse late body tissue reactions in clinical cases with as-polymerized PLLA plates and screws (Bergsma et al. 1995a). The tissue reactions have occurred at the late stage of degradation, between 3.3 to 5.7 years, when the degrading PLLA had fragmented and disintegrated into very slowly degrading crystal particles that have a needle-like structure. Contrary to these observations, Suuronen et al. reported that the degradation mediated crystallite particle formation with self-reinforced PLLA plates in sheep mandible did not show clinically manifested foreign-body reactions during the four to five year follow-up (Suuronen et al. 1998b). According to Böstman and Pihlajamäki, the degradation behaviour of the material strongly influences the biocompatibility of a degradable fixation device (Böstman and Pihlajamäki. 2000). On the other hand, its implantation site significantly influences the degradation; if there is insufficient drainage of by-products in the surrounding tissue or when the cellular clearing capacity may be overloaded, even the slow-degrading and amorphous polymers may provoke osteolytic changes (Weiler et al. 2000). The foreign-body reactions typically occur with pure PGA implants with 5 % in clinical cases, whereas with slower degrading lactide-based polymers the incidence ratio is lower than with PGA, even rare. Although the use of materials with low crystallinity has been advocated for medical purposes, the concerns about the poor biocompatibility of PGA implants do not necessarily apply to other materials with appropriate tissue response. (Böstman and Pihlajamäki. 2000, Weiler et al. 2000)

Because the polymer characteristics that affect biocompatibility include molecular weight, thermal history, residual monomer content, the degree of crystallinity and the porosity of the implant as well as the presence of additives as impurities in the polymer, and the method of fabrication and sterilization of the implants (Böstman and Pihlajamäki. 2000), different

approaches have been taken to confront the challenges related to the problem of biocompatibility and long-term tissue reactions. One approach to deal with the high crystallinity and long degradation times of PLLA is to manipulate the PLLA by pre-degrading it into a lower molecular weight polymer and simultaneously lowering the crystallinity by increasing the D-content in a lactide copolymer (Bergsma et al. 1995b). The influence of processing on the degradation behaviour both *in vitro* and *in vivo* can be seen by comparing studies conducted by Cordewener et al. with as-polymerized P(L/D)LA 96L/4D (Cordewener et al. 1995) and Saikku-Bäcktröm et al. with self-reinforced P(L/D)LA 96L/4D (Saikku-Bäckström et al. 1999). The mechanical properties of the as-polymerized P(L/D)LA 96L/4D (residual monomer content 1.8 wt-%) deteriorated and were lost completely seven weeks after implantation in rats (Cordewener et al. 1995), whereas the self-reinforced P(L/D)LA 96L/4D (residual monomer content 0.16 wt-%) showed only a slight decrease in mechanical properties during a 24-week subcutaneous implantation in rabbits (Saikku-Bäckström et al. 1999).

Well-tolerated biodegradable lactide copolymers with intermediate absorption characteristics include PLGA 80L/20G that degrades slow enough to not overwhelm the body's local ability to clear the degradation products, yet fast enough to demonstrate clearance after approximately one year (Tiainen et al. 2004). Compared to PLLA or P(L/D)LA 96L/4D, PLGA 80L/20G degrades faster and already after 24 weeks a significant change in the morphology occurs and the material's polarizing activity in the microscopic analysis disappears. In 1.5 years, the amount of biomaterial decreases remarkably, but nearly all of the remnants of the PLGA material are still detectable inside foamy macrophages (Tiainen et al. 2004).

The degradation of P(L/DL)LA 70L/30DL and PLGA 85L/15G in patients has been studied in the maxillofacial region up to 24 months during a five year period (Landes et al. 2006a). The simultaneously conducted *in vitro* study showed that the *in vitro* degradation rates were statistically significantly faster than in patients. Both copolymers decomposed reliably in patients with foreign-body reactions being minor with no inhibition of decomposition: PLGA within 12 months and P(L/DL)LA within 24 months and left only extremely small granules that turn to powder upon touch (Landes et al. 2006b). According to Rokkanen et al., the advances of bioabsorbable implants are beneficial, because osteoporosis associated with rigid metallic implants can be avoided (Rokkanen et al. 2000). Furthermore, the avoidance of implant removal procedures results in financial benefits and psychological advances and the bioabsorbable devices are especially suitable for arthroscopic and other minimally-invasive surgical procedures (Rokkanen et al. 2000).

2.5. Shape-memory polymers and the shape-memory effect

Shape-memory polymers are stimuli-sensitive materials that have the ability to change their shape under the influence of a material-specific stimulus. The shape-memory within polymers is created by deforming a polymer with shape-memory ability from its initial shape to a second, temporary shape, and freezing the deformed shape in order to store the load and orientation given to the polymer chains in the deformation process. This new and temporary shape is transformed back towards the original state by exposing the material to a specific stimulus e.g. heat or light (Lendlein and Kelch. 2002, Lendlein and Langer. 2002, Lendlein et al. 2005). The basic principle of shape-memory is presented in Figure 4.

Shape-recovery is caused by a stimuli-responsive increase in the molecular movements of the polymer chains that have been energetically unable to move in the entropically unfavourable and temporary shape. The shape-memory effect in polymers is not related to a specific material property, but to a combination of polymer structure, morphology and the delicate deformation process in creating and fixing the temporary shape. This new and advantageous property has been predicted to enable the development of novel, active medical devices and new surgical procedures, e.g. in the field of minimally invasive surgery, cardiovascular applications and controlled drug delivery (Behl and Lendlein. 2007b, Lendlein and Langer. 2002, Wache et al. 2003, Wischke et al. 2009, Chen et al. 2007, Venkatraman et al. 2006, Wischke and Lendlein. 2010, Metcalfe et al. 2003, Nagahama et al. 2009).

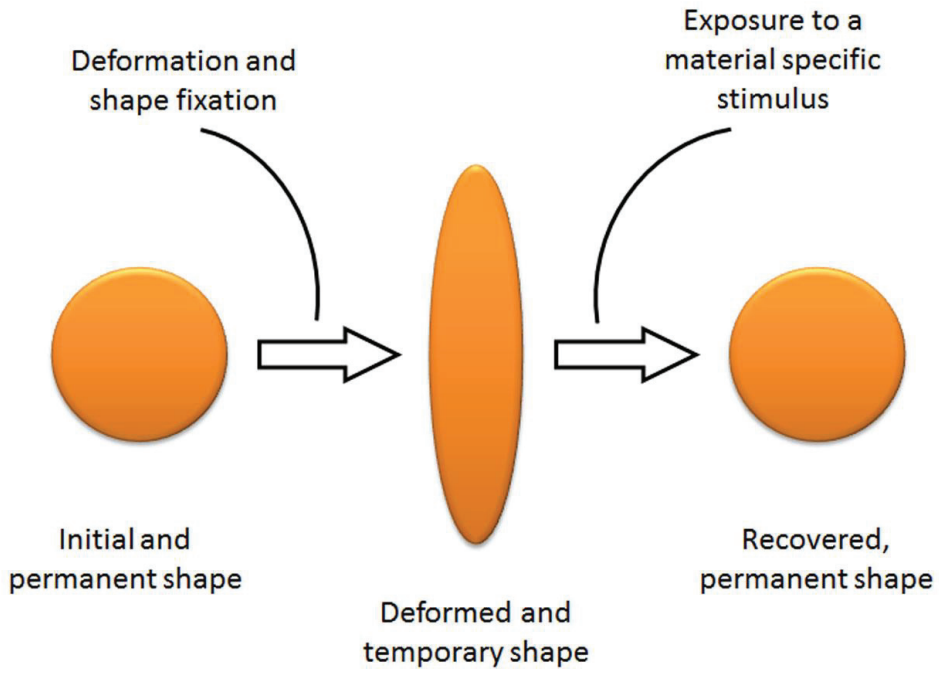

Figure 4. Schematic presentation of the basic principle of shape-memory

2.5.1. Thermally induced shape-memory effect in polymers

Shape-memory, which is triggered by an increase in the polymer's temperature, is termed the thermally induced shape-memory effect. It is based on increased molecular movements that occur when the temperature of the polymer is increased to a level where the state of the polymer changes from glassy to rubber-elastic. In the rubber-elastic state, the rotation around the segment bonds becomes increasingly unimpeded, and this enables the molecular chains to energetically take up more equivalent conformations. Typically, the macromolecules form compact random coils that are entropically more favourable than oriented conformations. According to the Bolzmann equation [Eq. 1, S = entropy, k = Bolzmann constant (1.38066×10^{-23} J/K)], if W expresses the probability of polymer chain conformation, the strongly coiled conformation with the maximum entropy represents the most probable state in an amorphous linear polymer. (Lendlein and Kelch. 2002, Rauwendaal. 2001)

$$S = k \ln W \qquad \text{(Eq. 1)}$$

A thermally induced shape-memory can be generated into a polymer if the strain given in the rubber-elastic state can be stabilized at the application temperature where the polymer will be used. The initial shape (i.e. the permanent shape) can be formed by conventional polymer processing methods such as melt-extrusion or injection moulding. Typically, the generation of the deformed temporary shape requires that the polymer has an inherent temperature sensitive mechanism to partially elastically orientate, but with still more stable molecular anchoring points that enable shape-recovery. Lendlein et al. term the elastically orientatable parts of the polymer the switching segment and the anchoring segments or molecular bonds the netpoints (Lendlein and Kelch. 2002, Lendlein et al. 2001, Lendlein and Langer. 2002). Because the inner energy of an ideal elastomer will not change during stretching, the Helmholz equation for free energy U is reduced according to Equation 2 (Lendlein and Kelch. 2002).

$$U = - T\Delta S \qquad \text{(Eq. 2)}$$

The switching segments, which act as the network chains of a cross-linked polymer or soft segments of a thermoplastic block copolymer, should be able to increase their flexibility as a function of temperature in the desired temperature range in order to initiate shape-recovery. The netpoints, which stabilize the permanent shape, can be either covalent bonds (chemical crosslinks) or hard polymer segments with a higher thermal transition temperature than the switching segments (physical crosslinks). For polymers with a low-degree of crosslinking and netpoints located far away from each other, the change in the polymer's free energy for the deformation of a standard volume is given by Equation 3., where N is the number of chain segments between the netpoints and λ_x, λ_y, λ_z are the elongation ratios presented in the three dimensions. (Lendlein et al. 2001, Lendlein and Kelch. 2002, Behl and Lendlein. 2007a, Behl and Lendlein. 2007b, Lendlein and Langer. 2002)

$$U = \tfrac{1}{2} N k T(\lambda_x^2 + \lambda_y^2 + \lambda_z^2 - 3) \qquad \text{(Eq. 3)}$$

There are two possible thermal transitions (T_{trans}) that enable the molecular movement for the thermally induced shape-memory: the melting and the glass transition. In the case of melting used as the $T_{trans,}$ a strain-induced crystallization can be initiated by cooling the polymer below the T_{trans} value while maintaining the deformed shape. The immediate deformation is prevented by the crystallites formed in the cooling process. The shape-recovery is initiated by increasing the temperature over T_{trans}, which enables the reforming of the coil-like structures of the switching segments. The molecular mechanism of the thermally induced shape-memory effect is presented Figure 5 a) for a multiblock copolymer with $T_{trans} = T_m$ and in b) for a covalently cross-linked polymer with $T_{trans} = T_m$. (Lendlein et al. 2001, Lendlein and Kelch. 2002, Lendlein and Langer. 2002, Kim et al. 1996)

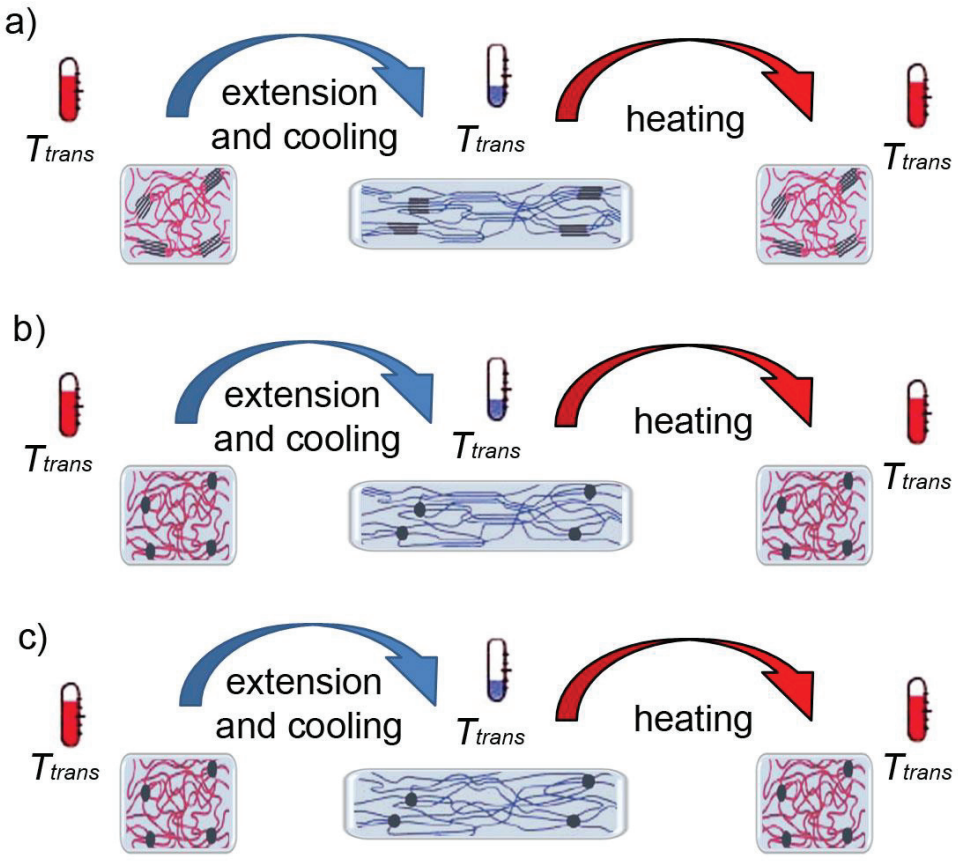

Figure 5. A schematic presentation of the molecular mechanism of the shape-memory effect a) a multiblock copolymer with $T_{trans} = T_m$, b) a covalently cross-linked polymer with $T_{trans} = T_m$, c) a polymer network with $T_{trans} = T_g$ (modified from Lendlein and Kelch. 2002)

For block copolymers with phase-separated morphology and different transition temperatures between the two or multiple phases, T_g can be used as the T_{trans} -temperature. In the case of copolymers that have almost complete phase separation, the T_{trans} is dictated by the T_g of the switching block; whereas with less phase-separated copolymers with short switching blocks, the T_{trans} is a mixture of the hard segments acting as the netpoints and the switching segment phase. In addition to block copolymers that form physical crosslinks, a shape-recovery effect with $T_{trans} = T_g$ can also be obtained with amorphous polymer networks (Alteheld et al. 2005). The molecular mechanism of the thermally induced shape-memory effect, where $T_{trans} = T_g$ is presented in Figure 5 c). (Alteheld et al. 2005, Behl and Lendlein. 2007b, Wischke et al. 2009, Lendlein and Kelch. 2002, Behl and Lendlein. 2007a)

In many medical applications, a device implanted into the human body is not necessarily needed after the healing of the tissue. This has led to the development of biodegradable shape-memory polymers because of their active and advantageous properties. Lendlein and Langer were among the first to develop biodegradable shape-memory polymers intended for medical applications (Lendlein and Langer. 2002). These biodegradable shape-memory polymers were based on phase-segregated multiblock copolymers coupled with 2,2,(4),4-trimethylhexanediisocyanate, in which oligo(ε-caprolactone)diol was the precursor of the switching segment and crystallizable oligo(*p*-dioxanone)diol-based hard segment provided the physical crosslinking in the polymer. The elongation at break was reported to be up to 1000 % and the shape-memory, which was based on $T_{trans} = T_m$, allowed the deformation between the permanent shape and the temporary shape up to 400 %. The shape-recovery was presented at 40 °C and occurred in seconds for a monofilament fibre. This type of shape-memory in biodegradable polymers was shown to have potentiality for intelligent self-tightening surgical sutures and its feasibility was shown in animal experiments on rats. (Lendlein and Langer. 2002)

Biodegradable shape-memory polymers with $T_{trans} = T_g$ have been developed from multiblock copolymers based on polylactide-co-poly(glycolide-co-caprolactone) (Min et al. 2005, Min et al. 2007), amorphous copolyester-urethane networks (Alteheld et al. 2005) and poly(urethane-urea) synthetized from poly(D,L-lactic acid) diols, hexamethylene diisocyanite and butanediamine (Wang et al. 2009). Both physical crosslinking as well as chemical crosslinks are used to determine the permanent shape of the polymers. Min et al. reported multiblock copolymers based on polylactide and poly(glycolide-co-caprolactone) in which the $T_{trans} = T_g$ varied in a small range from 40 to 49 °C (Min et al. 2005). The recovery speed for these multiblock copolymers was good compared with Lendlein's result (Lendlein and Langer. 2002), as the recovery time for curl-shaped films varied between 10 to 28 seconds at 45 °C. However, one must notice that the differences between the device shapes and the shape-recovery temperatures may have had an effect on the recovery rate.

In addition to the tailored biodegradable block copolymers or polymer networks, amorphous poly(D,L-lactide)/hydroxyapatite composites (Zheng et al. 2006) as well as semicrystalline

poly(L-lactide) (Wong and Venkatraman. 2010) have been reported to exhibit a thermally induced shape-memory effect. In the poly(D,L-lactide)/hydroxyapatite composites, the ceramic hydroxyapatite particles were reported to act as the stationary phase and the poly(D,L-lactide) as the mobile or flexible phase when the shape-recovery was initiated at 70 °C. Thermoplastic polymers may act as shape-memory materials, if the matrix is quickly deformed or orientated at a suitable temperature and subsequently cooled while maintaining the deformation. This type of shape-memory is generally considered to be based on the polymer chain entanglements, which are preserved and act as the netpoints determining the permanent shape. This is possible if the deformation process is so rapid that the polymer chains cannot either slip over each other or disentangle. With this type of polymer, the T_g will determine the T_{trans}. Wong and Venkatraman showed that shape-memory ability can be generated into poly(L-lactide), which is a semicrystalline polymer, if the orientation (i.e. the stretching) is done at an optimal temperature and with a relatively low orientation ratio (Wong and Venkatraman. 2010). In the case of PLLA, the degree of recovery has been reported to decrease with an increasing orientation ratio due to the increased strain-induced crystallization and the formation of microfibrillar structures. The shape-recovery is concentrated on the amorphous phase of this semicrystalline polymer and its recovery ratio is decreased with higher orientation ratios due to the chain slippage of the amorphous polymer chains. The temperature for the shape-recovery was 85 °C. The reported temperatures in which the shape-recovery was observed for poly(D,L-lactide)/hydroxyapatite composites (Zheng et al. 2006) as well as for PLLA (Wong and Venkatraman. 2010) were significantly higher than with the multiblock copolymers reported by Lendlein (Lendlein and Langer. 2002) or Min (Min et al. 2005).

2.5.2. Water-induced shape-memory effect

The temperatures required for the shape-transformation of biodegradable polymers are typically above human body temperature and thus in medical applications the excessive heating may be harmful to cells and the surrounding tissues. The high transformation temperatures can be avoided by copolymerizing flexible comonomers in order to increase the molecular mobility in temperatures close to human body temperature, but this may alter the mechanical properties as well as the degradation rate of the polymer. An effective way to avoid the high transformation temperatures in medical applications is to indirectly lower the T_{trans} by using water molecules that diffuse to the polymer matrix and lower the T_g of polymer. The net-T_g is thus a combination of the T_g of the polymer and the T_g of water (Hancock and Zografi. 1994, Oksanen and Zografi. 1993). The permanent shape can be generated with conventional methods similar to thermally induced shape-memory polymers. The temporary shape is created by first heating the polymer and then deforming and cooling the polymer while maintaining the deformation. (Behl and Lendlein. 2007a, Behl and Lendlein. 2007b)

Polyurethane-based polymers have been reported to decrease their T_g as a function of diffused water content, which is an effect that could be utilized in developing polymeric materials with shape-memory properties. The shape-memory effect reported by Huang et al. and Yang et al. (Huang et al. 2005, Yang et al. 2006) for a polyurethane, which was prepared from diphenylmethane-4,4'-diisocyanate, adipic acid, ethylene glycol, ethylene oxide, polypropyleneoxide, 1,4-butanediol and bisphenol A (MM3520 and MM5520, Mitsubishi Heavy Industries), was based on the polymer's ability to decrease its T_g from 35 °C to about 0 °C as a function of immersion time in water. The saturation of water for this polymer occurs after 240 h immersion at room temperature, but significant shape-recovery can be observed after about four hours. The molecular mechanism for the shape-memory effect was concluded to be the influence of diffused water molecules that weaken the hydrogen bonding between the N-H and C=O groups and thus causes a decrease in the T_g (Yang et al. 2006). The molecular mechanism is schematically presented in Figure 6. The diffused water in the polymer matrix can be split into two parts: the free water and the bound water. The free absorbed water has little effect on the T_g, while the bound water significantly reduces the T_g. The molecular mechanism for this type of polyurethane was complemented by Leng et al. (Leng et al. 2008) with the interpretation that the hydrogen bonding occurring after immersion is an indirect effect on the transition temperature and that only the flexibility of the polymer chains could be used to account for the decrease in T_{trans}.

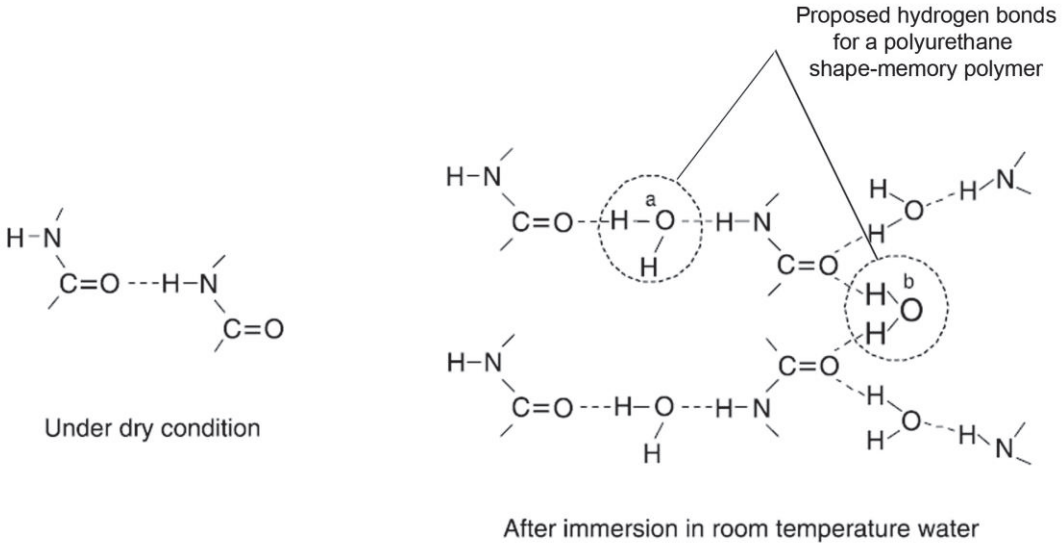

Figure 6. Effect of water on the hydrogen bonding in polyurethane shape-memory polymer (modified from Yang et al. 2006)

In addition to polyurethanes, the water-induced shape-memory effect has also been demonstrated with polymer networks based on poly[(rac-lactide)-co-glycolide] with 1,6-diisocyanato-2,2,4-trimethylhexane and 1,6-diisocyanato-2,2,4-trimethylhexane as

crosslinking molecules (Pierce et al. 2011). The crosslinkers were added as an isomeric mixture according to Alteheld et al. (Alteheld et al. 2005). These polymer networks decreased their T_g after immersion and the materials showed an equilibrated T_g-wet at 25 °C after 30 days in an aqueous environment at 37 °C. The programming of the shape-memory was done by deforming the polymers at 70 °C and fixing the temporary shape by cooling the polymer down to room temperature. The shape-memory effect was initiated in an aqueous environment at 37 °C within several hours, whereas no recovery was observed with samples immersed in 25 °C water up to one day. For the polymer networks, a difference in the shape recovery rate and ratio observed in the wet state at 37 °C was concluded to depend on the degree of crosslinking. The molecular mechanism behind the shape-memory effect initiated in an aqueous environment at 37 °C was concluded to be a combination of the thermally-induced shape-memory effect in the polymer networks and the plasticizing effect of water on the polymer chains acting as the switching segments (Pierce et al. 2011). Contrary to the hydrogen bonding reported for the shape-memory polyurethanes by Huang et al. (2005) and Yang et al. (2006), no bond weakening due to the diffusion of water was observed with the polymer networks. Thus, the decrease of the T_g was concluded to be due to the increased entropy of the PLGA domain (Pierce et al. 2011).

The plasticizing effect of water on the polymer's T_g is generally understood to depend on the polymer's chemical structure and the morphology. Despite its influence on a specific polymer, water is always present in the human body in every possible implantation site of any application. Polymers with a favourable and possibly tailored structure for possessing shape-memory properties are an effective method to control the shape-transformation rate and recovery ratio. Because the field of application in medicine is wide, different types of strategies for generating a water-induced shape-memory effect can be used for different applications. Steendam utilized the water-induced shape-memory behaviour of amorphous poly(D,L-lactide) powder particles in the controlled drug delivery of theophylline in an aqueous environment at 37 °C (Steendam. 2005, Steendam et al. 2001). In this shape-memory application, the poly(D,L-lactide) particles were mixed with the drug and then compacted into a cylindrical form in which the polymer particles were deformed and compressed together. After immersion at 37 °C, the diffusion of water into the poly(D,L-lactide) caused a reduction in the T_g of 10 to 15 °C and resulted in an entropy-driven relaxation of the plastically deformed polymer particles at temperatures around the glass transition of the hydrated polymer (Steendam et al. 2001). The drug release was initiated by a small shape-recovery of the deformed polymer particles that generated a structural deformation in the polymer-drug structure and enabled the drug to diffuse out of the compacted structure. A similar result showing a decrease in the T_g has also been reported by Blasi et al. for poly(DL-lactide-co-glycolide) in which diffusion water in the polymer matrix caused a decrease of T_g by 15 °C and levelling to ~30 °C before the degradation affected the T_g value (Blasi et al. 2005).

A shape-transformation of biodegradable medical devices *in vivo* has been reported for poly(D,L-lactide) by Tschakaloff et al. (1994) and for poly(L/DL-lactide) 70L/30DL by Guimarães-Ferreira et al. (2002). The shape-transformation for poly(D,L-lactide) reported by Tschakaloff et al. was in this case an unwanted effect for injection-moulded biodegradable plates designed for fractures of non-weight-bearing facial bones. The stability, tissue tolerance and degradation rates were found to be acceptable for clinical use, but the pre-bended angles in the plates were lost during the *in vivo* conditions. This type of lack of shape-stability was concluded to possess a severe risk if the plates were used in patients. A similar type of molecular movement *in vivo* was utilized in contractile plates studied for a potential device for the distraction of calvarial bone (Guimaraes-Ferreira et al. 2002). Here, the molecular movements of poly(L/DL-lactide) 70L/30DL activated by the *in vivo* environment were generated in a tube drawing method for a tubular billet that generated a biaxial orientation into the polymer. The oriented plates were able to freely contact ~30 % of their stretched length in an aqueous environment at 37 °C. When implanted into the bone island flaps of New Zealand white rabbits, the P(L/DL)LA 70L/30DL plates, termed cranio springs, could move the bone island and thus cause a distracted osteogenesis.

3. Materials and methods

3.1. Polymers and processing methods

Three different bioabsorbable polymers were used in this thesis. The used polymer and related publication are linked by a roman number after the material.

- Poly(L/D-lactide) 96L/4D, PURAC Biochem bv, Gorinchem, The Netherlands, inherent viscosities: 2.18 dl/g, 4.80 dl/g, and 6.26 dl/g, residual monomer content for all polymers < 0.05 % (reported by the manufacturer) (I)

- Poly(L-lactide-co-glycolide) 85L/15G (LG 857 S), Boehringer Ingelheim Pharma GmbH & Co. KG, Ingelheim am Rhein, Germany, inherent viscosity 5.5 to 6.1 dl/g, the measured residual lactide monomer concentration < 0.02 wt-% (II)

- Poly(D,L-lactide) (R207 S), Boehringer Ingelheim Pharma GmbH & Co. KG, Ingelheim am Rhein, Germany, inherent viscosity of 1.6 dl/g, the measured residual lactide monomer concentration 0.02 wt-% (III, IV)

3.1.1. Extrusion and melt-spinning

Before extrusion, the P(L/D)LA 96L/4D and PLGA 85L/15G polymer granules were vacuum dried at 100 °C for 16 hours and PDLLA polymer at 60 °C for 16 hours before use. Extrusions were carried out in a nitrogen atmosphere and fibre and die drawing in ambient conditions.

The fibre spinnings with P(L/D)LA 96L/4D were performed in a two-step melt-spinning/hot-drawing process using a single-screw Gimac TR melt-extruder with a screw diameter of 12 mm, an L/D of 24:1, and screw geometry of 1:1.237 (Gimac, Castronno, Italy). Two different dies, 8-filament (single orifice diameter 0.4 mm) and 12-filament (single orifice diameter 0.2 mm), were used in melt-spinnings. The extruder comprised six heating zones, three for the barrel, two for melt mixing and stabilizing, and one for the die. The used extruder zone temperatures are presented in Table 2 and the fibre diameters in Table 3. The screw rotation speed was 7-8 rpm. The abbreviation of P(L/D)LA 96L/4D polymers used in the fibre spinning are according to their inherent viscosities reported by the manufacturer: i.v. 2.18 dl/g (PLA22 and F22), i.v. 4.80 dl/g (PLA48 and F48) and i.v. 6.26 dl/g (PLA63 and F63).

Table 2. Extruder zone temperatures used in the melt-spinning processes (publication II)

Fiber	Polymer	Barrel 1	Barrel 2	Barrel 3	Nozzle 1	Nozzle 2	Nozzle 3
F22	PLA22	170	180	190	205	222	240
F48	PLA48	200	215	235	253	265	268
F63	PLA63	200	215	230	255	270	275

Table 3. Shapes and sizes of the melt-spun fibres and, extruded and oriented rods

Sample code	Shape - extruded	Diameter extruded [mm]	Shape - oriented	Diameter oriented [mm]
F22	fibre (round)	-	fibre (round)	0.04 ± 0.005
F48	fibre (round)	-	fibre (round)	0.07 ± 0.005
F64	fibre (round)	-	fibre (round)	0.08 ± 0.005
RM002	rod (round)	3.1 ± 0.1	rod (grooved)	1.6 ± 0.04
RM005	rod (round)	3.1 ± 0.1	rod (grooved)	1.6 ± 0.04
RM010	rod (round)	3.1 ± 0.1	rod (grooved)	1.6 ± 0.04
RM020	rod (round)	3.1 ± 0.1	rod (grooved)	1.6 ± 0.04
RM200	rod (round)	6.1 ± 0.1	rod (grooved)	3.4 ± 0.04
RM300	rod (round)	6.1 ± 0.1	rod (grooved)	3.4 ± 0.04
RM400	rod (round)	6.1 ± 0.1	rod (grooved)	3.4 ± 0.04
PDLLA$_{OP}$	rod (round)	6.6 ± 0.2	rod (grooved)	3.35 ± 0.1
PDLLA$_{OP}$	rod (round)	6.6 ± 0.2	rod (round)	3.2 ± 0.1

In order to study the effects of heat and shear stress on molecular degradation in the single-screw extruder barrel, samples were collected from the extracted screw from melt-spinnings done using the same parameters as in the original melt-spinnings. After stabilization of the spinning process, the die was removed, the screw was pushed out of the extruder barrel, and samples were collected immediately from screw pitches, that is, from the screw tip and from pitches 2, 4, 6, 7, 9, 12, and 15, as counted from screw tip to screw root. The samples were cooled in airflow immediately after harvesting and analysed by gel permeation chromatography.

The melt-extrusions to manufacture rods shape materials from PLGA 85L/15G (publication II) and PDLLA (publications III and IV) copolymers were performed by a co-rotating twin-screw extruder (Mini ZE 20*11.5 D, Neste Oy, Porvoo Finland) under nitrogen atmosphere. Sample materials were melt-extruded into round rods with the diameters of 3.1 ± 0.1 mm (II), 6.1 ± 0.1 mm (II) and 6.6 ± 0.2 mm (III, IV).

In order to produce biodegradable samples materials with various grades of lactide monomer, seven extrusion trials were carried out using PLGA 85L/15G polymer with various melt temperatures (Table 4). In extrusion trials 1-4 the sample materials were melt-extruded into 3.1 ± 0.1 mm and in extrusions trials 5-7 into 6.1 ± 0.1 mm round rods. The low lactide

monomer content of sample materials from extrusions 1-4 was thermally produced during the extrusion process, whereas in extrusions 5-7, L-lactide (L-lactide S, Boehringer Ingelheim Pharma GmbH & Co. KG, Ingelheim am Rhein, Germany) was added as a 4 wt-% premix to PLGA 85L/15G granules before feeding them into the extruder to produce high monomer level sample materials. The abbreviation of the PLGA 85L/15G samples are according to the residual lactide monomer (RM) contents measured after melt-extrusion such that RM003 contains 0.02 wt-% and RM200 2.0 wt-% of lactide monomer.

Table 4. Extrusion batch properties for PLGA 85L/15G polymer with various amounts of lactide monomer

Extrusion batch	Inherent viscosity (Raw material) [dl/g], n = 3	Extrusion melt temperature [°C]
1. RM003*	5.5	210
2. RM005*	5.5	256
3. RM010*	5.5	260
4. RM020*	6.1	262
5. RM200**	6.1	210
6. RM300**	6.1	210
7. RM400**	6.1	210

* Lactide monomer - thermally generated
** Lactide monomer - added as a premix (4.0 wt-%)
Deviation for inherent viscosity analysis ± 0.05 dl/g (equipment derived deviation)

3.1.2. Die drawing and generation of shape-memory by orientation-programming

The extruded PLGA 85L/15G rods were oriented in a die-drawing process into grooved shape with a maximum diameters of 1.60 ± 0.04 mm (extrusion 1-4) and 3.4 ± 0.04 mm (extrusion 5-7) (publication II). The PDLLA rods were deformed into grooved shape with a maximum diameter of 3.35 ± 0.1 mm (publication III, IV) as well as round shape with a diameter of 3.2 ± 0.1 mm (publication IV) in a process stated as orientation-programming which was used to generate an oriented temporary shape to the PDLLA polymer samples with water-induced shape-memory. The orientation-programming is a continuous polymer programming process, which is based on heating and deforming the polymer in temperatures above the glass transition temperature (T_g), but below the melting temperature. The deformed and uniaxially oriented polymer is subsequently cooled while maintaining the predefined tension within the entangled polymer chains (Figure 7). $PDLLA_{OP}$ is used as an acronym for the orientation-programmed PDLLA. The used drawing force in the orientation-programming

process was between 80-120 N, which coincide the tensional stress of 10-16 MPa. The shapes and sizes of the extruded and oriented rods used in this thesis are presented in Table 3.

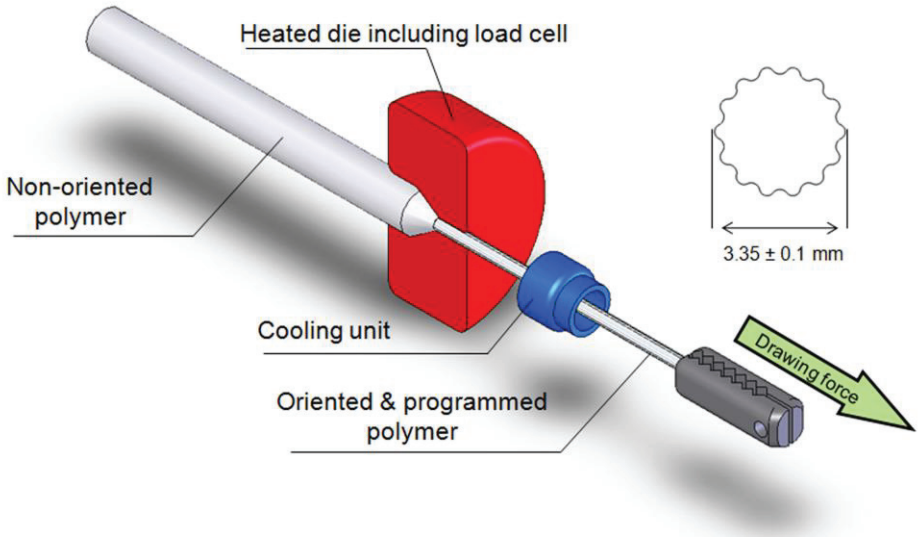

Figure 7. Principle of the orientation-programming process and the cross-section of an orientation-programmed grooved shaped polymer rod with diameter and tolerances (publication III)

3.1.3. Material sterilization by γ-irradiation

All sample materials were sterilized by γ-irradiation with a minimum radiation dose of 25 kGy by Gamma-Service Produktbestrahlung GmbH, Radeberg, Germany.

3.2. In vitro study and material characterization

The changes in the polymers' properties and shape were monitored *in vitro* at 37 ± 1 °C in two different buffer solutions: phosphate buffer solution (PBS, 3.54 g/dm^3 Na_2HPO_4–0.755 g/dm^3 NaH_2PO_4–5.9 g/dm^3 NaCl buffered saline) in publication (I) and Sörensen buffer solution in publication (II, III, and IV) both with volume/weight ratio greater than 30:1 (ml/g). The changes in the buffer solution pH were monitored weekly, and the pH was maintained in the range of 7.4 ± 0.2. The characterization methods for the polymers used in the thesis are summarized in Table 5. The incubation times varied between the different studies, the maximum length being 52 weeks.

Table 5. Summary of the characterization methods GPC = gel permeation chromatography, i.v. analysis = inherent viscosity analysis, DSC = differential scanning calorimetry, MDSC = modulated differential scanning calorimetry, GC = gas chromatography, SEM = scanning electron microscopy, FTIR = fourier transformation infrared spectroscopy

Extrusion batch	Orientation method	*In vitro* buffer solution	GPC	i.v. analysis	Mass loss	DSC	MDSC	Shear strength test	Bending strength test	Tensile strength	Melt viscosity	GC (lactide)	SEM	FTIR	Shape-transformation	Water absorption	Stress gen. & relax.	Pullout force
F22	Spin-drawing	PBS	x							x	x	x						
F48	Spin-drawing	PBS	x							x	x	x						
F63	Spin-drawing	PBS	x							x	x	x						
RM003	Die-drawing	Sörenssen		x	x	x		x	x			x	x		x			
RM005	Die-drawing	Sörenssen		x	x	x		x	x			x			x			
RM010	Die-drawing	Sörenssen		x	x	x		x	x			x			x			
RM020	Die-drawing	Sörenssen		x	x	x		x	x			x	x		x			
RM200	Die-drawing	Sörenssen		x		x		x				x			x			
RM300	Die-drawing	Sörenssen		x				x				x			x			
RM400	Die-drawing	Sörenssen		x		x		x				x			x			
$PDLLA_{OP}$	Orientation-programming	Sörenssen	x	x			x	x				x	x	x	x	x	x	x

3.3. Molecular weight and inherent viscosity measurements and determination of mass loss *in vitro*

The molecular weights (M_w, M_n), the calculated related values of polydispersity (PDI), and the intrinsic viscosity (I.v.) were determined by gel permeation chromatography (GPC). Two parallel samples with a volume of 150 µl and a concentration of 0.1 wt-% in chloroform were injected to PLgel 5-µm Guard precolumn and two PLgel 5-µm mixed-C columns (Polymer Laboratories, Amherst, USA) at a flow rate of 1.0 ml/min. The system comprised a detector (Waters 410 RI Differential Refractometer Detector), pump (Waters M515 HPLC-Pump), and auto-sampler (Waters 717P plus Autosampler) (Waters Operating Corporation, Milford, USA). Universal calibration was obtained for PDLLA ($k = 5.45 \times 10^{-4}$ dl/g, $a = 0.73$), and the mean values of results were used. The inherent viscosity (i.v.) was measured by viscometric analysis (Lauda PSV1, Lauda-Königshofen, Germany) with Ubbelohde capillars (Schott-Instrument, Mainz, Germany) in chloroform at 25 °C. The percentage mass loss was calculated according to equation 4, where m_i = initial weight and m_t = tested dry weight.

$$\text{mass loss [\% from initial]} = 100\% - [(m_i - m_t) / m_i] \times 100\% \qquad \text{(Eq. 4)}$$

3.4. Thermal analysis

The degradation-mediated crystallization of PLGA 85L/15G, measured as change in melting enthalpy, was monitored with a differential scanning calorimeter (DSC) (DSC Q1000, TA Instruments, New Castle, Delaware, USA). The analyses were performed with 5 to 10 mg vacuum dried samples in a temperature range from 10 to 200 °C with a heating rate of 20 °C/min. In the analysis the sum of the enthalpies of cold crystallization and melting was used.

The effect of water on the thermal properties of $PDLLA_{OP}$ was studied with a temperature-modulated differential scanning calorimeter (MDSC) (DSC Q1000, TA Instruments, New Castle, Delaware, USA). Analyses were performed on six parallel 5 to 10-mg samples in hermetically sealed pans with a temperature range of 5 to 80 °C, an amplitude of 0.16 s in publication (III) and 0.5 in publication (IV), a modulation period time of 40 s, and a heating rate of 1 °C/min. Excess moisture was carefully removed from sample surfaces before placing the samples in hermetically sealed pans. The glass transition temperature, evaluated as the extrapolated onset temperature (T_g-onset), and the enthalpy relaxation, evaluated by using an interpolated baseline, were monitored for seven days for non-γ-irradiated and γ-irradiated samples incubated at 37 ± 1 °C. In addition, γ-irradiated samples incubated at 2 ± 1 °C were monitored for seven days. Furthermore, a series of γ-irradiated samples were first incubated at 37 ± 1 °C *in vitro* for seven days and then vacuum dried for seven days at room temperature before MDSC-analysis.

3.5. Mechanical testing

The mechanical properties of the fibres during the hydrolysis were analysed by tensile tests (Instron 4411 Materials Testing Machine, Instron Ltd., High Wycombe, England). All tensile tests were run at ambient temperature with non-sterile and sterile fibres tested dry and fibres from *in vitro* samples tested wet. The testing parameters were: a grip distance of 50 mm, a load cell of 500 N, and a crosshead speed of 30 mm/min.

The mechanical properties of the oriented PLGA 85L/15G rods were tested by three-point bending and shear tests in an aqueous environment at 37 ± 1 °C (Lloyd 2000S, Lloyd Instruments Ltd., Fareman, Hampshire, UK and MTS Insight 30). The shear strength of the $PDLLA_{OP}$ rods with the programmed shape-memory was tested with samples, which shape-transformation was restricted (MTS Systems Corporation, Eden Prairie, MN USA). This was accomplished by placing the samples into custom-made hex-cylinders with water channels on each face of the hexagon prior to the incubation in buffer solution at 37 °C. A sample with the length of 30 mm was placed inside three 10-mm hex-cylinders with a central cavity diameter of 3.44 mm. Shear tests were performed with samples placed inside the hex-cylinders by fixing the lateral hex-cylinder to a holder and shearing the sample by pulling the

middlemost cylinder upwards (basic shear strength test principle with hex-cylinders is shown in Figure 8.

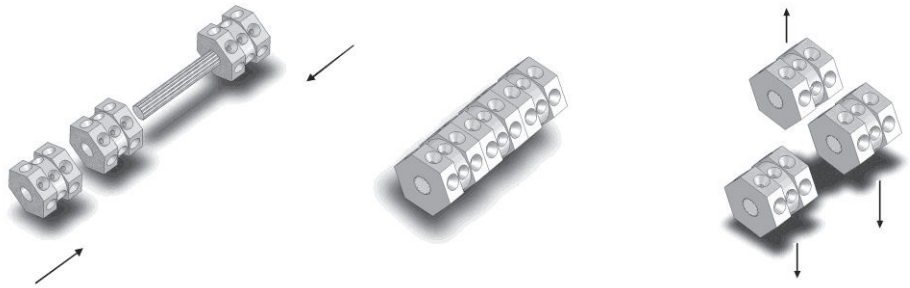

Figure 8. Schematic of a shear test with hex-cylinders (Publication III)

3.6. Melt viscosity measurements

A rotational rheometer (Physica MCR-301, Anton Paar Ostfildern, Germany) was used to measure the viscosities of the P(L/D)LA 96L/4D raw materials in a nitrogen atmosphere at 220 °C, 230 °C, 240 °C and 250 °C. The temperatures were selected based on the processing temperatures used in the fibre spinning process. Plate-plate geometry was used with a diameter of 25 mm and a gap size of 1 mm for three parallel measurements.

3.7. Analysis of lactide monomer content

Lactide monomer content was measured from all samples after melt-processing using gas chromatography (GC) (DC8000, CE Instruments, Rodano, Italy) and an flame ionization detector (FI-detector) after chloroform dilution (Rambol Analytics Oy, Lahti, Finland). The measuring resolution was 0.02 wt-%, and a mean of three parallel measurements were used to determine the monomer content. The release of lactide monomer from the polymer matrix *in vitro* at 37 °C was measured from samples containing 2.0 to 4.0 wt-% of lactide monomer (publication II).

3.8. Scanning electron microscopy

Structural changes in the oriented polymer matrix due to the hydrolysis and the transformation of the oriented structure were monitored by a scanning electron microscope (SEM) (Jeol JSM-T1000, Tokyo, Japan) with selected samples. SEM-samples were frozen in liquid nitrogen and broken along their longitudinal axis, and the fracture surface was used for SEM imaging.

3.9. Fourier transformation infrared spectroscopy

Fourier transform infrared spectroscopy (FTIR) was used to study the interactions between water and PDLLA-polymer chains (Spectrum One FT-IR Spectrometer, Perkin Elmer, Shelton, USA). Eight scans with the resolution of 4 cm^{-1} were carried out for each spectrum from 4000 to 450 cm^{-1} in a transmission mode and the resulting spectra were converted to absorbance format, after which they were processed further with data tune-up. The repeatability in the evaluations was ± 1 cm^{-1}. The sample films were prepared by solution casting in puriss grade acetone (NF ≥ 99 %). Both non-γ-irradiated and γ-irradiated films were scanned before vacuum drying, as vacuum dried and after immersion in a 37 °C deionized water bath, where the samples were held up to seven days**.** All IR spectra were normalized with respect to the spectrum of vacuum-dried selected film (Film 1), which removes the error caused by the different thicknesses of the samples. Normalization was carried out by using the signal of the asymmetric bending of the CH_3 group at 1454 cm^{-1} that exists in all samples.

3.10. Shape and structural transformation and water absorption *in vitro*

The shape transformation rate and extent of the $PDLLA_{OP}$ samples was monitored by measuring the radial expansion and longitudinal contraction. The water absorption of the samples was determined by weighing wet samples after carefully removing excess water from the sample surface and by comparing wet sample weights to initial dry ones. In publication III, the samples were monitored up to 10 weeks *in vitro* at 37 ± 1 °C (n = 10), at room temperature (21 ± 1 °C) *in vitro* (n=3) and dry at 37 ± 1 °C (n=3) and in publication IV one week at 37 ± 1 °C and at 2 ± 1 °C.

3.11. Stress generation and stress relaxation of orientation-programmed PDLLA

The stress generation and stress relaxation behaviour of both non-γ-irradiated and γ-irradiated $PDLLA_{OP}$ samples were monitored in Sörensen buffer solution at 37 ± 1 °C. The equipment in the tests comprised a temperature-controlled water bath with a temperature sensor (1.5 mm K-type thermocouple, Nokeval, Nokia, Finland), a process automation controller (National Instruments, Fieldpoint 2015, Austin, Texas, USA), a transducer (Gefran 40B 96, Gefran S.p.A, Provaglio d'Iseo, Italy), and a load cell (Gefran OC 50/500N, Gefran S.p.A, Provaglio d'Iseo, Italy). The samples were attached to the load cell with a gauge length of 20 ± 1 mm such that any free shape transformation was restrained and the force generation was monitored at time periods 1, 3, and 10 weeks. The stress generation tests were combined with stress relaxation: after one week an external force of 200 N was applied to γ-irradiated sample and 250 N to non-γ-irradiated sample. Due to lower mechanical properties a lower external force was used for γ-irradiated samples. Figure 9 presents the measuring method and exemplary data for the stress generation and stress relaxation, which were cycled over a ten-week period for non-γ-irradiated samples and over a five-week period for γ-irradiated samples.

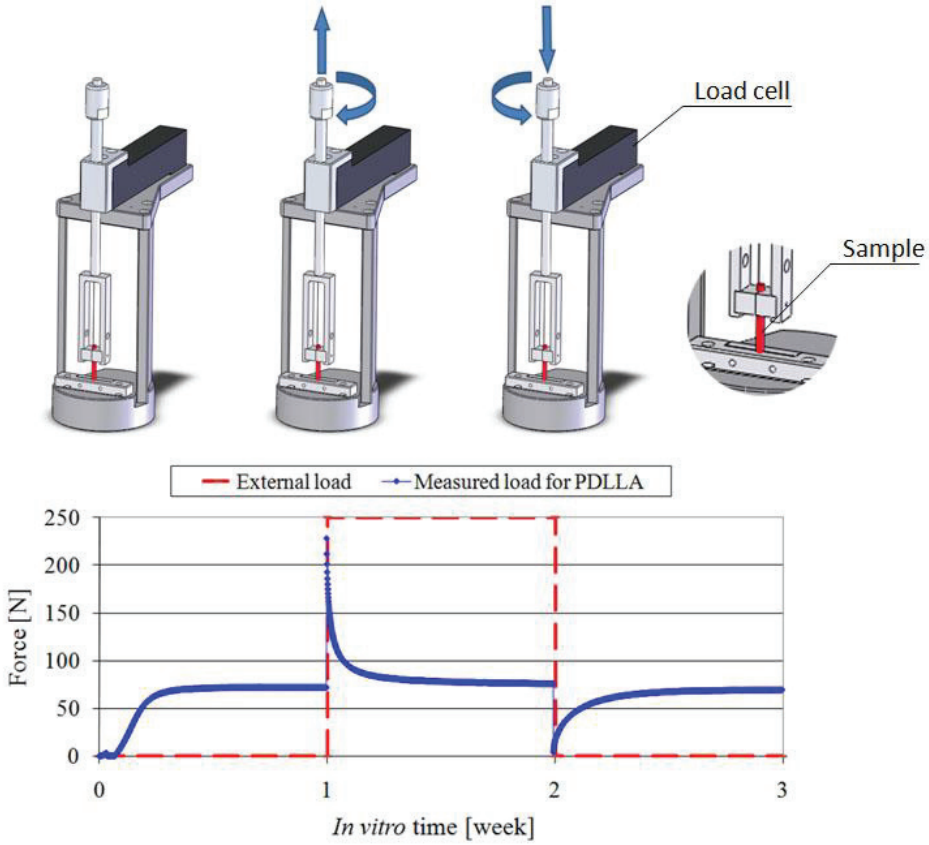

Figure 9. Measuring method and system for cycled stress generation and stress relaxation (publication III)

3.12. Pull-out test

The influence of the shape-transformation on the pull-out strength *in vitro* at 37 °C was studied by inserting the grooved shaped $PDLLA_{OP}$ nails with the maximum diameter of 3.35 ± 0.1 mm, length of 40 ± 1 mm and a machined conical shape tip into solid rigid polyurethane blocks (Sawbones, density 0.32 g/cc) and testing the pull-out force (MTS Insight 30, MTS Systems Corporation, Eden Prairie, MN USA) as function of *in vitro*-time up to seven days. The $PDLLA_{OP}$ nails were inserted to a 3.2 mm drill hole to a depth of 20 mm into the blocks with 1 mm water channels with a distance of 2.5 mm on each side. To ensure moist conditions before inserting the nails into the block, both the drill holes and the $PDLLA_{OP}$ nails were rinsed with the buffer solution. The principle for the pull-out test is presented in Figure 10.

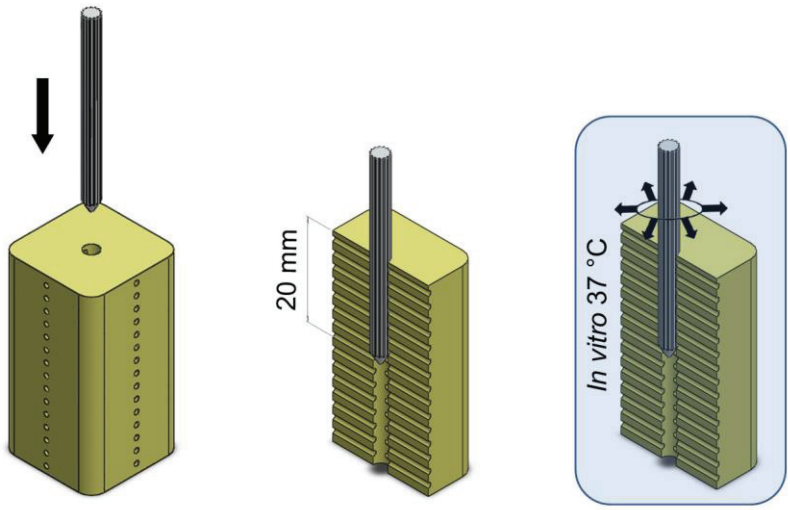

Figure 10. Schematic of the pull-out test *in vitro* at 37 °C with the grooved shaped $PDLLA_{OP}$ nails (publication IV)

4. Results

4.1. Molecular degradation and generation of lactide monomer in the melt-extrusion process

The effects of the melt-extrusion and gamma irradiation on M_n, M_w, i.v. of the polymer used in the thesis are shown in Table 6. In the case of P(L/D)LA 96L/4D, which was used for the melt-spinning with the single screw extruder, the initial molecular weight had significant effect on the degradation in the melt. PLA22, with low molecular weight compared to PLA48 and PLA 63, showed no change in its molecular weights, whereas the decreases in M_w were 50 % for PLA48 and 63 % for PLA63. Differences in molecular weights after melt-spinning were evened out in gamma irradiation, which decreased the M_w the melt-spun fibres by 73 % (F22), 79 % (F48), and 75 % (F63) (Table 6). The molecular weights of all the P(L/D)LA 96L/4D samples were nearly the same after melt-processing and sterilization despite the molecular weights of the raw materials or melt-spun fibres. Despite the similar molecular weights after extrusion and γ-irradiation, the L-lactide content of the melt-spun fibres differed significantly being < 0.02 wt-% for F22, 0.09 wt-% for F48, and 1.90 wt-% for F63.

The generation of lactide monomer into PLGA 85L/15G in twin-screw extrusion correlated well with the applied melt temperatures; the higher the melt temperature, the higher the amount of lactide monomer and the more significant the drop in inherent viscosity. Because by premixing the lactide monomer with PLGA 85L/15G granules, lower melt temperatures could be used. The lower melt temperatures resulted in higher post-processing inherent viscosities compared to the samples, in which the lactide monomer was thermally generated. The decreases in the i.v. due to γ-irradiation were 67% (RM003), 57% (RM005), 53% (RM010), 59% (RM020), 58% (RM200), 63% (RM300), and 64% (RM400) (Table 6). As with the P(L/D)LA 96L/4D fibres, the γ-irradiation evened out the post-processing i.v.-values of the PLGA 85L15G sample materials such that the difference between their maximum (RM400, 4.4 dl/g) and minimum (RM010, 2.4 dl/g) dropped by 78 % (RM400, 1.58 dl/g and RM010, 1.14 dl/g).

The i.v. of the melt-extruded PDLLA decreased from the initial 1.6 dl/g to 1.5 dl/g. No generation of lactide monomer was observed as the measured lactide monomer concentration was < 0.02 wt-%. The γ-irradiation decreased the i.v. of the PDLLA to 0.9 dl/g. Table 6 presents the results on the production of bioabsorbable fibres (F22, F48 and F63), rods (RM003 – RM400 and two reference materials) and the $PDLLA_{op}$ shape-memory copolymer rods with or without various amounts of lactide monomer, generated either thermally or by melt-mixing.

Table 6. Effects of melt-processing and γ-irradiation on polymer characteristic

Extrusion batch	Inherent viscosity (Raw material) [dl/g], n = 3	Inherent viscosity (Extruded) [dl/g], n= 3	Inherent viscosity (γ-irradiated) [dl/g], n= 3	M_n/M_w (Raw material) [g/mol], n = 2	Mn/Mw (Extruded) [g/mol], n= 2	Mn/Mw (γ-irradiated) [g/mol], n= 2	Extrusion melt temperature [°C]	L-lactide content (Residual monomer, RM) [wt-%], n = 2 ([a] = 3)	Melting enthalpy (γ-irradiated) [J/g], n =3
F22	2.18	-	-	55000 / 100400	63000 / 106000	16000 / 28000	-	< 0.02 [a]	-
F48	4.8	-	-	100400 / 271000	61000 / 137000	17000 / 29000	-	0.09 ± 0.01 [a]	-
F63	6.26	-	-	215000 / 344000	67000 / 128000	18000 / 32000	-	1.9 [a]	-
RM003*	5.5	3.9	1.3	-	-	-	210	0.03 ± 0.01	2.7 ± 0.8
RM005*	5.5	2.7	1.2	-	-	-	256	0.05 ± 0.01	6.2 ± 4.5
RM010*	5.5	2.4	1.1	-	-	-	260	0.10 ± 0.01	3.3 ± 2.1
RM020*	6.1	2.8	1.2	-	-	-	262	0.20 ± 0.01	3.1 ± 1.3
RM200**	6.1	3.7	1.6	-	-	-	210	2.0 ± 0.1	4.8 ± 1.8
RM300**	6.1	4.3	1.6	-	-	-	210	3.0 ± 0.1	-
RM400**	6.1	4.4	1.6	-	-	-	210	4.0 ± 0.1	5.7 ± 0.9
RM% < 0.02, D=2.7 mm	6.5	4.0	1.5	-	-	-	210	< 0.02	1.2 ± 0.5
RM% < 0.02, D=3.2 mm	6.5	4.2	1.5	-	-	-	210	< 0.02	2.9 ± 1.9
PDLLA$_{OP}$	1.6	1.5	0.9	127000 / 235000	11600 / 222000	56000 / 109000	-	0.02	-

* Lactide monomer - thermally generated
** Lactide monomer - added as a premix (4.0 wt-%)
Deviation for inherent viscosity analysis ± 0.05 dl/g (equipment derived deviation)
Sample series D = 2.7 mm and D = 3.2 mm with no measurable amount of lactide monomer are included as reference meterial

4.1.1. Molecular degradation in the extruder barrel during melt-spinning

The thermal degradation of P(L/D)LA 96L/4D during the melt-spinning processes is presented in Figure 11. The melting was initiated in the early phase of the transition zone as the pitch 15 was the first pitch to yield molten polymer for sample harvesting. The initial molecular weight of the raw material had a significant effect on the degradation caused by the heat and shear stress such that the higher initial molecular weight the higher degree of molecular degradation in the length of the extruder barrel. Both PLA48 and PLA63 degraded significantly during the melt-spinning, whereas PLA22 did not show any degradation in the extruder. The thermal degradation of PLA 48 and PLA 63 continued up to the beginning of the metering zone, after which no further degradation could be observed in the length of the extruder barrel. The overall decrease in the M_w between pitches 24 and 6 was 27% for PLA48 and 55% for PLA63.

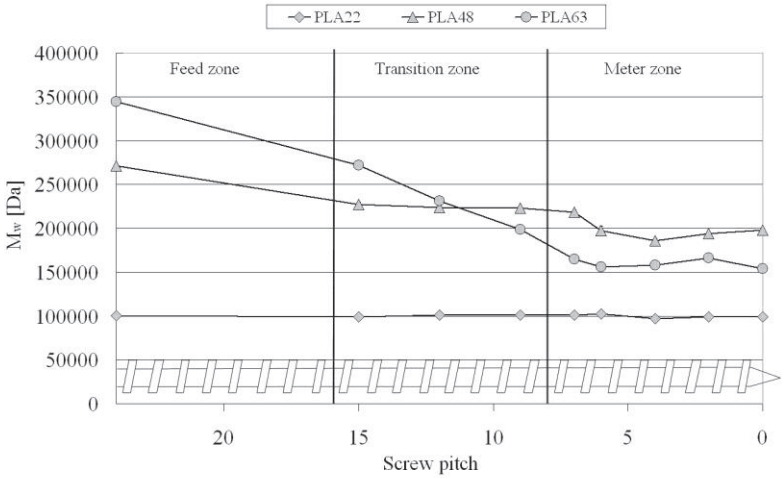

Figure 11. Decrease of molecular weight of P(L/D)LA 96L/4D copolymers with different initial molecular weights in the extruder barrel during the melt-spinnings (publication I)

4.1.2. Viscosity and shear stress at the extrusion temperatures

The P(L/D)LA 96L/4D copolymers used in the melt-spinning processes differed significantly between their viscosities and melt behaviour. PLA22, with the lowest initial molecular weight showed typical shear thinning behaviour, and its viscosities corresponded with the test temperatures. PLA48 and PLA63 showed significantly higher melt viscosities than PLA22, but unlike PLA22 they could not reach their zero viscosity level at shear rates between 0.1–10.0 1/s. PLA48 and PLA63 were shear-thinning as the measured viscosity decreased with increasing shear rate. The melt viscosities were similar between PLA48 and PLA63 at 240 °C and 250 °C with shear rates between 0.1–10.0 1/s, but at 220 °C and 230 °C the high viscosities caused an interruption to the analysis due to maximum torque level of the measuring system. The viscosity results measured with a rotational rheometer of PLA22 and PLA48 are presented in Figure 12.

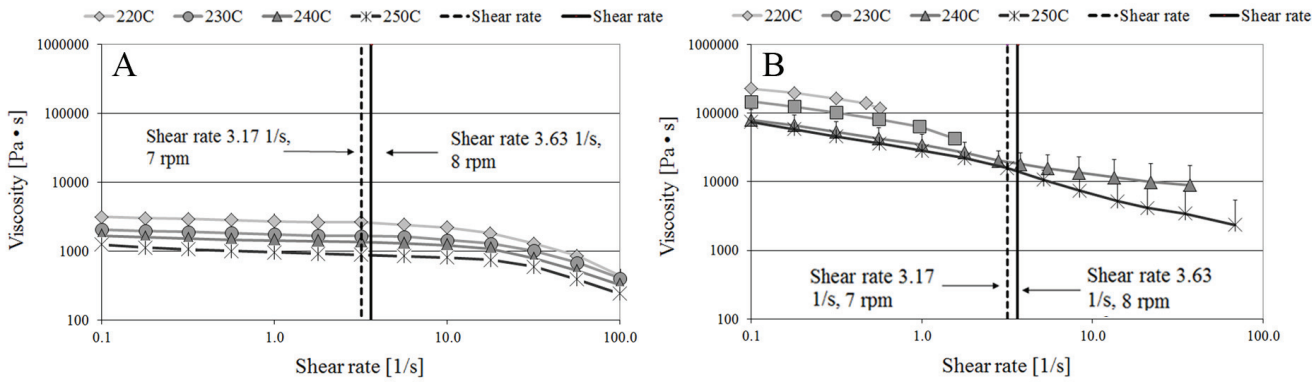

Figure 12. Melt viscosities of PLA22 (A) and PLA48 (B) on logarithmic scale, n = 3 (modified from publication I)

The shear rate in the screw channel was approximated according to equation 5 (Giles et al. 2005) by using a flat plate approximation and assuming pure drag flow. In equation 5: γ = shear rate, N = screw revolution speed (rpm), D = outer screw diameter and h = flight depth.

$$\gamma = \frac{\pi D N}{h \times 60}$$

(Equation 5)

The screw used in the melt-spinning had the following dimensions: D = 11.9 mm, h = 1.375 mm (in the metering zone). With the screw revolutions 7 - 8 rpm, the approximation of shear rates yields: 3.17 1/s when N=7 (rpm) and 3.63 1/s when N=8 (rpm). This approximation gives a mean value for the shear rates occurring in the melt-spinning processes. The equation 5 is reasonable to apply in the metering zone, where the polymer is molten. It is obvious that the shear rate changes between the screw sections and, especially at beginning of the screw, the non-molten material creates a more complex situation, to which the equation does not apply.

4.2. Effects of lactide monomer on the properties of lactide based polymers *in vitro*

4.2.1. Effect of lactide monomer on the hydrolytic degradation rate of lactide copolymers

The melt-spun fibres had similar molecular weights at the beginning of the *in vitro* test series, because the γ-irradiation had levelled the differences between the molecular weights of melt-spun fibres. As can be seen from Figure 13 the degradation rate between the fibres *in vitro* at 37 °C differed significantly despites the similarity in the pre-hydrolysis molecular weights. Although the F63 (1.9 wt-% lactide monomer) was the thickest fibre in the test series with the average diameter of 80 ± 5 μm, it was most affected by the hydrolytic environment of the fibres. On the other hand F22 (< 0.02 wt-% lactide monomer) was the thinnest of the melt-spun fibres with the diameter of 40 ± 5 μm, but it was only minorly affected by the hydrolysis. The decrease in M_w of F63 was 84% during 24 week follow ups, whereas the decrease in M_w of F48 was 61% and F22 only 10%.

The oriented and γ-irradiated PLGA 85L/15G rods had similar results in their hydrolysis behaviour than the P(L/D)LA 96L/4D fibres; the higher the lactide monomer content prior *in vitro*, the higher rate of molecular degradation *in vitro* at 37 °C (Figure 14). The influence of the lactide monomer on the hydrolytic degradation of PLGA 85L/15G is clearly evident. Even small amounts lactide monomer (e.g. 0.20 wt-%) affected the degradation rate:

specimens with a low monomer content (RM003 - RM020) took 6 to 14 weeks to reach 0.8 dl/g and 10 to 18 weeks to reach 0.6 dl/g. RM300 and RM400 with high initial monomer contents showed similar degradation rates regardless of a significant difference in their monomer contents. The decrease of i.v. appeared linear up to 0.4-0.2 dl/g, after which the hydrolysis rate measured as i.v. slowed down significantly, leveling at 0.1 dl/g for up to 52 weeks.

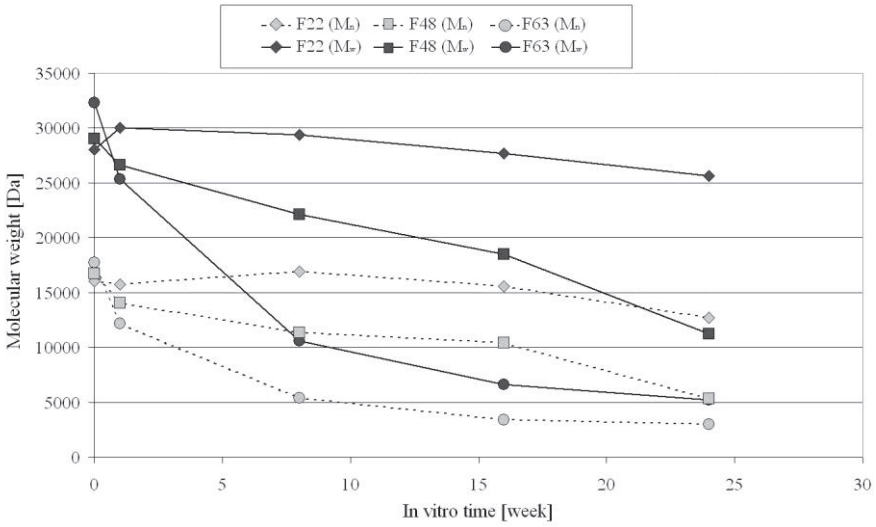

Figure 13. The effects of hydrolytic degradation on M_n and M_w of the melt-spun and γ-irradiated fibres (publication I)

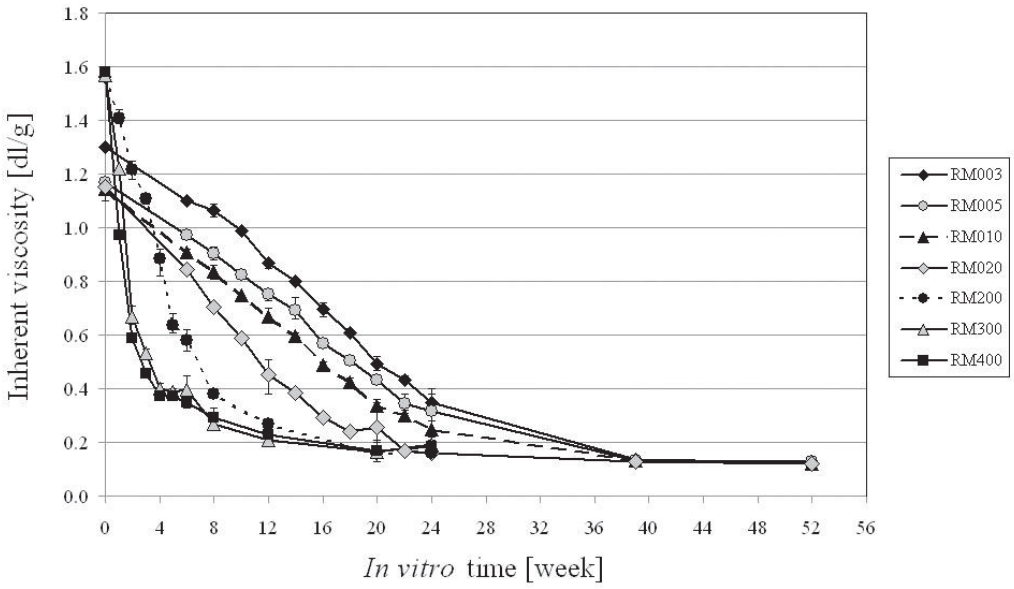

Figure 14. Decrease of i.v. of PLGA 85L/15G with lactide monomer contents ranging from 0.03 to 4.0 wt-%, n = 3 (publication II)

4.2.2. Strength retention of lactide copolymers with various residual lactide monomer contents *in vitro*

The tensile strength retention *in vitro* at 37 °C correlates well with the loss of molecular weight with the P(L/D)LA 96L/4D fibres with various amounts of lactide monomer (Figure 15). From the fibres, F22 lost only 11 % of its initial tensile strength during a 24 week incubation period, whereas the loss of tensile strength with F63 was significantly faster compared to F22 or F48, and after 8 weeks the fibres could no longer be tested for tensile strength, because the lack of mechanical properties.

The mechanical properties of the oriented PLGA 85L/15G rods measured as the shear strength and the bending load were affected by the lactide monomer accelerated degradation. Even in small amounts (≤ 0.20 wt-%) of lactide showed differences in the strength retention between the samples (Figure 16). A notable effect was that the shear strength of the samples was only slightly affected by hydrolytic degradation before reaching the critical zone, after which it plunged. This effect could be seen for both the thermally generated materials and those containing melt-mixed lactide monomer. A limit time value of maintaining 80 % of initial shear strength was 16 weeks for RM003, 14 weeks for RM005, 12 weeks for RM010, 8 weeks for RM020, 6 weeks for RM200, 2 weeks for RM300, and only one week for RM400. Similar results were also obtained with samples tested by bending test. After a molecular-degradation-rate-dependent length of a stable level, their maximum bending load dropped substantially (Figure 17). The bending load test could show the decrease of ductility up to a critical level of degradation after which the samples were broken down during the test instead of ductile bending.

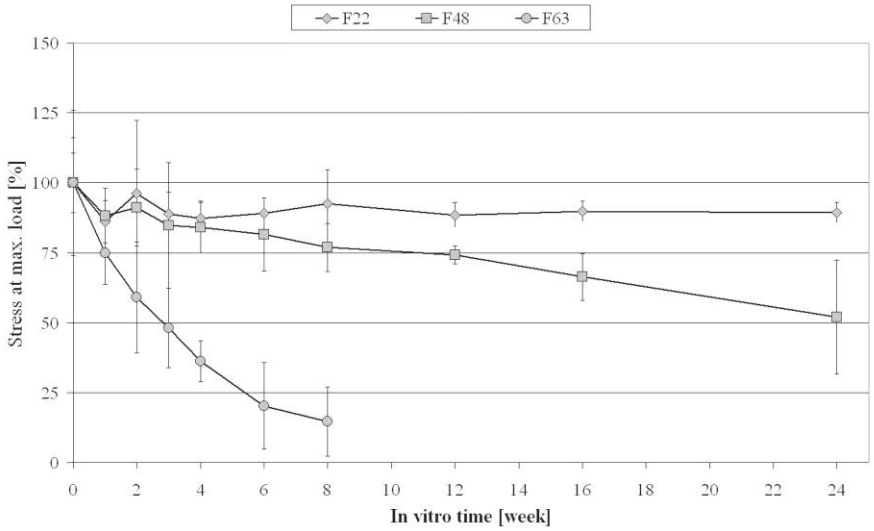

Figure 15. Effect of hydrolytic degradation on tensile strength retention P(D/L)LA 96L/4D with various residual monomer contents *in vitro* at 37 °C (n = 5) (publication I)

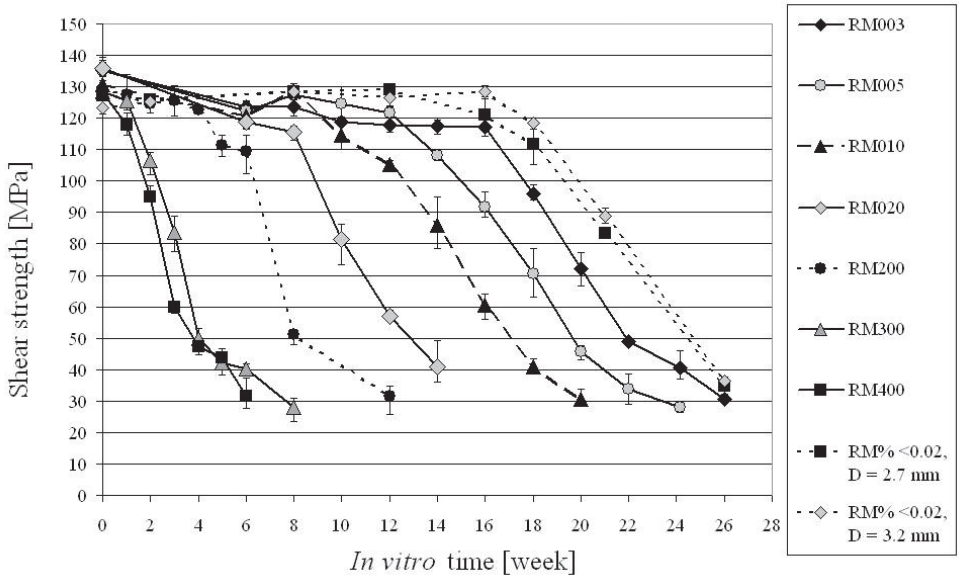

Figure 16. Effect of lactide monomer on shear strength retention of PLGA 85L/15G with various lactide monomer contents (n = 3). Sample series of 2.7 mm and 3.2 mm are included in the figure as reference material with < 0.02 wt-% of measured lactide monomer (publication II)

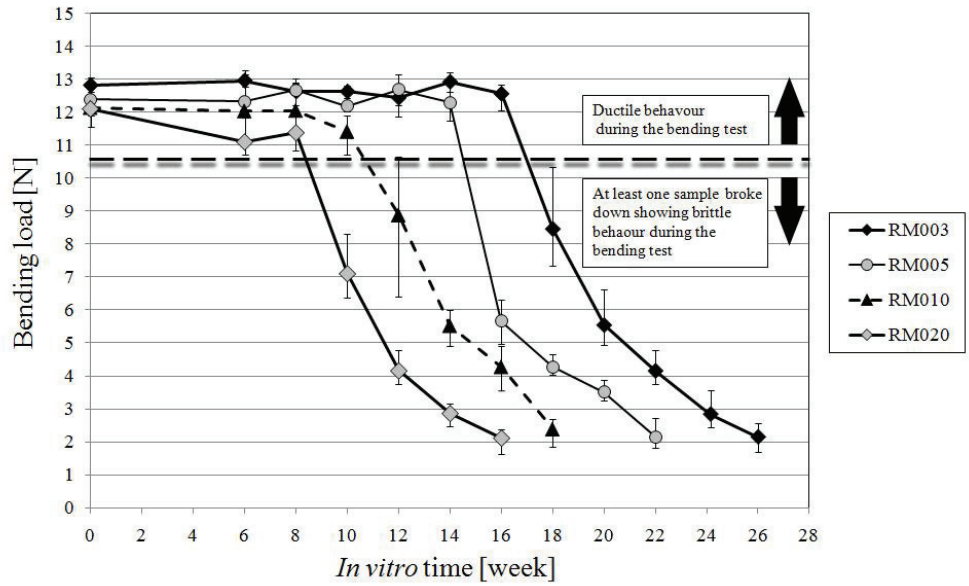

Figure 17. Effect of hydrolytic degradation on maximum bending load of PLGA 85L/15G with various lactide monomer contents (n = 3) (publication II)

The initial shear strength of orientation-programmed and γ-irradiated PDLLA (lactide monomer < 0.02 wt-%) was 85 MPa, which decreased to the range of 30 MPa in a 16-week test period (Figure 18). At this period, the molecular-weight-depended i.v. dropped down to 0.5 dl/g. A sharp drop in the shear strength compared to the load carrying capability was

observed during the first two weeks. This difference was noticed to be a result of the shape transformation in the initially grooved samples, which expanded into a tube-like inner cavity of the hex-cyliders used in the shear test. The small shape transformation, which changed the orientation ratio of the sample materials, affected the measured shear strength.

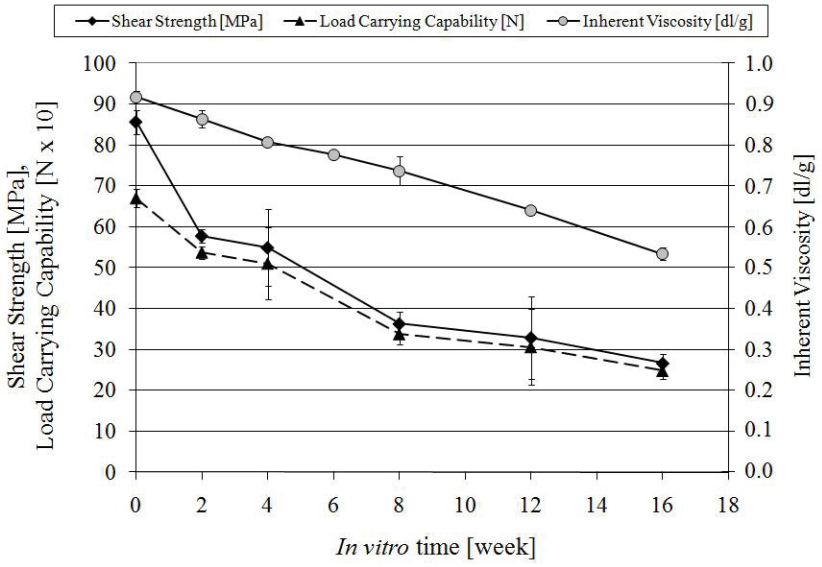

Figure 18. Strength retention and decrease of i.v. of γ-irradiated $PDLLA_{OP}$ due to hydrolytic degradation at 37 °C *in vitro* (n = 3) (publication III)

4.2.3. Effects of lactide monomer on the crystallinity, mass loss and dimensional stability of PLGA 85L/15G during hydrolysis

During the hydrolysis of the PLGA 85L/15G, the crystallinity measured as the as the increase in melting enthalpy, increased against degradation time and depended on the degradation rate of the polymer samples (Figure 19). A significantly faster crystallization during the hydrolysis *in vitro* at 37 °C was observed with the samples containing 2 and 4 wt-% compared to those with a monomer content of 0.03 to 0.20 wt-%. The mass loss of the oriented PLGA 85L/15G rods followed the same order in mass reduction as the drop in inherent viscosities. As presented in Figure 20, the mass loss initiated between the i.v. values of 0.38 - 0.43 dl/g and occurred after 22 weeks for RM003, 20 weeks for RM005, 18 weeks for RM010, and 14 weeks for RM020. Depending of their lactide monomer content, the samples with thermally generated lactide monomer lost 2 to 25 % of their dry weight during the 26-week follow up period.

The oriented PLGA 85L/15G rods changed their shape in small scale towards the non-oriented state at 37 °C *in vitro*. The minor shape transformation was measured as the as radial expansion of the samples' diameter and longitudinal contraction. The radial expansion of the

maximum diameter of the PLGA 85L/15G rods is presented in Figure 21. The shape transformation was linked with the degradation rate and thus correlated with the lactide monomer content. In an aqueous environment at 37 °C the samples with high monomer content, from 2 to 4 wt-%, were dimensionally more instable than those with a monomer content between 0.03 and 0.20 wt-%. The maximum shape transformation (5 %) measured as the radial expansion of the diameter was reached with samples containing lactide monomer of 3 and 4 wt-%. After reaching this magnitude of shape transformation their diameter started to decrease due to the substantial degradation and after 8 weeks the diameter and length of samples with 2-4 wt-% of monomer could no longer be measured because of material fragmentation.

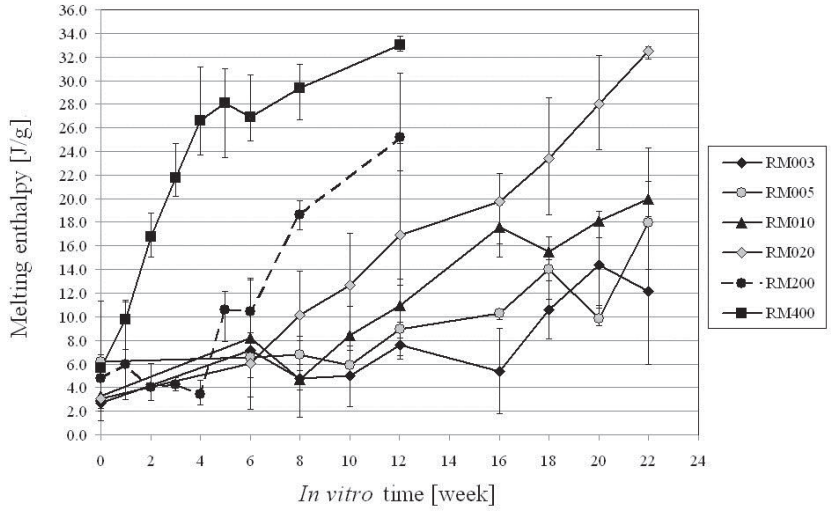

Figure 19. Melting enthalpy of PLGA 85L/15G with various lactide monomer contents *in vitro* (n = 3), presented as the sum of cold crystallization and melting enthalpies (publication II)

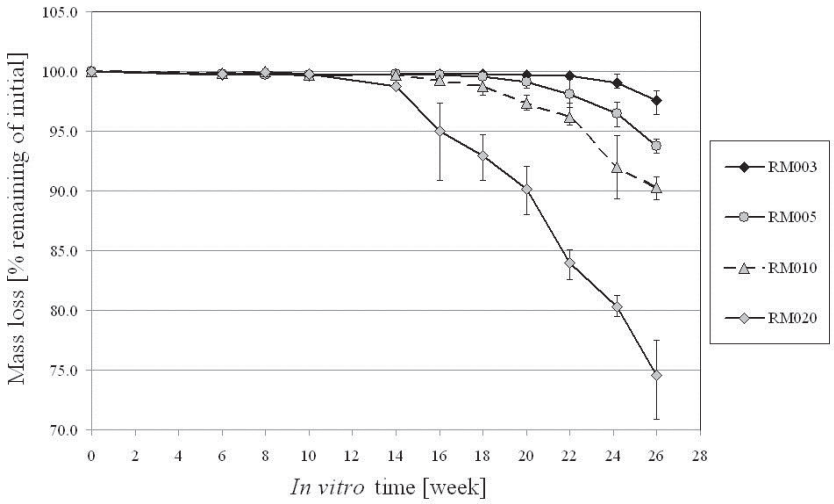

Figure 20. Mass loss of PLGA 85L/15G with various lactide monomer contents *in vitro* (n = 3) (publication II)

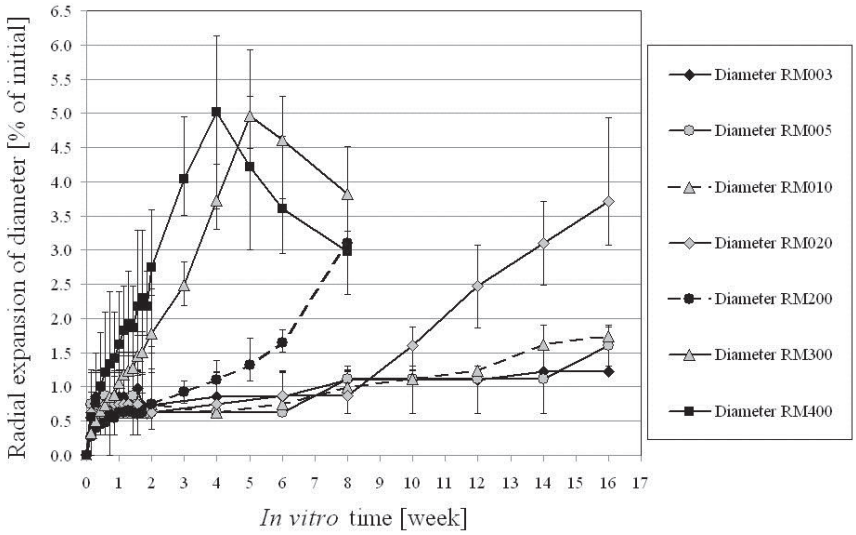

Figure 21. Radial expansion of the diameter of PLGA 85L/15G (n = 5 for RM003-RM020, n = 10 for RM200-RM400) (publication II)

4.2.4. Release of lactide monomer from the oriented PLGA 85L/15G matrix *in vitro* at 37 °C

The lactide monomer content in the aqueous environment at 37 °C was monitored with the high-monomer samples (RM200, RM300 and RM400), which were melt-processed from the premix of L-lactide and PLGA 85L/15G. During the incubation the monomer content rapidly decreased such that after four weeks no lactide monomer was measured in samples that initially contained 3-4 wt-% of lactide monomer (Figure 22). Samples with initial lactide monomer content of 2 wt-% had only 6 % of the initial content remaining after four weeks *in vitro.*

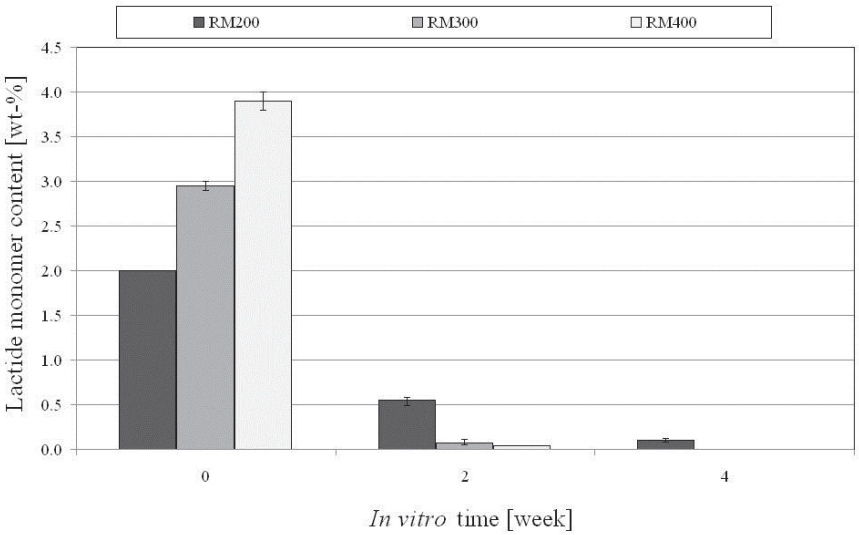

Figure 22. Changes in lactide monomer contents at 37 °C *in vitro* (publication II)

4.3. Water-induced shape-memory effect of PDLLA

4.3.1. Effects of the orientation-programming and γ-irradiation on the thermal properties of PDLLA

The orientation-programming, which is based on heating, deforming and cooling the polymer, affected both the T_g-onset as well as the enthalpy relaxation of the PDLLA. The measured T_g-onset of PDLLA increased during the orientation-programming process from ~50 °C to ~56 °C and at the same time generated an enthalpy relaxation peak to the T_g-zone. The γ-irradiation, which was used as the sterilization method, decreased the T_g-onset by ~1 °C, but did not have a significant effect on the area of the enthalpy relaxation peak of the orientation programmed $PDLLA_{OP}$ (Figure 23).

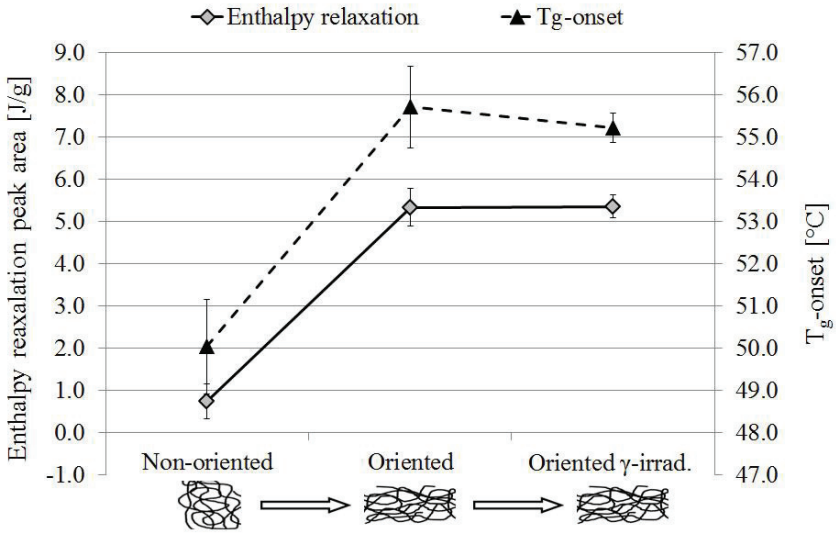

Figure 23. Effect of orientation-programming and γ-irradiation on enthalpy relaxation and T_g of PDLLA (n = 6) (publication IV)

4.3.2. Shape-recovery of orientation-programmed $PDLLA_{OP}$ in aqueous environment at 37 °C

The shape-recovery of $PDLLA_{OP}$ towards the non-oriented shape started in the 37 °C buffer solution within 24 hours for both non-γ-irradiated (i.v. 1.5 dl/g) and γ-irradiated (i.v. 0.9 dl/g) $PDLLA_{OP}$ polymers (Figures 24 and 25). The shape-recovery rate, measured as the radial expansion of the diameter, was faster with the γ-irradiated $PDLLA_{OP}$ than with the non-γ-irradiated and the recovery rate of the γ-irradiated $PDLLA_{OP}$ was accelerated after three-day incubation at 37 °C whereas the recovery rate for the non-γ-irradiated $PDLLA_{OP}$ remained constant up to 10 days. The shape-recovery ratios measured as a function of radial expansion during a ten-week *in vitro* test were: 94 % for non-γ-irradiated samples and 97 % for γ-

irradiated samples. The longitudinal contraction for both non-γ-irradiated and γ-irradiated $PDLLA_{OP}$ during the 10 weeks *in vitro* at 37 °C was 74 % of the initial length (Figure 25). As seen from Figure 24 and Figure 25 the γ-irradiation increased notably the shape-recovery rate but had no significant effect on their shape-recovery ratio. The shape-recovery of the γ-irradiated $PDLLA_{OP}$ was unsymmetrical as the radial expansion was faster at the ends of the rods, which seemingly curved outwards after four-day incubation. After the seven-day incubation the shape-recovery measured from the ends of the γ-irradiated round shaped $PDLLA_{OP}$ rods was 59 % whereas from the middle of the sample the shape-recovery was 46 %. No shape-transformation was detected for the γ-irradiated $PDLLA_{OP}$ in an aqueous environment at 2 °C temperature during a seven-day incubation period and samples tested dry at 37 °C or at 21 °C *in vitro* showed no appreciable shape-recovery over the ten-week test. The indicative equations calculated from the shape-recovery curves presented in Figure 24 are:

$PDLLA_{OP}$: $y = 0.0773x^4 - 1.8041x^3 + 12.656x^2 - 14.595x + 5.8075$, $R^2 = 0.99$

γ-irradiated $PDLLA_{OP}$: $y = 0.4131x^3 - 8.3609x^2 + 53.331x - 11.892$, $R^2 = 0.9723$

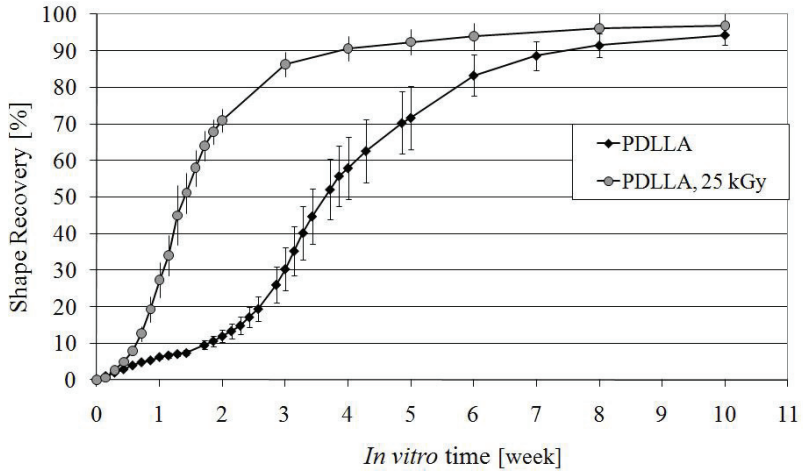

Figure 24. Shape-recovery of $PDLLA_{OP}$ towards the non-oriented shape *in vitro* at 37 °C measured as radial expansion of the diameter from the middle of the sample (n = 10) (publication III)

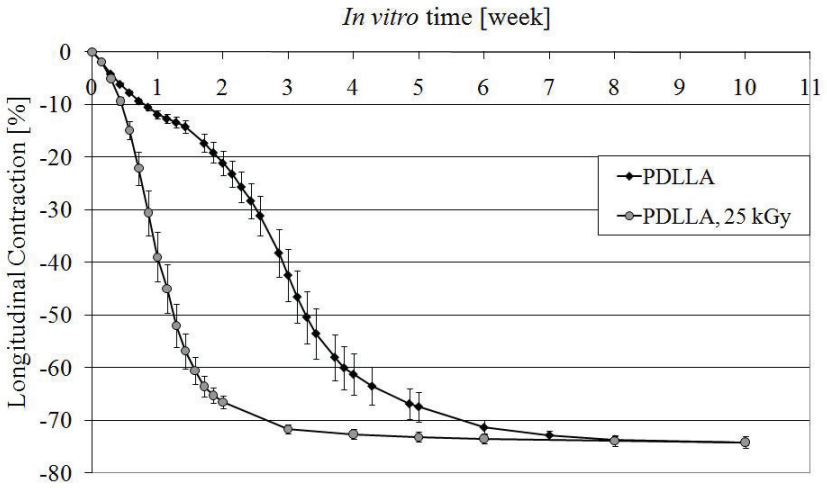

Figure 25. Longitudinal contraction of the $PDLLA_{OP}$ towards the non-oriented shape *in vitro* at 37 °C (n = 10) (publication III)

The change in the orientation-programmed structure can be clearly seen in the SEM images (Figure 26), which show the changes in the initially oriented structure *in vitro* at 37 °C. In Figure 26, the initiation of a shape-recovery-derived deorientation is clearly visible after five days. The fully oriented structure had transformed into alternating-oriented and non-oriented zones after three weeks *in vitro* at 37 °C.

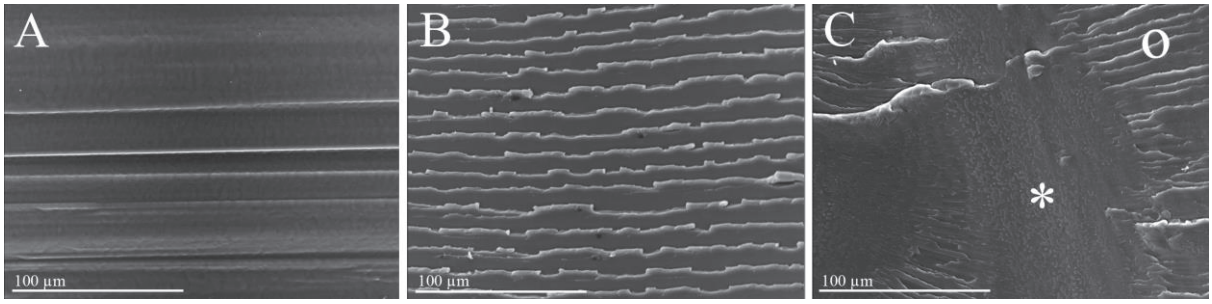

Figure 26. SEM images of longitudinal fracture surface of γ-irradiated $PDLLA_{OP}$; initial orientation-programmed structure (A), 5 d *in vitro* (B), and 21 d *in vitro* (C); oriented structure visible as horizontal lines in all images and as bands of oriented (o) and deoriented (*) zones after 21 d *in vitro* (publication III)

4.3.3. Water absorption and change of thermal properties of orientation-programmed $PDLLA_{OP}$ *in vitro*

When submerged into the buffer solution both non- and γ-irradiated samples absorbed small amounts (0.6 – 1.0 wt-%) of water (Figure 27). Both the incubation temperature and the molecular weight had an effect on the absorption of water. The main water absorption

occurred during the first two days, after which the polymers' water content was stabilized at 37 °C. The water absorption of $PDLLA_{OP}$ at 2 °C was slower and did not reach a stable level during the seven day test. The water content at 37 °C of non-γ-irradiated $PDLLA_{OP}$ samples remained stable for the whole 10-week period, whereas the water absorption of γ-irradiated $PDLLA_{OP}$ samples started to increase again very slowly after five weeks *in vitro* possibly due to the molecular degradation.

The small amount of absorbed water in the PDLLA polymer matrix had a pronounced effect on the thermal properties of the sample materials. The dry T_g –onset of $PDLLA_{OP}$, which was in the range of 56-57 °C for non-γ-irradiated samples and 55 °C for γ-irradiated samples (Table 7 and Figure 28), dropped dramatically already after 24 hours *in vitro* at 37 °C to 46 °C and 42 °C, respectively. Though the analysed T_g-onset for both non-γ-irradiated and γ-irradiated $PDLLA_{OP}$ was above 40 °C even after the stable level of water had been reach, a 2 % deviation of the baseline, indicating the start of the T_g range, can be seen already after 24 hours below 37 °C with γ-irradiated samples (Table 7). The *in vitro*-temperature had a clear effect on the T_g-drop with the $PDLLA_{OP}$ samples. The T_g-onset for the γ-irradiated $PDLLA_{OP}$ decreased to 46 °C during the seven day *in vitro* period at a temperature of 2 °C. When the diffused water was removed by vacuum drying at room temperature, the T_g-onset of the γ-irradiated $PDLLA_{OP}$ shifted back towards its original value, but the original dry-T_g of the oriented form was not fully reached as the T_g-onset leveled at 51 °C. However, the T_g-onset of the non-oriented PDLLA (~50 °C) was reached**,** which showed that the change of T_g in the shape-memory was thermally reversible.

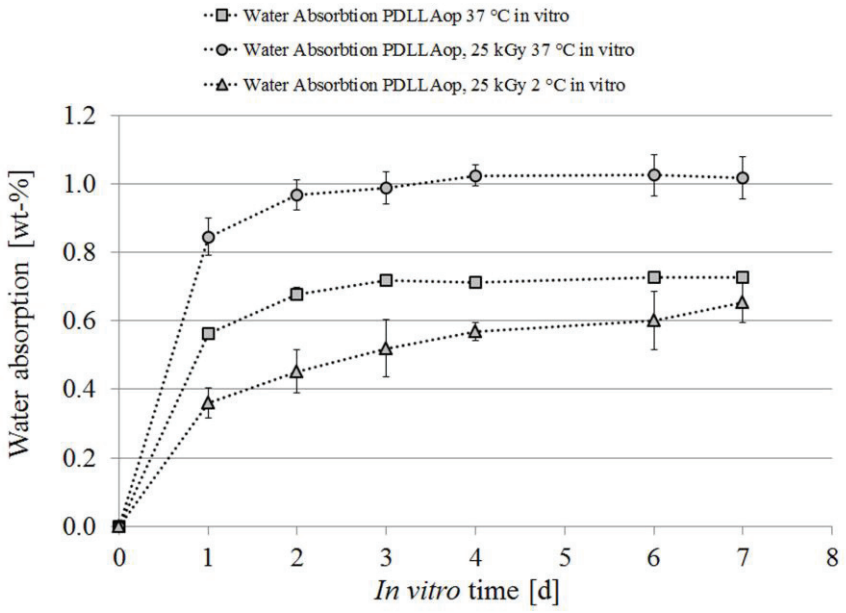

Figure 27. Water absorption measured as the weight increase of the $PDLLA_{OP}$ *in vitro* (n = 6) (publication IV)

Table 7. T_g-onset and MDSC-curve baseline deviations (2-5 %) indicating the start of the T_g-range of $PDLLA_{OP}$ at various incubation time points, n=6 (publication (III)

	PDLLA				
In vitro time [d]	Tg-onset [°C]	2 % dev. [°C]	3 % dev. [°C]	4 % dev. [°C]	5 % dev. [°C]
0	56.6 ± 0.8	50.6 ± 3.8	51.8 ± 3.7	52.6 ± 3.1	53.8 ± 0.4
1	45.8 ± 0.4	40.3 ± 0.9	41.3 ± 0.6	42.0 ± 0.6	42.4 ± 0.6
3	45.0 ± 0.4	38.7 ± 2.9	39.9 ± 2.2	40.8 ± 1.4	41.5 ± 1.0
7	44.2 ± 0.4	37.9 ± 2.1	39.3 ± 1.2	40.5 ± 0.8	41.0 ± 0.8

	PDLLA 25 kGy				
In vitro time [d]	Tg-onset [°C]	2 % dev. [°C]	3 % dev. [°C]	4 % dev. [°C]	5 % dev. [°C]
0	55.3 ± 0.3	48.0 ± 2.1	52.1 ± 0.3	52.3 ± 0.3	52.5 ± 0.3
1	42.2 ± 0.8	36.7 ± 1.7	37.9 ± 1.4	38.7 ± 1.2	39.3 ± 1.0
3	40.8 ± 0.7	35.2 ± 2.7	36.4 ± 3.2	38.0 ± 1.7	38.8 ± 1.5

The orientation-programming process generated a large enthalpy relaxation peak to the T_g-range, but already after 24 hours at 37 °C the peak was markedly changed with γ-irradiated samples, but no change was observed with the non-γ-irradiated $PDLLA_{OP}$ (Figure 29). The diffusion of water into the polymer matrix did not have such a straight-forward effect on the enthalpy relaxation of $PDLLA_{OP}$ as on the T_g as can be observed from the calculated values of the enthalpy relaxation peak areas presented as a function of *in vitro*- time in Figure 29. The enthalpy relaxation peak area for the non-γ-irradiated $PDLLA_{OP}$ remained unchanged during the seven day follow up period *in vitro* at 37 °C, whereas the enthalpy relaxation peak area for the γ-irradiated $PDLLA_{OP}$ decreased by 50 %. The γ-irradiated $PDLLA_{OP}$ samples showed that the diffused water had a powerful effect on the thermal properties of the $PDLLA_{OP}$ even at an incubation temperature of 2 °C as the enthalpy relaxation peak area decreased 23 % after a seven day incubation period. The vacuum drying at room temperature only minutely increased the peak size of the enthalpy relaxation of γ-irradiated $PDLLA_{OP}$ compared to those analyzed as wet, which indicates a non-reversible morphological change due to molecular movements in an aqueous environment at 37 °C. The non-γ-irradiated and non-oriented PDLLA, which was used as reference material, showed an aging-type behavior when incubated at 37 °C. The enthalpy relaxation peak area of the non-oriented PDLLA increased by six-fold during the first 24 hours after which no significant changes were observed.

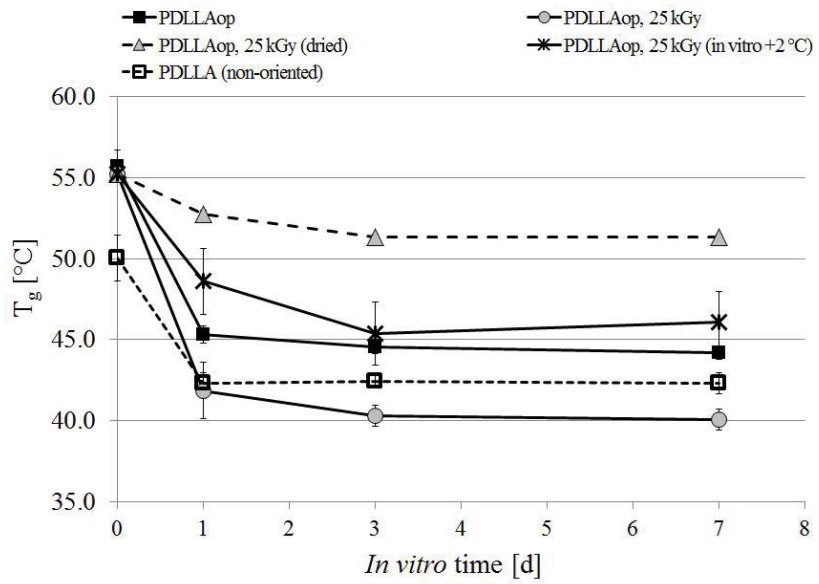

Figure 28. Enthalpy relaxation changes $PDLLA_{OP}$ and PDLLA *in vitro* (n = 6) (publication IV)

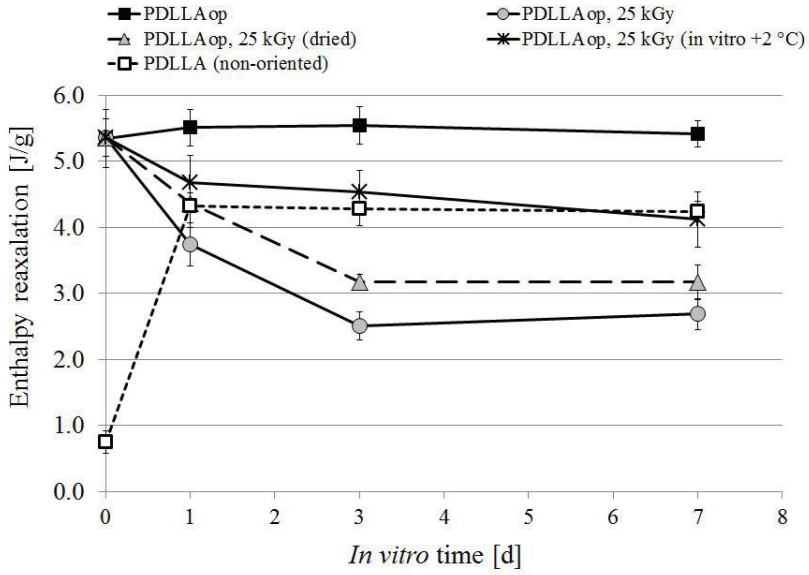

Figure 29. Enthalpy relaxation changes $PDLLA_{OP}$ and PDLLA *in vitro* (n = 6) (publication IV)

4.3.4. Change of spectroscopic properties in an aqueous environment

After immersion of the PDLLA samples, the main changes in the FTIR spectra could be seen in the intensities and locations of the peaks created by the IR absorptions of the OH bonds of the water molecules absorbed into the polymer matrix (3651–3657 cm^{-1} and 1625–1630 cm^{-1}), of the OH bonds of the polymer (3547–3569 cm^{-1}), and of the C=O bonds of the polymer

(1748–1765 cm^{-1} and the overtone at 3504–3509 cm^{-1}). The change of intensities and the shifting of the bands were the most significant during the first day of immersion and further observations showed that after the first day the positions of the bands moved only slightly or remained unaltered. The shift of the ν(OH) absorption band of water to a lower wavenumber in water treated Film 1, Film 1s (Figure 30), Film 2, and Film 2s from approximately 3656–3660 cm^{-1} to 3652–3653 cm^{-1} after the first day and to approximately 3651–3652 cm^{-1} after the seven days of immersion indicates that the amount of intermolecular hydrogen bonding between water molecules increased as function of the immersion time. The increase in this intensity corresponds to the amount of water absorbed into the polymer matrix during the immersion period. The FTIR spectra also indicate that the ν(OH) PDLLA absorption band, which originates from the OH groups of the original polymer, shifts to a higher wavenumber when the polymer has been immersed in water for one day, i.e. from 3565 cm^{-1} to 3568 cm^{-1} in Film 1 and from 3548 cm^{-1} to 3568 cm^{-1} in Film 1s. The ν(OH) PDLLA peak shifted only by 1 cm^{-1} during the second day of immersion and remained constant until the seventh day of immersion and the intensity increased slightly until the second day, but remained unchanged after that.

The absorption band at 3505 cm^{-1} is associated with an overtone of carbonyl stretching vibrations, ν(C=O), of the polymer occurring in the range of 1765–1748 cm^{-1}. In the non-γ-irradiated PDLLA films, the position of this overtone peak shifted only slightly (1 cm^{-1}) to a lower wavenumber after immersion of one day and remained unaltered until the seventh day of immersion (Figure 30). This shift is interpreted as a hydrogen bonding interaction between the C=O groups of the PDLLA polymer and water making the stretching vibrations of this group energetically slightly easier. The intensity of the peak increased during the first two days after which the change was stabilized up 7 days. The peak in the γ-irradiated films shifted 2 cm^{-1} during the first day and 3 cm^{-1} in total during the seven days of immersion. The larger shift towards lower energy could be interpreted as an increased opportunity for hydrogen bonding to take place between the C=O groups and water after γ-irradiation, that shortens the polymer chains and increases the flexibility of the chains compared to before γ-irradiation.

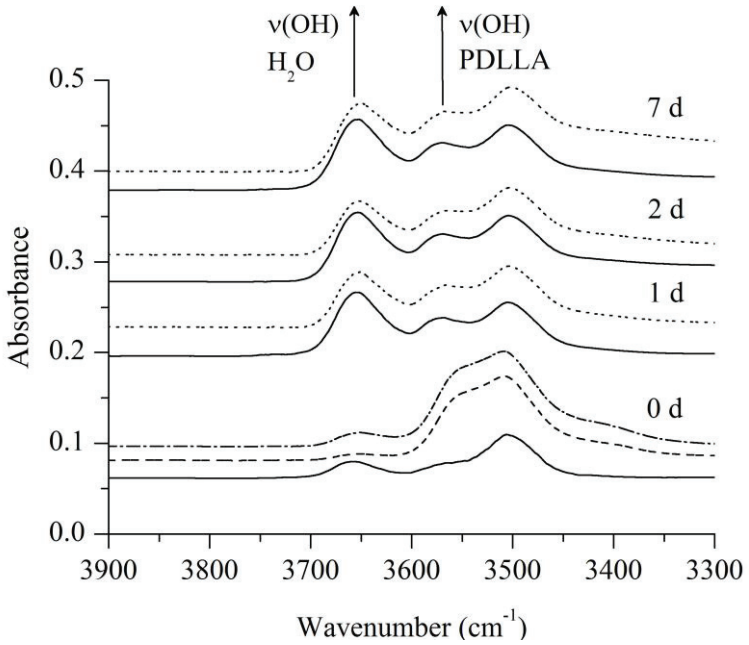

Figure 30. FTIR spectra of Film 1 (solid lines) and Film 1s (dotted lines) in the region of 3900–3300 cm^{-1} before (0 d) and after immersion in water for one, two, and seven days. The spectrum of Film 1 after drying in vacuum (the lowest line) was used as a reference for normalization. The dash-dotted line (-·-) represents Film 1s before γ-irradiation and the dashed line (- -) directly below it is the same film after γ-irradiation and vacuum drying, but before exposure to water. The directions of the changes in the intensities due to water treatment are indicated with arrows. (publication IV)

The peaks within the strong, broad and split ν(C=O) stretching band of PDLLA at 1748–1765 cm^{-1} (Figures 31a and 31c) shifted to lower wavenumbers by 1–7 cm^{-1} when the films were immersed to water. Compared to the non-γ-irradiated PDLLA the shift of wavenumbers was clearer for the γ-irradiated PDLLA films due to the lower molecular weight polymer chains. The direction of the shift indicates that the stretching of the C=O bond becomes easier with the presence of water. This phenomenon can be interpreted as an increase in the hydrogen bonding interaction between water molecules and the C=O groups of the polymer. During the first two days, the intensity of the band increased pronouncedly, especially in the non-γ-irradiated films. Such an increase in the intensity indicates that more C=O groups become hydrogen-bonded when the amount of water increases and the saturation level is approached or achieved within the immersion period. Moreover, the intensity of the peak at the lowest wavenumber, 1748–1750 cm^{-1}, increased with respect to the highest wavenumber peak at 1765 cm^{-1}. The weak band appearing at approximately 1626 cm^{-1} after immersion in water for one day (Figure 31b and 31d) is due to the H–O–H bending of free water. This band was removable from the films by drying the films at 37 °C. When studying carefully the spectral lines, it is observed that even in the non-vacuum dried films was a small amount of water that absorbed infrared light at a slightly lower wavenumber than after immersion.

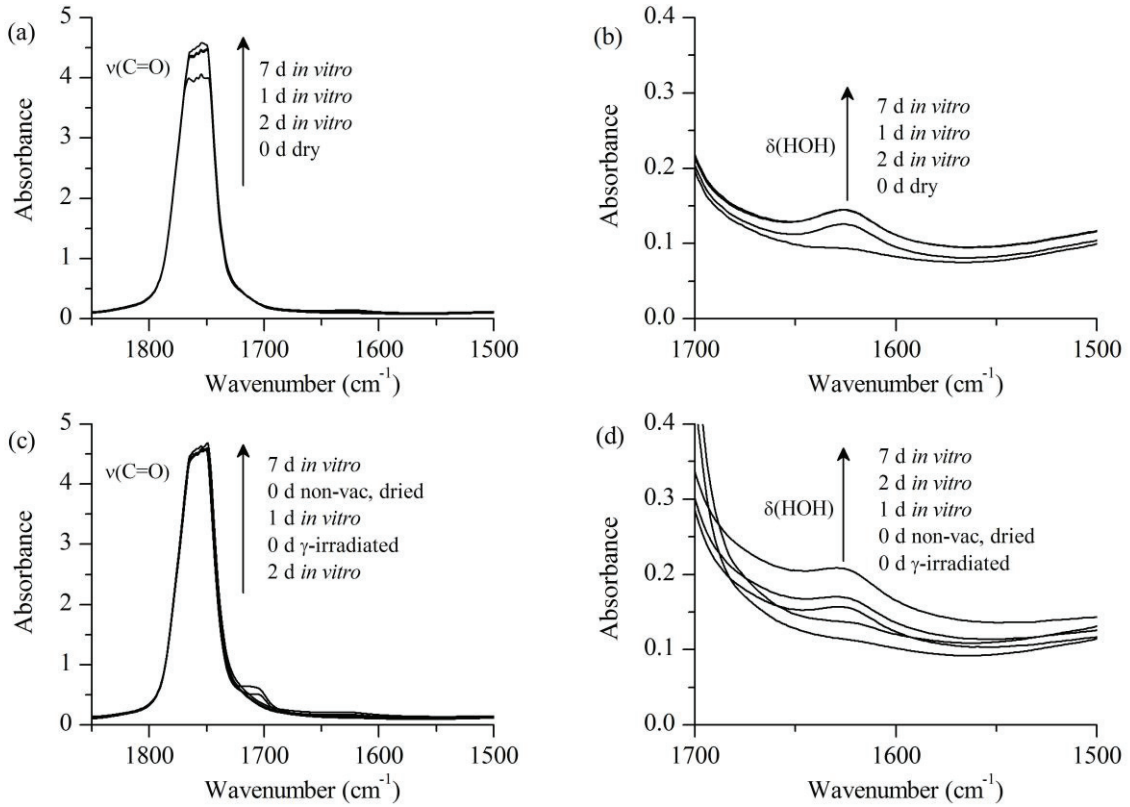

Figure 31. FTIR spectra of Film 1 in the regions of (a) 1850–1500 cm^{-1} and (b) 1700–1500 cm^{-1} together with the spectra of γ-irradiated Film 1s (c) and (d) in the same regions, respectively (publication IV)

4.3.5. Stress generation and stress relaxation of orientation-programmed $PDLLA_{OP}$ at 37 °C *in vitro*

The stress generation and stress relaxation test executed with the $PDLLA_{OP}$ showed that after submerging the samples in a 37 °C aqueous environment, stress generation occurred at the earliest in 30 minutes and at the latest in 15 hours. The orientation-programmed polymers could generate a stress level of approximately 10 MPa in an aqueous environment at 37 °C, which accorded with the tensile stress applied in the orientation-programming process (10-15 MPa). The molecular degradation, which had occurred during the γ-irradiation, had a significant effect on their stress generating capability: the maximum generated stress for γ-irradiated samples was 7 to 8 MPa, and the $PDLLA_{OP}$ samples could not maintain a steady contracting stress as the non-γ-irradiated $PDLLA_{OP}$ (Figure 32). During the 10-week test period *in vitro* at 37 °C the measured stress dropped by 96 % in the γ-irradiated sample, but only by 19 % in the non-γ-irradiated sample.

The $PDLLA_{OP}$ showed a tendency to recall the original and programmed tension despite the external loading in the cycled stress generation and stress relaxation test (Figure 33). When the external load was cycled according to Figure 33 B, the polymer was first able to generate a contracting force, which accorded with that used in the orientation-programming, but when

the material was subjected to an external tensional force greater than one used the orientation-programming, it stress relaxed back to the programmed level. After removal of all load and generated stress such that no load could be measured, the programmed material tended to contract and generate a stress that again accorded with that used in the orientation-programming.

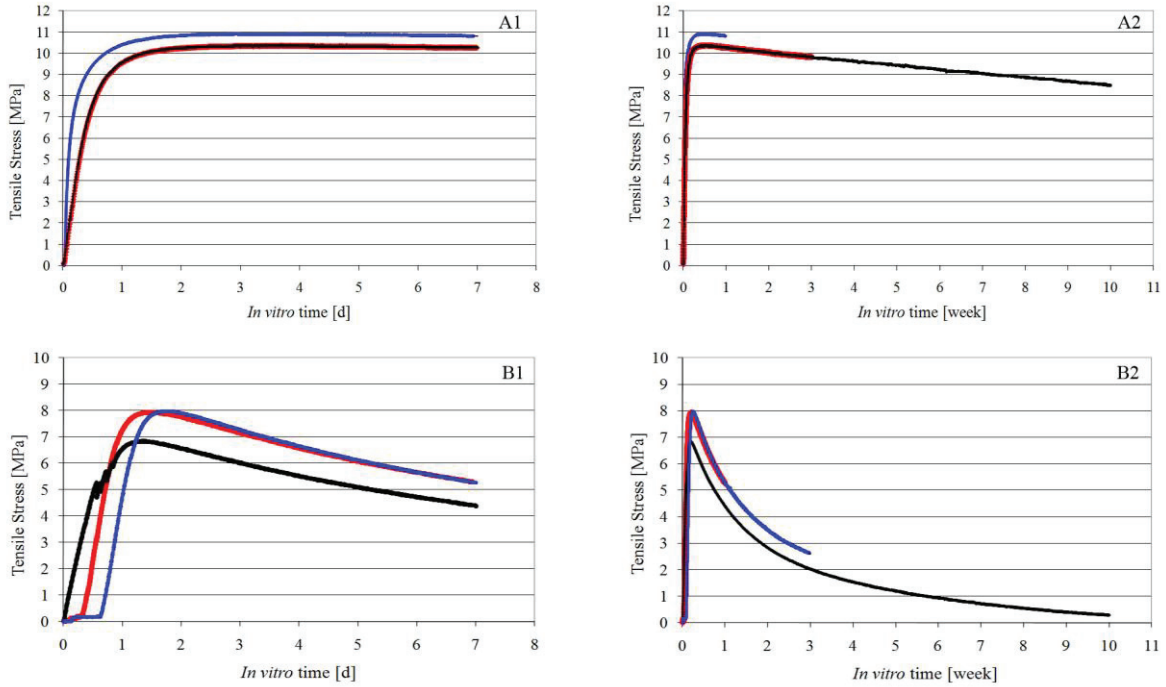

Figure 32. Generation of tensile stress due to restrained shape transformation of $PDLLA_{OP}$ (A) and γ-irradiated $PDLLA_{OP}$ (B); short-term force generation (A1, B1) at left, long-term (A2, B2) at right, curve colours identify the samples in the long- and short-term tests (publication III)

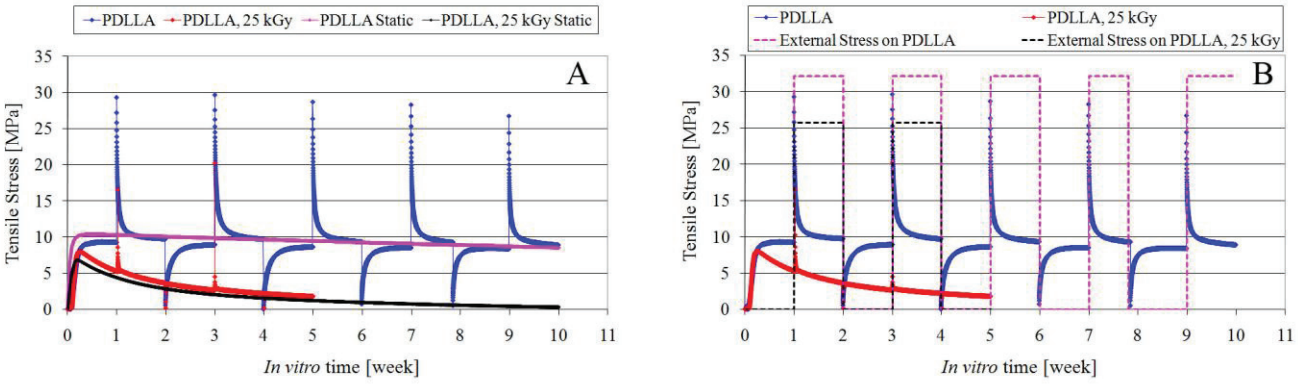

Figure 33. Cycled stress generation and stress relaxation of $PDLLA_{OP}$ compared to a static, non-cycled, stress generation test (A), combined stress generation and stress relaxation of PDLLA and applied external stress (B) (publication III)

4.3.6. Effect of the shape-memory effect on the pull-out force of $PDLLA_{OP}$ nails

The results of the pull-out force as function of time *in vitro* at 37 °C of the γ-irradiated grooved-shaped $PDLLA_{OP}$ nails in a polyurethane block model are presented in Figure 34. After immersion the initial pull-out strength of the nails was maintained for the first 24 hours after which the pull-out force was significantly increased due to the shape-memory effect activated by the 37 °C aqueous environment. The shape-transformation of the $PDLLA_{OP}$ nails implanted in a tight drill hole generated a 110 % increase in the pull-out force during a three-day incubation period and after seven days the pull-out force had increased 360 %. The $PDLLA_{OP}$ nails were visually observed to expand where they could, simultaneously contracting in the direction of their longitudinal axis, mainly outside the test blocks.

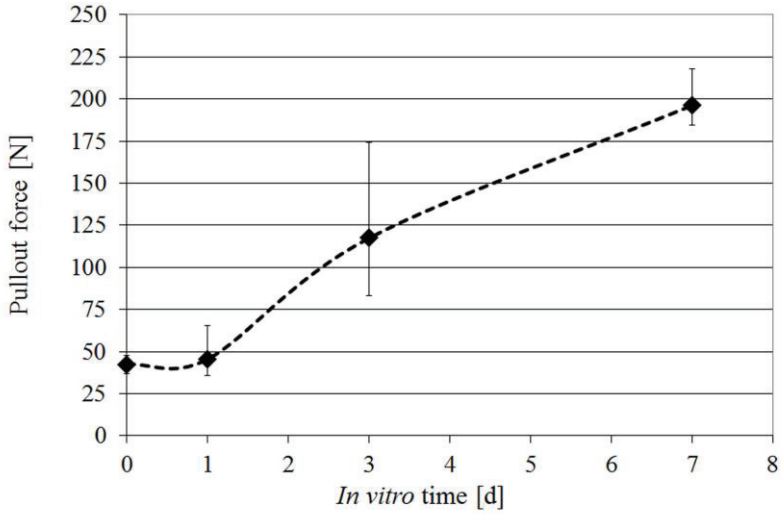

Figure 34. Pull-out force of the γ-irradiated grooved shaped $PDLLA_{OP}$ nails *in vitro* at 37 °C (n = 3, error bars show the min. and max. values) (publication IV)

5. Discussion

5.1. The effects of melt-extrusion on the molecular weight and the generation of the lactide monomer of lactide copolymers

In this study, two different lactide copolymers, P(L/D)LA 96L/4D and PLGA 85L/15G, were used to study the effects of melt-extrusion on the molecular degradation occurring during the melt-processing and the effects of the processing-derived degradation on performance in an hydrolytic environment. The P(L/D)LA 96L/4D copolymers with different initial molecular weights showed different degradation characteristics during the melt-spinning with a single-screw extruder: the higher the initial molecular weight, the stronger the molecular degradation, with the most degradation occurring in the length of the extruder barrel. The low-molecular-weight PLA22 (M_w 100400 g/mol) did not degrade in the melt-spinning process due to its lower melt-viscosity and lower shear stresses affecting the polymer melt compared to PLA48 (M_w 271000 g/mol) or PLA63 (M_w 344000 g/mol). The high-molecular-weight PLA48 and PLA63, on the other hand, degraded significantly in the extruder barrel. The degradation during the melt-extrusion was possibly due to the high shear stress caused by the extruder screw at the applied temperatures. The degradation process in the melt continued until the melt-viscosity and the molecular weight were low enough to withstand the shearing of the screw.

The molecular degradation of PLGA 85L/15G in the melt and the generation of lactide monomer correlated with the melt temperatures used, as the high melt temperatures caused higher molecular degradation and higher generation of lactide monomer than the lower melt temperatures. During the melt-extrusion, the decrease in the inherent viscosity was in the range of 29 - 56 % and the generated lactide monomer content with the thermally degraded PLGA 85L/15G was in the range of 0.03 - 0.2 wt-%. The effect of the shear stress generated by the extruder screw was observed with PLGA 85L/15G samples in which the lactide monomer was melt-mixed. The higher amount of lactide monomer mixed in the melt plasticized the polymer and thus decreased the effect of the shear stress on the polymer chains. Also, lower melt temperatures could be used to generate sample materials containing various amounts of monomer. The influence of the initial inherent viscosity of the polymer on the degradation sensitivity in the melt-extrusion process was also observed with the PDLLA which only had a minor drop in its inherent viscosity during the processing and no lactide monomer was generated thermally into the polymer.

Earlier studies in which lactide copolymers have been used in the melt-spinning process have reported a 50 % decrease in the i.v. of P(L/D)LA 96/4 with an i.v. of 4.21 dl/g (Kellomäki et al. 2000c) and a 47-62 % decrease with an i.v. of 5.48 dl/g (Ellä et al. 2010), a 31 % decrease in the M_w of P(L/DL)LA 92/8 with an M_w of 16,400 g/mol (Schmack et al. 2001) and a 68 % decrease in the viscometric molecular weight (M_v) of PLLA with an M_v of 330,000 Da

(Fambri et al. 1997). When comparing the results of this study with earlier studies, the molecular degradation in the melt could be minimized by choosing optimal molecular weight for the raw material and by using as low melt temperatures as possible.

An interdependency between molecular weight and melt viscosity was observed when analysing the rheological properties of the P(L/D)LA 96L/4D copolymers with a rotational rheometer. When measuring the melt-viscosities with the shear rates used in the single-screw extrusion, the viscosities of PLA48 and PLA 63 were observed to be significantly higher than with PLA22. The initial molecular weight also influenced the rheological behaviour in the melt, which is clearly seen when comparing the high-molecular-weight copolymers to the PLA22. The PLA22 showed typical shear-thinning behaviour, similar to that in (Schmack et al. 2004), but the viscosities of PLA48 and PLA63 decreased nearly linearly with an increasing shear rate. The decrease in viscosity during the rotational rheometric analysis of PLA48 and PLA63 is probably the result of the molecular chain degradation caused by the interaction of high temperatures (240-250 °C) and shear stress or from an edge fracture in the polymer melt during the measurements that caused an error in the analysis (Dealy. 1999).

With the melt-spinning setup and processing parameters used in the study with a single-screw extruder, the high-molecular-weight PLA48 and PLA63 degraded significantly due to the shear stress in the length of the extruder barrel caused by the extruder screw. The melt-viscosity seems to play a major role in the molecular degradation in the melt, because the screw extraction test showed that the molecular weight dropped until reaching a level in which the melt viscosity was low enough to halt the degradation caused by the shearing action of the screw in the extruder barrel. To reach low enough melt-viscosity in the extrusion with high-molecular-weight PLA48 and PLA63, higher extruder zone temperatures were required than with the low-molecular-weight PLA22. Due to the weak thermal stability of lactide-based polymers (Jamshidi et al. 1988), the high melt-temperature further accelerated the generation of lactide monomer in the small melt-flow-channels in the spinning dies.

The differences in the molecular weights and inherent viscosities of the melt-spun fibres and the extruded rods were evened out during the γ-irradiation. The decreases of M_w for the melt-spun fibres were 73 % (F22), 79 % (F48) and 75 % (F63), and for the extruded and die-drawn rods the decreases of i.v. were 67 % (RM003), 57 % (RM005), 53 % (RM010), 59 % (RM020), 58 % (RM200), 63 % (RM300), 64 % (RM400) and for the orientateon-programmed PDLLA 40 % during the γ-irradiation. The radiation seemed to cause more molecular degradation on the high molecular weight and high i.v. samples. This is possibly due to the γ-irradiation's random cleavage of the macromolecules: the irradiation in a bigger molecule causes a bigger drop in the average molecular weight than with initially lower molecular weight molecules. The γ-irradiation, however, has not been found to affect the lactide monomer contents of lactide copolymers, whether the materials contained lactide monomer or not prior to the γ-irradiation (Ellä et al. 2010). Previous studies that have reported the γ-irradiation of lactide-based polymers show similar magnitudes of degradation

as reported here. In (Ellä et al. 2007), the decrease in the M_w of P(L/D)LA 96/4 in γ-irradiation (25 kGy) was reported as 73 %, and in (Nuutinen et al. 2002) the decrease in the intrinsic viscosity of PLLA was 62 %. In both melt spinning and γ-irradiation (25 kGy), molecular degradation was reportedly 70 % in (Kellomäki et al. 2000c) and the decrease in i.v. ~80 % in (Kellomäki et al. 2000a) and 81 % in (Honkanen et al. 2003).

5.2. The effects of melt-extrusion derived lactide monomer on hydrolytic degradation characteristics of oriented lactide copolymers

The hydrolytic degradation of a lactide copolymer at the physiological temperature is significantly affected by the melt processing. The thermal degradation in the melt not only decreases the molecular weight of the polymers, but also affects the thermal generation of lactide monomer, which markedly affects the hydrolytic degradation rate at 37 °C *in vitro* (Ellä et al. 2010). The hydrolytic degradation of these polymers is a sum of complex interrelated events consisting of decreasing molecular weight, morphological changes and mass loss.

The effects of the lactide monomer can be clearly seen with the melt-spun and extruded lactide copolymers used in this study. Although the P(L/D)LA 96L/4D fibres and the PLGA 85L/15G rods with the thermally generated lactide monomer had the initial molecular weights and inherent viscosities in the same level, the hydrolytic degradation behaviour *in vitro* at 37 °C between the samples with different lactide monomer content differed significantly despite their shape and size. The molecular degradation monitored as the decrease in molecular weight or i.v. was dependent on lactide monomer content and showed a linear-type of decrease up to a specific level, after which the degradation rate slowed down. This effect was likely due to the faster hydrolysis of the amorphous phase of the oriented semicrystalline polymers that degraded to a level at which the molecular chain mobility in the oriented amorphous phase was sufficient enough to allow a cleavage-induced crystallization of the polymer chains to occur. This can be clearly seen with the PLGA 85L/15G samples. According to Zong et al. the hydrolytic degradation mediated increase in both the crystallinity and the more confined amorphous regions hinder the hydrolysis compared to the polymer chains in the amorphous gaps of the semicrystalline polymer**.** This is because the highly crystalline regions can possibly limit the penetration of water molecules into these amorphous regions (Zong et al. 1999). In addition, as the fraction of crystalline material increased due to the dilution of the amorphous regions out of the oriented polymer matrix, the degradation proceeded more slowly as only more ordered crystalline regions remained (King and Cameron. 1997).

The effects of even small amounts of lactide monomer can be seen in both the fibres and the rods. The drop in the molecular weight (M_w) of the fibres during the 24-week follow up time

was 84 % for F63 (monomer content 1.9 wt-%), 61 % for F48 (monomer content 0.09 wt-%) and 9 % for F22 (monomer content <0.02 wt-%). The rods showed a similar trend and although the degradation rates differed only slightly between RM005, RM010 and RM020, which all had the same initial i.v., degradation had significant long-term effects. This can be clearly seen when monitoring the time for the molecular degradation to reach the 0.6 dl/g limit. For RM005, RM010 and RM020, reaching this limit in i.v. took 16, 14 and 10 weeks, respectively. As presented in Figure 14, both thermally generated and melt-blended monomer affected the hydrolytic degradation rate of PLGA 85L/15G, which was further proportional to the samples' post-processing monomer content despite the elution of lactide monomer from the polymer matrix into the surrounding medium during the first weeks. The initial lactide monomer content in the polymer matrix most likely catalyzed the chain scission at 37 °C *in vitro*. This resulted in the formation of acidic end groups that further enhanced the rate of hydrolysis (Edlund and Albertsson. 2003, Tsuji and Ikada. 2000). An observation of this study that is especially significant is the generation of lactide monomer in the melt and its effects on the hydrolytic degradation. This observation is significant because the earlier studies have mostly focused on demonstrating the importance of polymer purity on the performance of the material (Kellomäki et al. 2003, Hyon et al. 1998). For both the fibres and the rods, the size did not play a key role in the degradation as both the thicker fibres and thicker rods degraded faster than the thinner ones, similar to the findings of (Ellä et al. 2010). No autocatalytic effect, similar to the findings of (Li et al. 1990c,Li. 1999), was observed with the oriented polymers. This could be due to the micro cavities generated in the orientation process that can ease the fluid exchange and prevent the accumulation of degradation products inside the polymer (Kellomäki et al. 2000a).

As generally understood, mechanical properties are related to the molecular weight of the polymer, but with thermally unstable and biodegradable polymers there are also other remarkable factors that influence mechanical properties such as monomer content. Strength retention *in vitro* can be controlled by control of the degradation rate because strength retention is likely to be related to the lactide monomer content of the melt-processed polylactide. The higher the monomer content, the more rapid is the decline in molecular weight and mechanical properties. The lactide monomer catalysed hydrolytic molecular degradation of the lactide copolymers and had a profound effect on the mechanical properties of the melt-spun fibres and the extruded and oriented rods. In the *in vitro* study with the P(L/D)LA 96L/4D fibres, the 12-week strength retentions of the melt spun and γ-irradiated fibres were 88 % for F22 and 74 % for F48. These results are better than or similar to those in (Ellä et al. 2007) and (Honkanen et al. 2003) in which P(L/D)LA 96L/4D fibres and yarns maintained 75 % and ~50 % of their initial ultimate tensile strength during hydrolysis over 13 weeks, respectively.

The effect of the lactide monomer catalyzed hydrolytic degradation is very clear when measuring the shear strength of the extruded and die-drawn rods. The shear strength first remained at a stable level minimum of 80 % of its initial value up to the critical stage of

molecular degradation, after which it started to decline rapidly. There seems to be a clear relationship between the molecular weight dependent inherent viscosity and the shear strength, so that when the i.v. reaches a critical level of 0.8 – 0.6 dl/g the molecular weight is so low that even small drops start to drastically affect the mechanical properties. The results show that even small quantities (0.05-0.20 wt-%) of lactide monomer catalyzed molecular degradation and resulted in a further loss of mechanical properties in PLGA 85L/15G at 37 °C *in vitro*. Compared to shear strength, the bending load of the PLGA 85L/15G samples was even more sensitive to degradation. This sensitivity to degradation is due to the degradation-induced crystallization in the oriented polymer matrix that transformed the oriented polymer from ductile to brittle. The increase in crystallinity was simultaneous and degradation-rate-dependent and most likely due to the degradation of the amorphous phase, which crystallized because of increased molecular mobility. Thus, this proportionally increased the volume of the polymer crystal phase (Zong et al. 1999, Li and Vert. 1994, Niiranen et al. 2004). As was the case with degradation, crystallization and structural change, mass loss also followed the degradation rate. Similar mass loss profiles for PLGA 85L/15G have been reported in (Ramchandani et al. 1997) in which the mass losses were comparable to RM003 and RM020.

A small dimensional transformation towards the original non-oriented shape was observed with the oriented PLGA 85L/15G *in vitro* at 37 °C. A radial expansion of the diameter and longitudinal contraction occurred simultaneously and the shape transformation tendency was related mainly to the degradation rate of the polymers. Thus, the high amounts of lactide monomer (2.0 – 4.0 wt-%) stimulated the transformation of the oriented structure of PLGA 85L/15G significantly more than small amounts of lactide monomer (0.03 - 0.20 wt-%). Because the small shape-recovery occurred before a significant decrease in i.v., the molecular movements are likely to be caused by the water-molecule-driven plasticization of the amorphous phase of the polymer (Blasi et al. 2005). The higher shape-recovery ratios, a maximum of 5 %, observed with the high lactide monomer containing samples (RM200 – RM400) are likely to be due to the relaxation of the amorphous phase between the crystallites. This phenomenon pulls the adjacent crystal lamella closer together and thus further advances the shape transformation (Zong et al. 1999, King and Cameron. 1997).

5.3. Degradation data based simplified model for degradation-related strength retention

The hydrolytic degradation data gathered from studies with PLGA 85L/15G (publication II) enabled the construction of a simplified model for degradation-related strength retention. The model presented in Figure 35 is based on the observations of the effects of lactide monomer on the hydrolytic degradation rate and that the mechanical properties significantly decline in the i.v. range of 0.8-0.6 dl/g. This model uses the calculated time-values of the degradation reaching the 0.6 dl/g and 0.8 dl/g limits and assumes that the polymer loses its shear strength

at below 80 % of the initial value. This simplified model enables the prediction of the strength retention of PLGA 85L/15G in a hydrolytic environment at 37 °C with lactide monomer content up to 0.2 wt-%. The high lactide monomer contents are not included in the model, because the melt-mixed monomer might not be as homogenously distributed in the polymer matrix and can thus cause unreliable results.

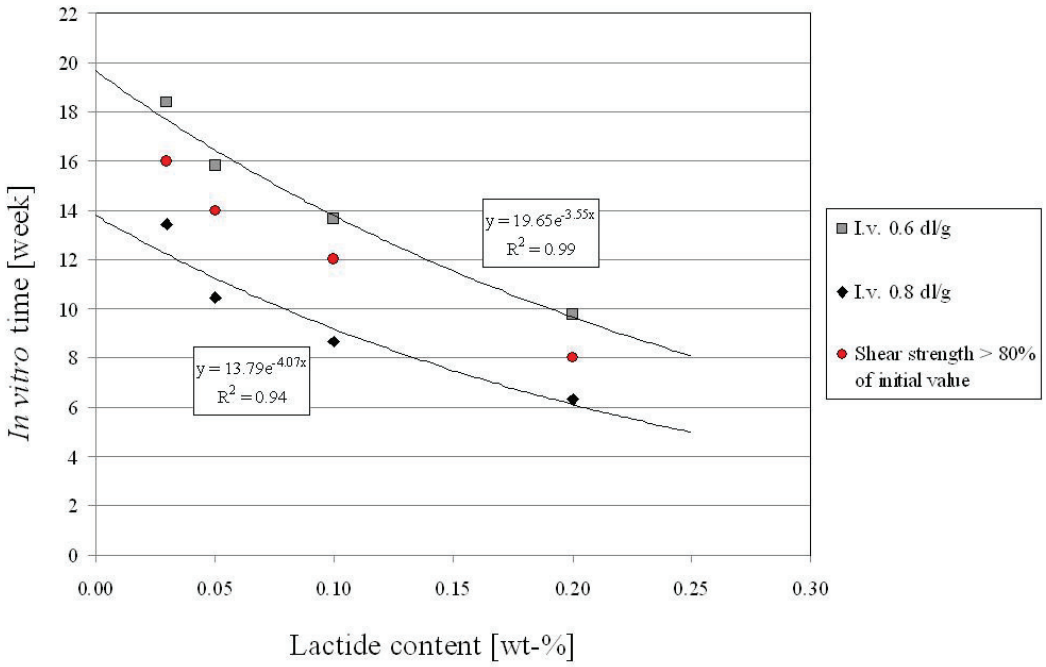

Figure 35. Simplified model of strength retention of PLGA 85L/15G with various amounts of lactide monomer showing maximum (i.v. 0.6 dl/g) and minimum (i.v. 0.8 dl/g) limiting values for strength retention and fitted curves with equations [Lactide content ≤ 0.20 wt-%]; measured true values for strength retention time are shown with red bullets (publication II)

The hydrolytic degradation data was further refined into a mathematical equation defining the surface that has been fitted based on the measurement results using the surface fitting toolbox in Matlab®. In Figure 36, a surface model and equation for the surface with an R^2-value of 0.99 that describes the strength retention and its relation to *in vitro*-time and lactide monomer content is presented. Although the calculated equation represents the degradation phenomena well, due to its R^2-value it is only suitable within the range of lactide contents and *in vitro*-times used in the measurements. Despite the limiting factors of the two models, they provide an estimation of the strength retention time *in vitro* at 37 °C for PLGA 85L/15G with various lactide monomer contents. The models are important because they clearly show the significant effects of even small amounts of lactide monomer on the strength retention of PLGA 85L/15G. Furthermore, the methodology of the models can possibly be applied to other lactide-based polymers as well. Consequently, the presented models are useful in

predicting and controlling hydrolytic degradation *in vivo* and in setting up a quality control system in the manufacture of bioabsorbable medical devices using melt processing.

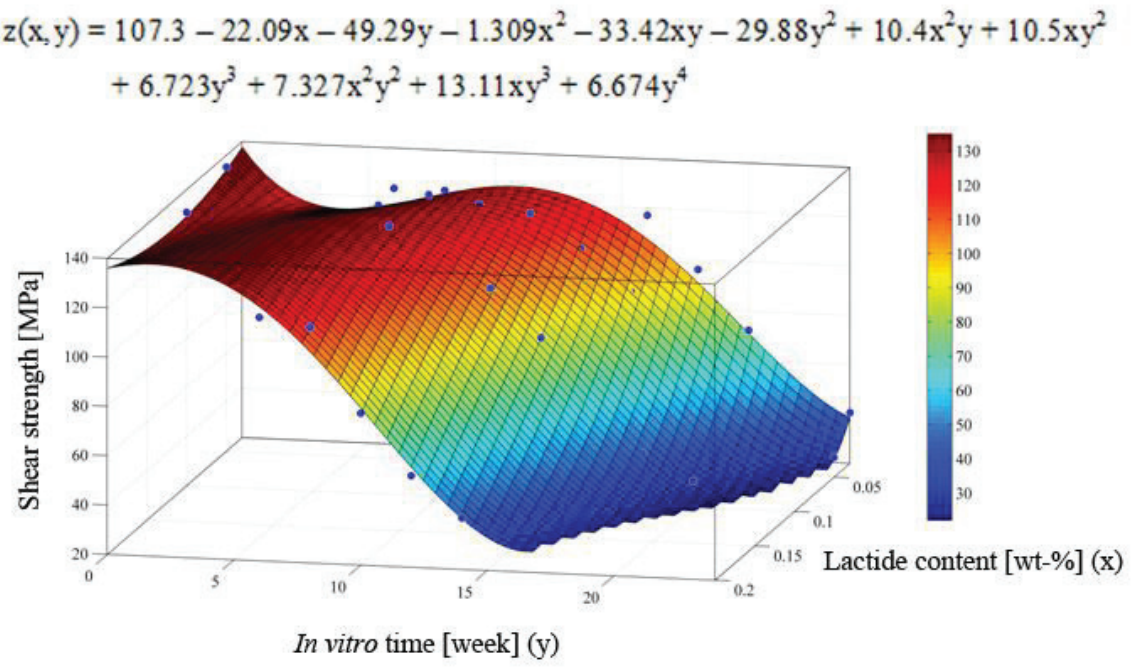

Figure 36. Mathematical model and equation for strength retention (z) of PLGA 85L/15G at 37 °C *in vitro* with various lactide monomer contents (x) as a function of *in vitro* time (y) R^2=0.99 (publication II)

5.4. Water-induced shape-memory of poly(D,L-lactide) generated by orientation-programming process

The shape-memory properties of amorphous PDLLA were generated in an orientation-programming process in which PDLLA is deformed into a temporary shape that is triggered to shape-recover in an aqueous environment at the physiological temperature, i.e. 37 °C. In the orientation-programming process, the polymer chains are first heated and strained, while simultaneously applying tensional stress to the polymer. The polymer chains are then immediately cooled down while maintaining the deformation, tension and polymer chain entanglements. During the shape-transformation process, the chain entanglements act as physical crosslinks that determine the permanent shape.

When the polymer chains are forced from their initially non-organized amorphous molecular structure into an oriented, more organized and less preferred state, the entropy in the system decreases as the number of possible molecular conformations decreases (Steendam. 2005, Wischke and Lendlein. 2010). This change in the polymer's morphology due to the

orientation-programming process is detected in thermal analysis (MDSC) as an enthalpy relaxation peak in the glass transition zone. The morphological transformation increases the analyzed T_g-value and the T_g-range and resembles a typical aging process in polymers in which the segmental mobility drives the polymers towards volume relaxation and a reduction in free volume (Pan et al. 2007, Hutchinson et al. 1999, Rault. 2006, Bailey et al. 2002). The difference to a typical polymer aging process is, however, that the smaller enthalpy and free volume in the $PDLLA_{OP}$ is caused by actively stretching the polymer chains that generates a strain-induced oriented morphology that requires more energy to finish the glass transition process than the original non-oriented structure (Lee et al. 2010, Stoclet et al. 2010).

The $PDLLA_{OP}$ expressed a shape-memory effect in an aqueous environment at 37 °C due to the effect of a small amount of diffused water (~1 wt-%) that caused a significant decrease in the T_g (12-15 °C) of the $PDLLA_{OP}$ after immersion (Blasi et al. 2005, Steendam. 2005). These molecular movements are based on the ability of amorphous $PDLLA_{OP}$ to exhibit a significant entropy-driven molecular mobility below its T_g, which involves the relaxation of small molecular groups with sufficient mobility (Hancock et al. 1995, Steendam et al. 2001, Steendam. 2005). Because the molecular motions are limited due to the T_g-onset of dry PDLLA (55-57 °C), the molecular movement that causes a shape-transformation in macroscopic scale are limited at 37 °C when the polymer is dry. However, the larger molecular movements, seen as shape-transformation, can appear when the time-scale of the larger molecular movement is reduced by lowering the glass transition temperature by plasticizing molecules that diffuse into the amorphous polymer matrix. The T_g-onset decreased and leveled at 45 °C for the non-γ-irradiated $PDLLA_{OP}$ and at 40 °C for the γ-irradiated $PDLLA_{OP}$, after a constant level of water in the polymer matrix had been reached. Even though the analysed T_g-onset was observed above the physiological temperature, the molecular movements are possible because glass transition is not a single temperature but occurs in a range in which the polymer changes from glassy to rubbery. By analysing the inflection point of the MDSC-curve (Table 7), it can be clearly seen that after 24 hours a 2 % deviation from the baseline of the MDSC curve occurs below 37 °C with γ-irradiated $PDLLA_{OP}$. This marks the start of the glass transition zone just below the physiological temperature and enables a slow shape-recovery towards the non-oriented state.

In an aqueous environment at 37 °C, the higher molecular weight non-γ-irradiated $PDLLA_{OP}$ was more resistant to the diffusion of water at 37 °C than the γ-irradiated $PDLLA_{OP}$, which led to a lower plasticization of the non-γ-irradiated $PDLLA_{OP}$. Samples tested at 2 °C showed that the water absorption of the γ-irradiated $PDLLA_{OP}$ was significantly weaker than it was at 37 °C and resulted in a significantly smaller T_g-drop due to a smaller number of diffused water molecules in the polymer matrix than at 37 °C. Steendam et al. have reported similar results regarding the stabilization of the water content and the effect of molecular weight on the T_g of PDLLA (Steendam et al. 2001). The increase of the T_g by the removal of the diffused water by vacuum drying at room temperature indicates that the change of T_g is thermally reversible with PDLLA.

The molecular weight of $PDLLA_{OP}$ had a significant effect on the shape-recovery rate, but not on the shape-recovery ratio during a 10-week follow up *in vitro* at 37 °C between the non-γ-irradiated and γ-irradiated samples. The molecular weight drop in the oriented state due to the γ-irradiation affected the water absorption as well as the enthalpy of the orientation-programmed polymers. When the T_g of the polymer decreased near the physiological temperature due to the diffusion of water, the probability of molecular movements at 37 °C increased (Hancock et al. 1995) and the simultaneous increase of enthalpy and free volume, seen as the decrease of the enthalpy relaxation peak, enabled the glass transition process to finish with a lower amount of energy (Pan et al. 2007). Thus, the significantly slower shape-recovery of the non-γ-irradiated $PDLLA_{OP}$ compared to the γ-irradiated $PDLLA_{OP}$ in a 37 °C aqueous environment can be explained by the lower concentration of plasticizing water and the lower enthalpy of the higher molecular weight polymer even with the maximum level of diffused water in the polymer matrix. The enthalpy relaxation that was observed in the non-γ-irradiated $PDLLA_{OP,}$ even after a stable level of water in the polymer matrix had been reached, caused the observed T_g-value to shift to a higher temperature due to a longer relaxation time than with the γ-irradiated $PDLLA_{OP}$ (Matsuoka and Bair. 1977). The phenomenon leads to a paradoxical result of a shifted T_g-range, even though the initiation of the glass transition process would have been at nearly the same temperature range (Höhne et al. 2003). The results of this study show that the molecular movements seen in macroscopic scale for γ-irradiated $PDLLA_{OP}$ are the result of two thermal changes that occur in an aqueous environment at 37 °C: a decrease in the T_g and a simultaneous decrease in the enthalpy relaxation.

The molecular mechanism behind the water-induced shift of the glass transition zone studied by FTIR spectroscopy showed that the diffusion of water to the polymer matrix affected the intermolecular dipole–dipole and/or hydrogen bonding of the PDLLA chains. The changes in the FTIR spectra of the PDLLA were seen in the intensities and locations of the peaks created by the IR absorptions of the OH bonds of the water molecules absorbed into the polymer matrix (Braun et al. 2006, Silverstein et al. 2005), of the OH bonds of the polymer (Gonçalves, C., M., B. et al. 2010) and of the C=O bonds of the polymer (Gonçalves, C., M., B. et al. 2010, Zhang et al. 2005). The most significant changes occurred during the first day *in vitro*. In the polymer matrix, the water molecules both separated the chains as well as interacted with them. This led to the disruption of the interaction (dipole–dipole and/or hydrogen bonding) between the polar OH groups and the other polar groups of the original polymer. Thus, the IR absorption (i.e. stretching) of the chain end O–H bonds became energetically slightly more difficult. The effect possibly competes and overlaps with the hydrogen bonding interaction between water molecules and the OH end groups of the polymer that has the tendency to move the stretching band slightly back to a lower wavenumber and to increase the intensity of the peak. Furthermore, the ν(C=O) stretching band shifted clearly to lower wavenumbers in the immersed γ-irradiated films. When a water molecule is hydrogen-bonded to two C=O groups at a time, the C=O absorption appears at a lower wavenumber than when only one water molecule is hydrogen-bonded to one C=O

group (Yang et al. 2006, Puffr and Šebenda. 1967). The weak and removable band appearing at ~1626 cm^{-1} after one day *in vitro* at 37 °C was due to the H–O–H bending of free water. In previous studies (Herrera-Gómez et al. 2001, Blasi et al. 2005), the different fractions of water adsorbed in hydrophilic materials have been assigned. One fraction, so called bound water, which corresponds to the first water layer in contact with the adsorbing solid, absorbs at a lower wavenumber ~1640 cm^{-1}. The other fraction, which corresponds to the absorbed water layers on top of the first layer, absorbs at a higher wavenumber ~1656 cm^{-1}**.** In the case of polyurethane, it has been shown that the bound water causes a decrease in the glass transition temperature of the polymer (Yang et al. 2006, Leng et al. 2008). The absorbed water in the polymer matrix also weakens the hydrogen bonding between the chains and causes a significant decrease in the glass transition temperature. Our results of the interaction between the PDLLA and water are in agreement with results of the polyurethane shape-memory polymer and show that a similar type of change in the thermal properties also enables the molecular movements in bioabsorbable PDLLA in the physiological environment.

When shape transformation was restricted in an aqueous environment at 37 °C, the $PDLLA_{OP}$ could generate a predefined level of stress measured as compression. The compressive stress generated *in vitro* at 37 °C was of the same level as the tensile stress used in the orientation-programming. This clearly indicates that the programming load could be stored in the polymer and mobilized by the 37 °C aqueous environment. Although the γ-irradiation had a positive effect on the shape-recovery rate, it significantly affected the stress generation capability of $PDLLA_{OP}$. The effect of γ-irradiation on the stress generation capability lowered the maximum generated stress and caused the polymer to stress relax due to the tension it had first generated. This was possibly due to chain slippage in the lower-molecular-weight polymer chain. With fewer possible chain entanglements (physical crosslinks) than non-γ-irradiated $PDLLA_{OP}$ with a higher molecular weight, the γ-irradiated $PDLLA_{OP}$ could not generate or maintain the programmed level of compression. Another affect factor could be the initial T_g of the γ-irradiated $PDLLA_{OP}$ that was lower than that of non-γ-irradiated $PDLLA_{OP}$ and thus enabled more molecular movement and chain slippage. The initial stress generated by non-γ-irradiated $PDLLA_{OP}$ also decreased, but the small stress relaxation was related more to the rate of degradation that caused similar chain slippage than to the γ-irradiated $PDLLA_{OP}$. The loading in orientation-programming clearly determines the stress level, or more precisely, the stress profile to which orientation-programmed PDLLA tends to adapt despite the external forces affecting it.

Compared to the thermally-stimulated shape-memory polymers that are typically directly heated over their transition temperature (Lendlein and Langer. 2002, Wischke and Lendlein. 2010), or to the highly tailored lactide and glycolide polymer networks showing water-induced shape-memory effect at 37 °C (Pierce et al. 2011), the shape transformation of $PDLLA_{OP}$ was slow in a physiological environment. However, the $PDLLA_{OP}$ did not need any external energy to start its shape-recovery, but was activated by the simulated

physiological environment and it presented good mechanical properties even after γ-irradiation and a linear hydrolytic degradation profile at 37 °C *in vitro*. Thus, the advantage of the orientation-programming is that it not only yields novel shape-transformation properties, but also simultaneously acts as a reinforcing method whereby polylactide copolymers can be processed into strong and ductile biodegradable medical materials (Törmälä. 1992). The pull-out test with the grooved shaped $PDLLA_{OP}$ nails presented the efficacy of the water-induced shape-memory of $PDLLA_{OP}$. The initial pull-out strength and the fixation stability was due to the tight fitting of the grooved shaped $PDLLA_{OP}$ nail and the longer stability and locking due to the shape-memory effect activated by the 37 °C aqueous environment. Thus the water-induced shape-memory of $PDLLA_{OP}$ can be successfully used in increasing the functionality and fixation reliability of bioabsorbable medical devices such as nails or tacks used for bone fracture or ligament fixation.

6. Conclusions

On the basis of the result presented and discussed in this thesis, it can be concluded that:

In melt-processing the rheological properties of lactide copolymers significantly influence the molecular degradation and the generation of lactide monomer in the melt. For high-quality melt-extrusion and to minimize the processing-derived molecular degradation, the melt-temperature and the shear stress affecting the polymer chains should be optimized by either raw material selection or the modification of the melt-processing system itself.

With lactide copolymers, the process-generated or melt-mixed lactide monomer significantly affects the material performance in a hydrolytic environment at 37 °C, as the rate of hydrolysis is dependent on the lactide monomer content. An important observation is that even small amounts of pre-hydrolysis lactide monomer have an effect in the long term especially on the polymer's mechanical properties and its degradation-induced increase in crystallinity.

The mechanical properties of oriented PLGA 85L/15G are maintained up to a specific molecular weight-dependent i.v.-range and then lost rapidly. Because the rate of the molecular degradation is dependent on the lactide monomer content, the time to this drop-zone can be predicted. This observation opens up a new possibility to control and program the degradation rate and enables the quality control of medical devices based on oriented PLGA 85L/15G. The same principle can be possibly applied with other lactide copolymers with similar hydrolytic degradation behavior, as well.

A water-induced shape-memory that is activated in an aqueous environment at 37 °C, without external energy, can be generated into amorphous PDLLA without chemical modifications by an orientation-programming process that generates a novel oriented and entangled structure for PDLLA. The tensional stress given to the PDLLA in the orientation-programming determines the stress generation and stress relaxation behavior when the shape-transformation is restricted in an aqueous environment at 37 °C. The trigger for this shape-memory is the combination of the effects of diffused water molecules in the polymer matrix and thermal activation by the physiological temperature.

The main phenomena affecting the molecular movements in an aqueous environment at the physiological temperature are caused by the disruption of the intermolecular dipole–dipole and/or hydrogen bonding of the orientation-programmed PDLLA chains due to the diffused water that further decreases the initiation of the T_g-range slightly below the physiological temperature. The γ-irradiation accelerates the shape-recovery by decreasing the enthalpy relaxation: the energy needed to finish the glass transition process, of $PDLLA_{OP}$. This novel shape-memory-function can be easily applied to increase the functionality and reliability of bioabsorbable fixation devices and ease of operation procedures.

References:

Ajioka M, Suizu H, Higuchi C, Kashima T. 1998. Aliphatic polyesters and their copolymers synthesized through direct condensation polymerization. Polym Degrad Stab 59:137-143.

Alteheld A, Feng Y, Kelch S, Lendlein A. 2005. Biodegradable, amorphous copolyester-urethane networks having shape-memory properties. Angew Chem Int Ed 44:1188-1192.

Andriano KP, Pohjonen T, Törmälä P. 1994. Processing and characterization of absorbable polylactide polymers for use in surgical implants. J Appl Biomater 5:133-140.

Bailey NA, Sandor M, Kreitz M, Mathiowitz E. 2002. Comparison of the enthalpic relaxation of poly(lactide-co-glycolide) 50:50 nanospheres and raw polymer. J Appl Polym Sci 86:1868-1872.

Behl M, Lendlein A. 2007a. Actively moving polymers. Soft Matter 3:58-67.

Behl M, Lendlein A. 2007b. Shape-memory polymers. Materials Today, 10:20-28.

Bendix D. 1998. Chemical synthesis of polylactide and its copolymers for medical applications. Polym Degrad Stab 59:129-135.

Bergsma JE, De Bruijn WC, Rozema FR, Bos RRM, Boering G. 1995a. Late degradation tissue response to poly(L-lactide) bone plates and screws. Biomaterials 16:25-31.

Bergsma JE, Rozema FR, Bos RRM, Boering G, De Bruijn WC, Pennings AJ. 1995b. In vivo degradation and biocompatibility study of in vitro pre-degraded as-polymerized polylactide particles. Biomaterials 16:267-274.

Blasi P, D'Souza SS, Selmin F, DeLuca PP. 2005. Plasticizing effect of water on poly(lactide-co-glycolide). J Control Release 108:1-9.

Böstman O, Pihlajamäki H. 2000. Clinical biocompatibility of biodegradable orthopaedic implants for internal fixation: A review. Biomaterials 21:2615-2621.

Braun B, Dorgan JR, Dec SF. 2006. Infrared spectroscopic determination of lactide concentration in polylactide: An improved methodology. Macromolecules 39:9302-9310.

Breitenbach J. 2002. Melt extrusion: from process to drug delivery technology. E J Pharm Biopharm 54:107-117.

Cam D, Marucci M. 1997. Influence of residual monomers and metals on poly (L-lactide) thermal stability. Polymer, 38:1879-1884.

Chen M-C, Tsai H-W, Chang Y, Lai W-Y, Mi F-L, Liu C-T, Wong H-S, Sung H-W. 2007. Rapidly self-expandable polymeric stents with a shape-memory property. Biomacromolecules 8:2774-2780.

Cicero JA, Dorgan JR, Garrett J, Runt J, Lin JS. 2002a. Effects of molecular architecture on two-step, melt-spun poly(lactic acid) fibers. J Appl Polym Sci 86:2839-2846.

Cicero JA, Dorgan JR, Janzen J, Garrett J, Runt J, Lin JS. 2002b. Supramolecular morphology of two-step, melt-spun poly(lactic acid) fibers. J Appl Polym Sci 86:2828-2838.

Cordewener FW, Rozema FR, Bos RRM, Boering G. 1995. Material properties and tissue reaction during degradation of poly (96L/4D-lactide) - A study in vitro and in rats. J Mater Sci Mater Med 6:211-217.

Dealy JM. 1999. Melt rheology and its role in plastics processingtheory and applications. Dordrecht:Kluwer Academic Publishers.

Edlund U, Albertsson A-C. 2003. Polyesters based on diacid monomers. Adv Drug Deliv Rev 55:585-609.

Eling B, Gogolewski S, Pennings AJ. 1982. Biodegradable materials of poly(L-lactic acid): 1. Melt-spun and solution-spun fibres. Polymer 23:1587-1593.

Ellä V, Gomes M, Reis R, Törmälä P, Kellomäki M. 2007. Studies of P(L/D)LA 96/4 non-woven scaffolds and fibres; properties, wettability and cell spreading before and after intrusive treatment methods. J Mater Sci Mater Med 18:1253-1261.

Ellä V, Nikkola L, Kellomäki M. 2010. Process-induced monomer on a medical-grade polymer and its effect on short-term hydrolytic degradation. J Appl Polym Sci .

Fambri L, Pegoretti A, Fenner R, Incardona SD, Migliaresi C. 1997. Biodegradable fibres of poly(L-lactic acid) produced by melt spinning. Polymer, 38:79-85.

Fan Y, Nishida H, Shirai Y, Endo T. 2004. Thermal stability of poly (L-lactide): Influence of end protection by acetyl group. Polym Degrad Stab 84:143-149.

Furukawa T, Matsusue Y, Yasunaga T, Shikinami Y, Okuno M, Nakamura T. 2000. Biodegradation behavior of ultra-high-strength hydroxyapatite/poly (L-lactide) composite rods for internal fixation of bone fractures. Biomaterials 21:889-898.

Giles HFJ, Wagner JRJ, Mount EM. 2005. Extrusion - The Definitive Processing Guide and Handbook:79-81.

Gogolewski S, Mainil-Varlet P. 1997. Effect of thermal treatment on sterility, molecular and mechanical properties of various polylactides. 2. Poly(L/D-lactide) and poly(L/DL-lactide). Biomaterials 18:251-255.

Gonçalves, CMB, Coutinho JAP, Marrucho IM. 2010. Optical properties. in: Auras RA, Lim L, Selke SEM, Tsuji H, editors. Poly(lactic acid): Synthesis, structures, properties, processing, and applications (Wiley Series on Polymer Engineering and Technology). New Jersey:John Wiley & Sons. p 97-112.

Guimaraes-Ferreira J, Gewalli F, David L, Maltese G, Heino H, Lauritzen C. 2002. Calvarial bone distraction with a contractile bioresorbable polymer. Plast Reconstr Surg 104:1325-1331.

Gupta AP, Kumar V. 2007. New emerging trends in synthetic biodegradable polymers - Polylactide: A critique. Eur Polym J 43:4053-4074.

Hancock BC, Zografi G. 1994. The relationship between the glass transition temperature and the water content of amorphous pharmaceutical solids. Pharmaceut Res 11:471-477.

Hancock BC, Shamblin SL, Zografi G. 1995. Molecular Mobility of Amorphous Pharmaceutical Solids Below Their Glass Transition Temperatures. Pharmaceut Res 12:799-806.

Herrera-Gómez A, Velázquez-Cruz G, Martín-Polo MO. 2001. Analysis of the water bound to a polymer matrix by infrared spectroscopy. J Appl Phys 89:5431-5437.

Hine PJ, Ward IM, Olley RH, Bassett DC. 1993. The hot compaction of high modulus melt-spun polyethylene fibres. J Mater Sci 28:316-324.

Höhne GWH, Hemminger WF, Flammersheim H-J. 2003. Differential scanning calorimetry, Second edition. Berlin:Springer-Verlag.

Honkanen PB, Kellomäki M, Lehtimäki MY, Törmälä P, Mäkelä S, Lehto MUK. 2003. Bioreconstructive joint scaffold implant arthroplasty in metacarpophalangeal joints: Short-term results of a new treatment concept in rheumatoid arthritis patients. Tissue Engineering 9:957-965.

Huang WM, Yang B, An L, Li C, Chan YS. 2005. Water-driven programmable polyurethane shape memory polymer: Demonstration and mechanism. Appl Phys Lett 86:114105.

Hutchinson JM, Smith S, Horne B, Gourlay GM. 1999. Physical aging of polycarbonate: enthalpy relaxation, creep response, and yielding behavior. Macromolecules 32:5046-5061.

Huttunen M, Törmälä P, Godinho P, Kellomäki M. 2008. Fiber-reinforced bioactive and bioabsorbable hybrid composites. Biomedical Materials 3.

Huttunen M, Ashammakhi N, Törmälä P, Kellomäki M. 2006. Fibre reinforced bioresorbable composites for spinal surgery. Acta Biomaterialia, 2:575-587.

Hyon S-H, Jamshidi K, Ikada Y. 1998. Effects of residual monomer on the degradation of DL-lactide polymer. Polym Int 46:196-202.

Hyon S-H, Jamshidi K, Ikada Y. 1997. Synthesis of polylactides with different molecular weights. Biomaterials 18:1503-1508.

Jacobsen S, Fritz H-G, Degée P, Dubois P, Jérôme R. 2000. New developments on the ring opening polymerisation of polylactide. Ind Crop Prod 11:265-275.

Jamshidi K, Hyon S-H, Ikada Y. 1988. Thermal characterization of polylactides. Polymer 29:2229-2234.

Jani MM, Silva MJ, Gregush RV, Matava MJ. 2004. Mechanical properties of bioabsorbable meniscal arrows as a function of tear location: An ex vivo experimental study. Am J Sports Med 32:666-674.

Joziasse CAP, Veenstra H, Grijpma DW, Pennings AJ. 1996. On the chain stiffness of poly(lactide)s. Macromol Chem Physic 197:2219-2229.

Juuti H, Kotsar A, Mikkonen J, Isotalo T, Talja M, Tammela TLJ, Törmälä P, Kellomäki M. 2012. The effect of pH on the degradation of biodegradable poly(L-lactide-co- glycolide) 80/20 urethral stent material in vitro. J Endourol 26:701-705.

Kellomäki M, Paasimaa S, Törmälä P. 2000a. Pliable polylactide plates for guided bone regeneration: Manufacturing and in vitro. Proc Inst Mech Eng Part H J Eng Med 214:615-629.

Kellomäki M, Törmälä P. 2003. Processing of resorbable poly- α-hydroxy acids for use as tissue-engineering scaffolds. In: Hollander AP, Hatton PV, editors. Methods in molecular biology, vol 238: Biopolymer methods in tissue engineering. Totowa, NJ:Humana Press Inc. p 1.

Kellomäki M, Pohjonen T, Törmälä P. 2003. Self Reinforced Polylactides. In: Arshady R, editor. Biodegradable Polymers. London:Citus Books. p 212.

Kellomäki M, Niiranen H, Puumanen K, Ashammakhi N, Waris T, Törmälä P. 2000b. Bioabsorbable scaffolds for guided bone regeneration and generation. Biomaterials, 21:2495-2505.

Kellomäki M, Puumanen K, Waris T, Törmälä P. 2000c. In vivo degradation of composite membrane of P(ε-CL/L-LA) 50/50 film and P(L/D)LA 96/4 mesh. Materials for Medical Engineering. p 79-85.

Kim BK, Lee SY, Xu M. 1996. Polyurethanes having shape memory effects. Polymer 37:5781-5793.

King E, Cameron RE. 1997. Effect of hydrolytic degradation on the microstructure of poly(glycolic acid): An X-ray scattering and ultraviolet spectrophotometry study of wet samples ultraviolet. J Appl Polym Sci 66:1681-1690.

Kricheldorf HR. 2001. Syntheses and application of polylactides. Chemosphere 43:49-54.

Kricheldorf HR, Lee S-R. 1995. Polylactones: 32. High-molecular-weight polylactides by ring-opening polymerization with dibutylmagnesium or butylmagnesium chloride. Polymer 36:2995-3003.

Landes C, Ballon A, Roth C. 2006a. Maxillary and Mandibular Osteosyntheses with PLGA and P(L/DL)LA Implants: A 5-Year Inpatient Biocompatibility and Degradation Experience. Plast Reconstr Surg 117:2347.

Landes CA, Ballon A, Roth C. 2006b. In-patient versus in vitro degradation of P(L/DL)LA and PLGA. J Biomed Mater Res - Part B Appl Biomat 76:403-411.

Lee SC, Han JI, Jeong YG, Kwon M. 2010. Strain-induced enthalpy relaxation in Poly(lactic acid). Macromolecules 43:25-28.

Lendlein A, Schmidt A, Langer R. 2001. AB-polymer networks based on oligo(ε-caprolactone) segments showing shape-memory properties. PNAS 98:842.

Lendlein A, Jiang H, Junger O, Langer R. 2005. Light-induced shape-memory polymers. Nature 434:879-882.

Lendlein A, Kelch S. 2002. Shape-memory polymers. Angew Chem Int Ed 41:2034-2057.

Lendlein A, Langer R. 2002. Biodegradable, elastic shape-memory polymers for potential biomedical applications. Science 296:1673-1676.

Leng J, Lv H, Liu Y, Du S. 2008. Comment on "water-driven programable polyurethane shape memory polymer: Demonstration and mechanism" [Appl. Phys. Lett. 86, 114105 (2005)]. Appl Phys Lett 92.

Li S, Garreau H, Vert M. 1990a. Structure-property relationships in the case of the degradation of massive poly(α-hydroxy acids) in aqueous media - Part 3 Influence of the morphology of poly(L-lactic acid). J Mater Sci Mater Med 1:198-206.

Li S, McCarthy S. 1999. Further investigations on the hydrolytic degradation of poly (DL-lactide). Biomaterials 20:35-44.

Li S, Vert M. 1994. Morphological changes resulting from the hydrolytic degradation of stereocopolymers derived from L- and DL-lactides. Macromolecules 27:3107-3110.

Li SM, Garreau H, Vert M. 1990b. Structure-property relationships in the case of the degradation of massive aliphatic poly-(α-hydroxy acids) in aqueous media - Part 1: Poly(dl-lactic acid). J Mater Sci Mater Med 1:123-130.

Li SM, Garreau H, Vert M. 1990c. Structure-property relationships in the case of the degradation of massive poly(α-hydroxy acids) in aqueous media - Part 2 Degradation of lactide-glycolide copolymers: PLA37.5GA25 and PLA75GA25. J Mater Sci Mater Med 1:131-139.

Li S. 1999. Hydrolytic degradation characteristics of aliphatic polyesters derived from lactic and glycolic acids. J Biomed Mater Res 48:342-353.

Lim L-T, Auras R, Rubino M. 2008. Processing technologies for poly(lactic acid). Prog Polym Sci 33:820-852.

Majola A. 1991. Fixation of experimental osteotomies with absorbable polylactic acid screws. Ann Chir Gynaecol 80:274-281.

Majola A, Vainionpää S, Rokkanen P, Mikkola H-M, Törmälä P. 1992. Absorbable self-reinforced polylactide (SR-PLA) composite rods for fracture fixation: strength and strength retention in the bone and subcutaneous tissue of rabbits. J Mater Sci Mater Med 3:43-47.

Malin M, Hiljanen-Vainio M, Karjalainen T, Seppälä J. 1996. Biodegradable lactone copolymers. II. Hydrolytic study of ε-caprolactone and lactide copolymers. J Appl Polym Sci 59:1289-1298.

Manninen MJ. 1993. Self-reinforced poly-L-lactide screws in the fixation of cortical bone osteotomies in rabbits. J Mater Sci Mater Med 4:179-185.

Matsuoka S, Bair HE. 1977. The temperature drop in glassy polymers during deformation. J Appl Phys 48:4058-4062.

Maurus PB, Kaeding CC. 2004. Bioabsorbable implant material review. Oper Techn Sport Med 12:158-160.

Metcalfe A, Desfaits A, Salazkin I, Yahia L, Sokolowski WM, Raymond J. 2003. Cold hibernated elastic memory foams for endovascular interventions. Biomaterials 24:491-497.

Mikkonen J, Uurto I, Isotalo T, Kotsar A, Tammela TLJ, Talja M, Salenius J-P, Törmälä P, Kellomäki M. 2009. Drug-eluting bioabsorbable stents – An in vitro study. Acta Biomaterialia 5:2894-2900

Min C, Cui W, Bei J, Wang S. 2007. Effect of comonomer on thermal/mechanical and shape memory property of L-lactide-based shape-memory copolymers. Polym Adv Technol 18:299-305.

Min C, Cui W, Bei J, Wang S. 2005. Biodegradable shape-memory polymer - Polylactide-co-poly(glycolide-co-caprolactone) multiblock copolymer. Polym Advan Technol 16:608-615.

Nagahama K, Ueda Y, Ouchi T, Ohya Y. 2009. Biodegradable shape-memory polymers exhibiting sharp thermal transitions and controlled drug release. Biomacromolecules 10:1789-1794.

Nakamura T, Hitomi S, Watanabe S, Shimizu Y, Jamshidi K, Hyon S-H, Ikada Y. 1989. Bioabsorption of polylactides with different molecular properties. J Biomed Mater Res 23:1115-1130.

Niemelä T. 2005. Effect of β-tricalcium phosphate addition on the in vitro degradation of self-reinforced poly-l,d-lactide. Polym Degrad Stab, 89:492-500.

Niiranen H, Pyhältö T, Rokkanen P, Kellomäki M, Törmälä P. 2004. In vitro and in vivo behavior of self-reinforced bioabsorbable polymer and self-reinforced bioabsorbable polymer/bioactive glass composites. J Biomed Mater Res Part A 69A:699-708.

Nordström P, Pohjonen T, Törmälä P, Rokkanen P. 2002. Shear-load carrying capacities of the distal rat femora after osteotomy fixed with self-reinforced polyglycolic acid and poly-L-lactic acid pins. J Mater Sci Mater Med 13:65-68.

Nuutinen J, Clerc C, Virta T, Törmälä P. 2002. Effect of gamma, ethylene oxide, electron beam, and plasma sterilization on the behaviour of SR-PLLA fibres in vitro. J Biomat Sci Polym Ed 13:1325-1336.

Oksanen CA, Zografi G. 1993. Molecular mobility in mixtures of absorbed water and solid poly(vinylpyrrolidone). Pharm Res 10:791-799.

Pan P, Zhu B, Inoue Y. 2007. Enthalpy relaxation and embrittlement of poly(L-lactide) during physical aging. Macromolecules 40:9664-9671.

Pegoretti A, Fambri L, Migliaresi C. 1997. In vitro degradation of poly(L-lactic acid) fibers produced by melt spinning. J Appl Polym Sci 64:213-223.

Peltoniemi HH, Tulamo R-M, Toivonen T, Hallikainen D, Törmälä P, Waris T. 1999. Biodegradable semirigid plate and miniscrew fixation compared with rigid titanium fixation in experimental calvarial osteotomy. J Neurosurg 90:910-917.

Penning JP, Dijkstra H, Pennings AJ. 1993. Preparation and properties of absorbable fibres from -lactide copolymers. Polymer, 34:942-951.

Perego G, Cella GD, Bastioli C. 1996. Effect of molecular weight and crystallinity on poly(lactic acid) mechanical properties. J Appl Polym Sci 59:37-43.

Pierce BF, Bellin K, Behl M, Lendlein A. 2011. Demonstrating the influence of water on shape-memory polymer networks based on poly[(rac-lactide)-co-glycolide] segments in vitro. Int J Artif Organs 34:172-179.

Pihlajamäki H, Böstman O, Manninen M, Päivärinta U, Rokkanen P. 1994. Tissue-implant interface at an absorbable fracture fixation plug made of polylactide in cancellous bone of distal rabbit femur. Arch Orthop Trauma Surg 113:101-105.

Pihlajamäki H, Böstman O, Tynninen O, Laitinen O. 2006a. Long-term tissue response to bioabsorbable poly-l-lactide and metallic screws: An experimental study. Bone 39:932-937.

Pihlajamäki H, Salminen S, Laitinen O, Tynninen O, Böstman O. 2006b. Tissue response to polyglycolide, polydioxanone, polylevolactide, and metallic pins in cancellous bone: An experimental study on rabbits. J Orthopaed Res 24:1597-1606.

Pirhonen E, Ellä V. 2008. Melt spinning. In: Wnek GE, Bowlin GL, editors. Encyclopedia of biomaterials and biomedical engineering. New York, USA: Informa Healthcare USA Inc. p 1816-1823.

Puffr R, Šebenda J. 1967. On the Structure and Properties of Polyamides. XXVII. The Mechanism of Water Sorption in Polyamides. J Polym Sci Part C: Polymer Symposia 16:79-93.

Ramchandani M, Pankaskie M, Robinson D. 1997. The influence of manufacturing procedure on the degradation of poly(lactide-co-glycolide) 85:15 and 50:50 implants. J Control Release 43:161-173.

Rault J. 2006. Aging of oriented polymer glasses. J Non Cryst Solids 352:4946-4955.

Rauwendaal C. 2001. Polymer extrusion. 4th ed. Cincinnati, OH: Hanser Gardner Publications.

Reed AM, Gilding DK. 1981. Biodegradable polymers for use in surgery — poly(glycolic)/poly(Iactic acid) homo and copolymers: 2. In vitro degradation. Polymer 22:494-498.

Rokkanen P. 2001. Bioabsorbable polymers for medical applications with an emphasis on orthopedic surgery. In: Dumitriu S, editor. Polymeric biomaterials, Second edition, Revised and expanded. NY, USA: Marcel Dekker Inc. p 545.

Rokkanen P, Böstman O, Vainionpää S, Vihtonen K, Törmälä P, Laiho J, Kilpikari J, Tamminmäki M. 1985. Biodegradable implants in fracture fixation: Early results of the treatment of fractures of the ankle. The Lancet 325:1422.

Rokkanen P, Böstman O, Hirvensalo E, Mäkelä E, Partio E, Pätiälä H, Vainionpää S, Vihtonen K, Törmälä P. 2000. Bioabsorbable fixation in orthopaedic surgery and traumatology. Biomaterials 21:2607-2613.

Saikku-Bäckström A, Tulamo R-M, Pohjonen T, Törmälä P, Räihä JE, Rokkanen P. 1999. Material properties of absorbable self-reinforced fibrillated poly-96L/4 D-lactide (SR-PLA96) rods; A study in vitro and in vivo. J Mater Sci Mater Med 10:1-8.

Schmack G, Jehnichen D, Vogel R, Tändler B, Beyreuther R, Jacobsen S, Fritz H-G. 2001. Biodegradable fibres spun from poly(lactide) generated by reactive extrusion. J Biotechnol 86:151-160.

Schmack G, Tändler B, Optiz G, Vogel R, Komber H, Häußler L, Voigt D, Weinmann S, Heinemann M, Fritz H-. 2004. High-speed melt spinning of various grades of polylactides. J Appl Polym Sci 91:800-806.

Schmack G, Tändler B, Vogel R, Beyreuther R, Jacobsen S, Fritz H-. 1999. Biodegradable fibers of poly(L-lactide) produced by high-speed melt spinning and spin drawing. J Appl Polym Sci 73:2785-2797.

Schwach G, Coudane J, Engel R, Vert M. 2002. Influence of polymerization conditions on the hydrolytic degradation of poly(DL-lactide) polymerized in the presence of stannous octoate or zinc-metal. Biomaterials 23:993-1002.

Shih C. 1995. Chain-end scission in acid catalyzed hydrolysis of poly(D,L-lactide) in solution. J Controll Release 34:9-15.

Shikinami Y, Okuno M. 1999. Bioresorbable devices made of forged composites of hydroxyapatite (HA) particles and poly-L-lactide (PLLA): Part I. Basic characteristics. Biomaterials 20:859-877.

Siemann U. 1985. The influence of water on the glass transition of poly(dl-lactic acid). Thermochim Acta 85:513-516.

Silverstein R, M., Webster F, X., Kiemle D. 2005. Spectrometric Identification of Organic Compounds. New York: John Wiley & Sons Inc.

Södergård A, Stolt M. 2002. Properties of lactic acid based polymers and their correlation with composition. Prog Polym Sci, 27:1123-1163.

Steendam R. 2005. Amylodextrin and poly(DL-lactide) oral controlled release matrix tablets; concepts for understanding their release mechanisms. Groningen: Stichting Drukkerij C. Regenboog.

Steendam R, van Steenbergen MJ, Hennink WE, Frijlink HW, Lerk CF. 2001. Effect of molecular weight and glass transition on relaxation and release behaviour of poly(-lactic acid) tablets. J Control Release 70:71-82.

Stoclet G, Seguela R, Lefebvre J-M, Rochas C. 2010. New insights on the strain-induced mesophase of poly(d, l-lactide): in situ WAXS and DSC study of the thermo-mechanical stability. Macromolecules 43:7228-7237.

Suuronen R. 1991. Comparison of absorbable self-reinforced poly-L-lactide screws and metallic screws in the fixation of mandibular condyle osteotomies: An experimental study in sheep. J Oral Maxillofac Surg 49:989-995.

Suuronen R, Pohjonen T, Hietanen J, Lindqvist C. 1998a. A 5-year in vitro and in vivo study of the biodegradation of polylactide plates. J Oral Maxillofac Surg 56:604-614.

Suuronen R, Pohjonen T, Hietanen J, Lindqvist C. 1998b. A 5-year in vitro and in vivo study of the biodegradation of polylactide plates. J Oral Maxillofac Surg 56:604-614.

Suuronen R, Pohjonen T, Taurio R, Törmälä P, Wessman L, Rönkkö K, Vainionpää S. 1992a. Strength retention of self-reinforced poly-L-lactide screws and plates: an in vivo and in vitro study. J Mater Sci Mater Med 3:426-431.

Suuronen R, Pohjonen T, Wessman L, Törmälä P, Vainionpää S. 1992b. New generation biodegradable plate for fracture fixation: comparison of bending strengths of mandibular osteotomies fixed with absorbable self-reinforced multi-layer poly-l-lactide plates and metallic plates - an experimental study in sheep. Clin Mater 9:77-84.

Tiainen J, Soini Y, Törmälä P, Waris T, Ashammakhi N. 2004. Self-reinforced polylactide/polyglycolide 80/20 screws take more than 1 1/2 years to resorb in rabbit cranial bone. J Biomed Mat Res - Part B Appl Biomat 70:49-55.

Törmälä P, Pohjonen T. 1995. Ultra-high strength bioabsorbable polymeric composites for surgical applications. In: Rokkanen P, Törmälä P, editors. Self-reinforced bioabsorbable polymeric composites in surgery. Tampere: Tampere University of Technology. p 1.

Törmälä P. 1992. Biodegradable self-reinforced composite materials; Manufacturing structure and mechanical properties. Clin Mater 10:29-34.

Törmälä P, Pohjonen T, Rokkanen P. 1998. Bioabsorbable polymers: Materials technology and surgical applications. Proc Inst Mech Eng Part H J Eng Med 212:101-111.

Törmälä P, Vainionpää S, Kilpikari J, Rokkanen P. 1987. The effects of fibre reinforcement and gold plating on the flexural and tensile strength of PGA/PLA copolymer materials in vitro. Biomaterials 8:42-45.

Tschakaloff A, Losken HW, von Oepen R, Michaeli W, Moritz O, Mooney MP, Losken A. 1994. Degradation kinetics of biodegradable dl-polylactic acid biodegradable implants depending on the site of implantation. Int J Oral Maxillofac Surg 23:443-445.

Tschoeke B, Flanagan TC, Koch S, Harwoko MS, Deichmann T, Ellä V, Sachweh JS, Kellomäki M, Gries T, Schmitz-Rode T, Jockenhoevel S. 2009. Tissue-engineered small-caliber vascular graft based on a novel biodegradable composite fibrin-polylactide scaffold. Tissue Engineering - Part A 15:1909-1918.

Tsuji H. 2002. Autocatalytic hydrolysis of amorphous-made polylactides: Effects of L-lactide content, tacticity, and enantiomeric polymer blending. Polymer 43:1789-1796.

Tsuji H, Fukui I. 2003. Enhanced thermal stability of poly(lactide)s in the melt by enantiomeric polymer blending. Polymer 44:2891-2896.

Tsuji H, Ikada Y. 2000. Properties and morphology of poly(L-lactide) 4. Effects of structural parameters on long-term hydrolysis of poly(L-lactide) in phosphate-buffered solution. Polym Degrad Stab 67:179-189.

Vainionpää S, Kilpikari J, Laiho J, Helevirta P, Rokkanen P, Törmälä P. 1987. Strength and strength retention vitro, of absorbable, self-reinforced polyglycolide (PGA) rods for fracture fixation. Biomaterials 8:46-48.

Van Nostrum CF, Veldhuis TFJ, Bos GW, Hennink WE. 2004. Hydrolytic degradation of oligo(lactic acid): A kinetic and mechanistic study. Polymer 45:6779-6787.

Venkatraman SS, Tan LP, Joso JFD, Boey YCF, Wang X. 2006. Biodegradable stents with elastic memory. Biomaterials 27:1573-1578.

Vert M, Chabot F. 1981. Stereoregular Bioabsorbable Polyesters for Orthopaedic Surgery. Makromol Chem Suppl 5.

Viljanen J, Pihlajamäki H, Kinnunen J, Bondestam S, Rokkanen P. 2001. Comparison of absorbable poly-L-lactide and metallic intramedullary rods in the fixation of femoral shaft osteotomies: An experimental study in rabbits. J Orthopaed Sci 6:160-166.

Viljanen JT, Pihlajamäki HK, Törmälä PO, Rokkanen PU. 1997. Comparison of the tissue response to absorbable self-reinforced polylactide screws and metallic screws in the fixation of cancellous bone osteotomies: An experimental study on the rabbit distal femur. J Orthopaed Res 15:398-407.

von Oepen R, Michaeli W. 1992. Injection moulding of biodegradable implants. Clin Mater 10:21-28.

Wache HM, Tartakowska DJ, Hentrich A, Wagner MH. 2003. Development of a polymer stent with shape memory effect as a drug delivery system. J Mater Sci Mater Med 14:109-112.

Wachsen O, Platkowski K, Reichert K-H. 1997. Thermal degradation of poly-L-lactide - studies on kinetics, modelling and melt stabilisation. Polym Degrad Stab 57:87-94.

Wang Y, Li Y, Luo Y, Huang M, Liang Z. 2009. Synthesis and characterization of a novel biodegradable thermoplastic shape memory polymer. Mater Lett 63:347-349.

Waris E, Ashammakhi N, Lehtimäki M, Tulamo R-M, Kellomäki M, Törmälä P, Konttinen YT. 2008. The use of biodegradable scaffold as an alternative to silicone implant arthroplasty for small joint reconstruction: An experimental study in minipigs. Biomaterials 29:683-691.

Weiler A, Reinhard MD, Hoffmann RFG, Stähelin AC, Helling H-J, Südkamp NP. 2000. Biodegradable implants in sports medicine: The biological base. Arthroscopy 16:305-321.

Weir NA, Buchanan FJ, Orr JF, Farrar DF, Boyd A. 2004. Processing, annealing and sterilisation of poly-L-lactide. Biomaterials, 25:3939-3949.

Williams DF. 1982. Biodegradation of surgical polymers. J Mater Sci 17:1233-1246.

Wischke C, Lendlein A. 2010. Shape-memory polymers as drug carriers-a multifunctional system. Pharm Res 27:527-529.

Wischke C, Neffe AT, Steuer S, Lendlein A. 2009. Evaluation of a degradable shape-memory polymer network as matrix for controlled drug release. J Control Release 138:243-250.

Wong YS, Stachurski ZH, Venkatraman SS. 2008. Orientation and structure development in poly(lactide) under uniaxial deformation. Acta Materialia 56:5083-5090.

Wong YS, Venkatraman SS. 2010. Recovery as a measure of oriented crystalline structure in poly(L-lactide) used as shape memory polymer. Acta Materialia 58:49-58.

Yang B, Huang WM, Li C, Li L. 2006. Effects of moisture on the thermomechanical properties of a polyurethane shape memory polymer. Polymer 47:1348-1356.

Yuan X, Mak AFT, Kwok KW, Yung BKO, Yao K. 2001. Characterization of poly(L-lactic acid) fibers produced by melt spinning. J Appl Polym Sci 81:251-260.

Zhang J, Duan Y, Sato H, Tsuji H, Noda I, Yan S, Ozaki Y. 2005. Crystal modifications and thermal behavior of poly(L-lactic acid) revealed by infrared spectroscopy. Macromolecules 38:8012-8021.

Zheng X, Zhou S, Li X, Weng J. 2006. Shape memory properties of poly(d,l-lactide)/hydroxyapatite composites. Biomaterials 27:4288-4295.

Zong X, Wang Z, Hsiao BS, Chu B, Zhou JJ, Jamiolkowski DD, Muse E, Dormier E. 1999. Structure and morphology changes in absorbable poly(glycolide) and poly(glycolide-co-lactide) during in vitro degradation. Macromolecules 32:8107-8114.

ORIGINAL PUBLICATIONS

Publication I

Paakinaho, K., Ellä, V., Syrjälä, S., Kellomäki, M.

Melt spinning of poly(L/D)lactide 96/4: Effects of molecular weight and melt processing on hydrolytic degradation

Polymer Degradation and Stability 94 (2009), pp. 438-442.

Polymer Degradation and Stability 94 (2009), pp. 438-442.

Melt-Spinning of Poly(L/D)lactide 96/4: Effects of Molecular Weight and Melt Processing on Hydrolytic Degradation

Paakinaho, K.[*1], Ellä, V. [1], Syrjälä, S.[2], Kellomäki, M. [1]*

[1]Deparment of Biomedical Engineering, Tampere University of Technology
Hermiankatu 12 B, P.O.Box 692, FI-33101 Tampere, Finland

[2]Department of Material Science, Tampere University of Technology
Korkeakoulunkatu 10, P.O.Box 527FI-33101 Tampere, Finland

**Corresponding author, Tel +358 40 849 0975; fax +358 3 3115 2250*
E-mail address: kaarlo.paakinaho@tut.fi,

Keywords: polylactide, degradation, molecular weight, melt-spinning, viscosity, monomer

Abstract

This study focused on determining the effects of molecular weight on the degradation of Polylactide 96L/4D in melt spinning and the effects of melt processing on hydrolytic degradation. Three polylactides with different inherent viscosities were melt-spun, and the fibres were studied *in vitro*. Results showed that during melt spinning high-molecular-weight polylactide degraded because polymer chains were subject to high shear stress and high melt temperatures, whereas a low-molecular-weight polylactide with low melt viscosity was not affected by melt processing. Most degradation occurred during the melting phase in the length of the extruder barrel. Lactide monomer, generated as the polymer degraded in the melt, significantly affected *in vitro* degradation such that the degradation rate was directly proportional to the lactide concentration of the polymer.

1. Introduction

Polylactides, which belong to the family of poly-α-hydroxy acids, constitute a biodegradable polymer family commonly used in medical applications. They are thermoplastic polyesters, whose polymer backbone is formed from lactic acid monomer units. The properties of the polymer enable production of different varieties of the material for various applications such as sutures, bone fixation devices, and tissue engineering scaffolds [1-5].

Polylactide fibres are well-functioning source material for production of biodegradable implants by means of common textile techniques [4,5] or for reinforcing polymer composites [6]. Different methods of spinning polylactide have been studied [7-9]; the studies have covered poly-L-lactide [10,11] as well as different lactide copolymers [12,13]. The copolymerization of lactide enantiomers affects the polymer's crystal structure, which with increasing crystallinity affects the polymer's melting temperature [12]. Reportedly, semicrystalline and amorphous polylactides also differ in their melt viscosity, the former having a higher melt viscosity than the latter [14].

Polylactides, as well as polyesters in general, are prone to thermal degradation. During melt processing, their molecular weight decreases due to the scission of polymer chains [15-17]. During melt processing, degradation increases because of moisture, residual monomers and oligomers, but especially because of residual catalytic metal components [15]. In a hydrolytic environment, the post-processing molecular weight is significant in light of the polymer's mechanical properties and its degradation time. The above are important factors in designing composite materials for a medical application, in which the initial strength and strength retention during healing are crucial, or for a tissue engineering scaffold to provide adequate support for seeded cells to grow.

Understanding the relationships between the factors affecting molecular degradation during melt processing helps produce advanced medical devices with suitable strength and degradation characteristics. Our objective was to study the melt spinning of various molecular-weight polylactides and the effects of melt processing on hydrolytic degradation *in vitro* after γ-irradiation.

2. Materials and methods

2.1 Materials

The polymers used in this study were medical grade P(L/D)LA 96/4 copolymers (PURAC Biochem bv) with inherent viscosities reported by the manufacturer of 2.18 dl/g (PLA22), 4.80 dl/g (PLA48), and 6.26 dl/g (PLA63). The residual monomer content of all polymers was <0.05 %.

2.2 Material characterization

The molecular weights (M_w, M_n), the calculated related values of polydispersity (PDI), and the intrinsic viscosity (i.v.) of the raw materials and produced fibres were determined by size exclusion chromatography (SEC), which was also used to monitor the rate of the fibres' hydrolytic degradation *in vitro*. Two parallel 150 µl samples with concentration of 0.1 weight-%, prepared in chloroform, were injected at a flow rate of 1.0 ml/min. The columns used for exclusion were a PLgel 5-µm Guard precolumn and two PLgel 5-µm mixed-C columns, manufactured by Polymer Laboratories, Amherst, USA. The detector (Waters 410 RI Differential Refractometer Detector), pump (Waters M515 HPLC-Pump), and auto-sampler (Waters 717P plus Autosampler) were manufactured by Waters Operating Corporation, Milford, USA. Universal Calibration was obtained for P(L/D)LA 96/4 ($k = 5.45 \times 10^{-4}$ dl/g, $a = 0.73$), and mean values of results were used.

Monomer determinations were performed in Lahti Research Laboratory (Lahti, Finland). The L-lactide content was measured using gas chromatography (DC8000, CE Instruments, Rodano, Italy) and an FI-detector after chloroform dilution. The measuring resolution was 0.02 %, and mean values of three parallel measurements were used to determine the monomer content of the processed fibres.

A rotational rheometer (Physica MCR-301, Anton Paar Ostfildern, Germany) was used to measure the viscosities of the three raw materials at four different temperatures, selected based on the processing temperatures of 220°C, 230°C, 240°C, and 250°C. A plate-plate geometry was used with a diameter of 25 mm and a gap size of 1 mm. Three parallel measurements were taken, and the mean values of the results were used.

2.3 Melt spinning

Before extrusion, the materials were dried in a vacuum heated to 100°C at a rate of 1°C/min, held there for 16 hours, and then allowed to cool to room temperature before use. Fibre spinning was done in a two-step melt spinning/hot-drawing process using a Gimac TR melt extruder with a screw diameter of 12 mm, an L/D of 24:1, and a screw geometry of 1:1.237, B.V.O (Gimac, Castronno, Italy). The extruder comprised six heating zones, the first three for the barrel, two for melt mixing and stabilizing, and one for the die. The extruder zone temperatures used for each material are shown in Table 1. Two different dies, 8-filament (single orifice diameter 0.4 mm) and 12-filament (single orifice diameter 0.2 mm), were used in melt spinning. Melt pressure was monitored during spinning with a melt pressure instrument in zone five (Dynisco pressure sensor, model TPT 484-7.5M-6/18-B379, Dynisco Instruments, USA). Extrusion was carried out in a nitrogen atmosphere and drawing in ambient laboratory conditions.

Table 1. Extruder zone temperatures [°C] for melt spinning

Fiber	Polymer	Barrel 1	Barrel 2	Barrel 3	Nozzle 1	Nozzle 2	Nozzle 3
F22	PLA22	170	180	190	205	222	240
F48	PLA48	200	215	235	253	265	268
F63	PLA63	200	215	230	255	270	275

For information on the effects of heat and shear stress on molecular degradation in the extruder barrel, three melt spinnings were done using the same parameters as in the original melt spinnings but with samples collected from the extracted screw. After the spinning stabilized, the die was removed, the screw was pushed out of the extruder barrel, and samples were collected immediately from screw pitches, that is, from the screw tip and from pitches 2, 4, 6, 7, 9, 12, and 15, as counted from screw tip to screw root. Immediately after harvesting, the samples were cooled in air flow and then analyzed by SEC.

2.4 γ-irradiation

After melt spinning and hot drawing, all specimens were γ-irradiated for sterility with a radiation dose of 25 kGy by a commercial supplier.

2.5 In vitro

To study the rate of hydrolytic degradation, fibres were placed in a phosphate buffer solution (PBS, 3.54 g/dm^3 Na_2HPO_4–0.755 g/dm^3 NaH_2PO_4–5.9 g/dm^3 NaCl buffered saline) at pH 7.40±0.05, and their degradation was monitored with tensile tests and SEC. Samples were incubated for 1, 2, 3, 4, 6, 8, 12, 16, and 24 weeks at 37°C. The buffer solution was changed fortnightly.

Tensile tests were run on the fibres to measure their tensile strength retention and to monitor indirectly their hydrolytic degradation (Instron 4411 Materials Testing Machine, Instron Ltd., High Wycombe, England). All tensile tests were run at ambient temperature with non-sterile and sterile fibres tested dry and fibres from *in vitro* specimens tested wet. The testing parameters were a grip distance of 50 mm, a load cell of 500 N, and a crosshead speed of 30 mm/min.

3. Results

3.1 Molecular degradation and monomer generation during melt spinning

The effects of melt spinning and gamma irradiation on M_n, M_w and i.v. are shown in Figure 1. The sample materials differed significantly in their thermal degradation: PLA22 showed no change in its molecular weights and i.v., whereas decreases in M_w and i.v. were 50 % and 34 % for PLA48 and 63 %

and 43 % for PLA63, respectively. Differences in molecular weight and i.v. after melt spinning were evened out in gamma irradiation, in which the decrease in M_w and i.v. in melt spun fibres was 73 % and 64 % for F22, 79 % and 71 % for F48, and 75 % and 66 % for F63, respectively. The molecular weights and i.v. of all specimens were nearly the same after both melt processing and sterilization despite the molecular weight and i.v. of the raw materials or melt-spun fibres. The L-lactide content of the melt-spun fibres was <0.02 w-% for F22, 0.09 w-% for F48, and 1.90 w-% for F63.

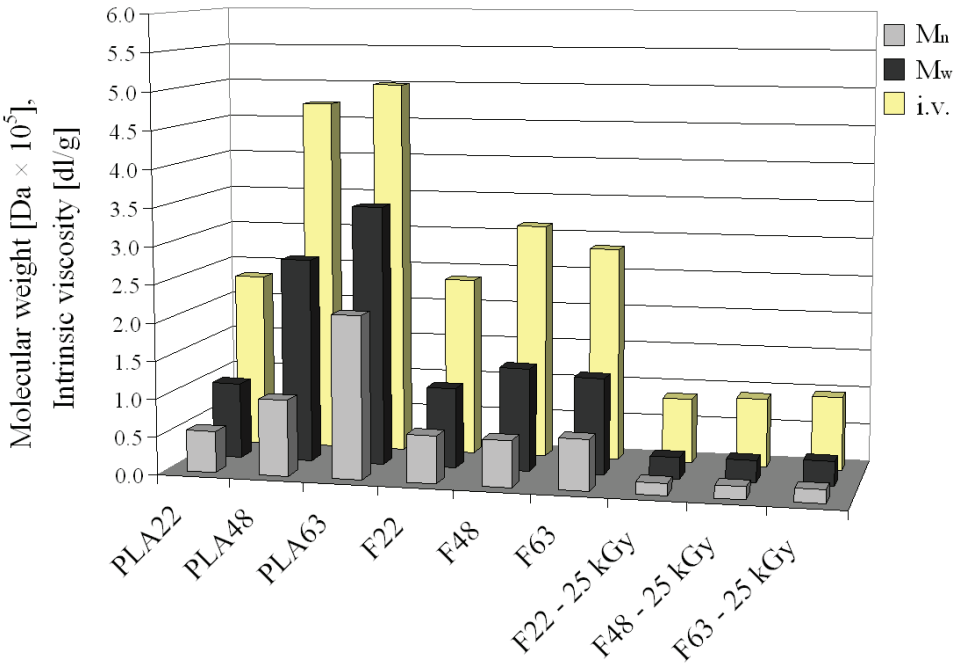

Figure 1. Effects of processing and sterilization on M_w, M_n and i.v., n=2.

3.2 Effects of shear stress and heat on molecular weight during extrusion

The effects of heat and shear stress on M_w and PDI in the length of the extruder barrel are shown in Figures 2 and 3. In the experiment, screw pitch 15, which is located immediately after the first heating zone in the extruder barrel, was the first pitch to yield molten polymer for sample harvesting. PLA48 and PLA63, which both degraded markedly during melt spinning, showed a gradual degradation profile in the extruder barrel. The M_w of both materials dropped to the beginning of the metering zone, after which virtually no further degradation took place in the length of the extruder barrel. The decrease in M_w between pitches 24 and 6 was 27% for PLA48 and 55% for PLA63. PLA22 did not show any degradation in the extruder.

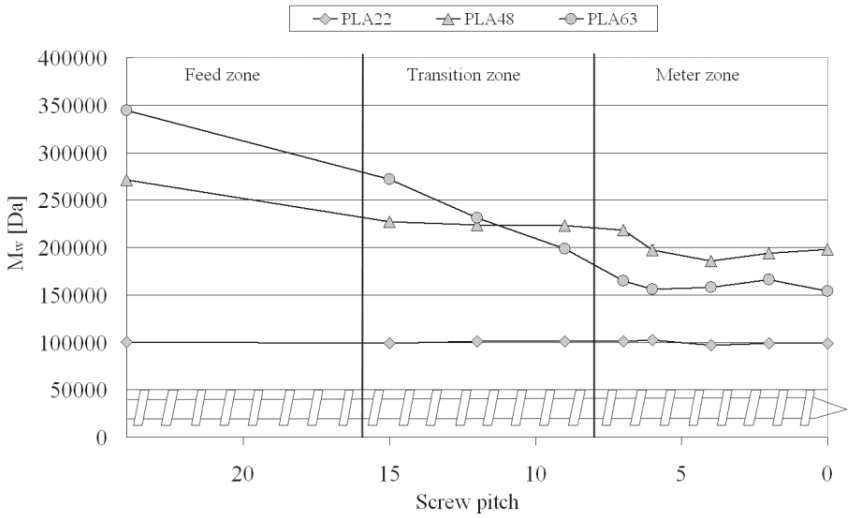

Figure 2. Schematic view of extruder screw and molecular degradation in extruder barrel during melt spinning, n=2.

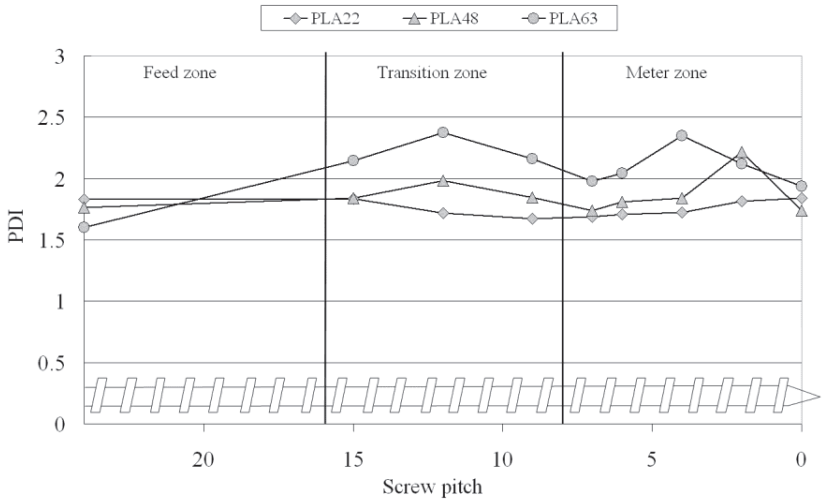

Figure 3. Schematic view of extruder screw and PDI changes in length of extruder barrel, n=2.

3.3 Viscosity and shear stress at extrusion temperatures

Figures 4-6 show viscosity results measured with a rotational rheometer. The three materials differed significantly in their melt viscosities and melt behaviour. PLA22 showed typical shear thinning behaviour, and its viscosities corresponded with the test temperatures. PLA48 and PLA63 were also

shear-thinning; however unlike PLA22, they did not reach their zero viscosity level at shear rates between 0.1–10.0 1/s. At 220°C and 230°C, their viscosities were so high that the test was interrupted because the rheometer reached its maximum torque. PLA48 and PLA63 showed similar melt viscosities at 240°C and 250°C with shear rates between 0.1–10.0 1/s. At higher shear rates, the viscosity of PLA48 started dropping more rapidly at 250°C than at 240°C, at which the viscosity slope was nearly linear. In rotational rheometric analysis with plate-plate or cone-plate geometries, polymer melts undergo various instabilities when shear velocity is increased, the so-called edge fracture being the most common [18]. It was thus impossible to gain reliable measurement data at high shear velocities (>10.0 1/s).

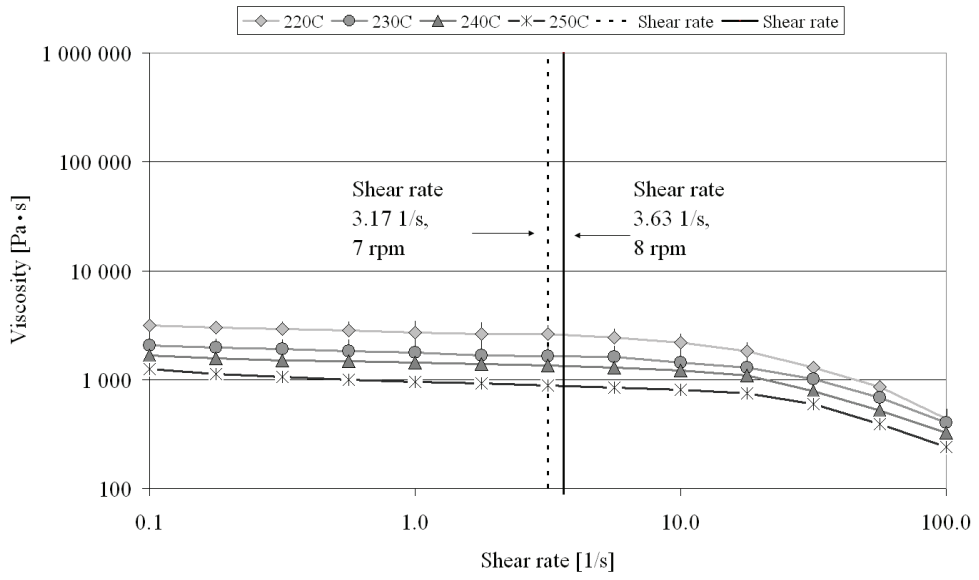

Figure 4. Viscosity at different temperatures of PLA22 on logarithmic scale, n=3.

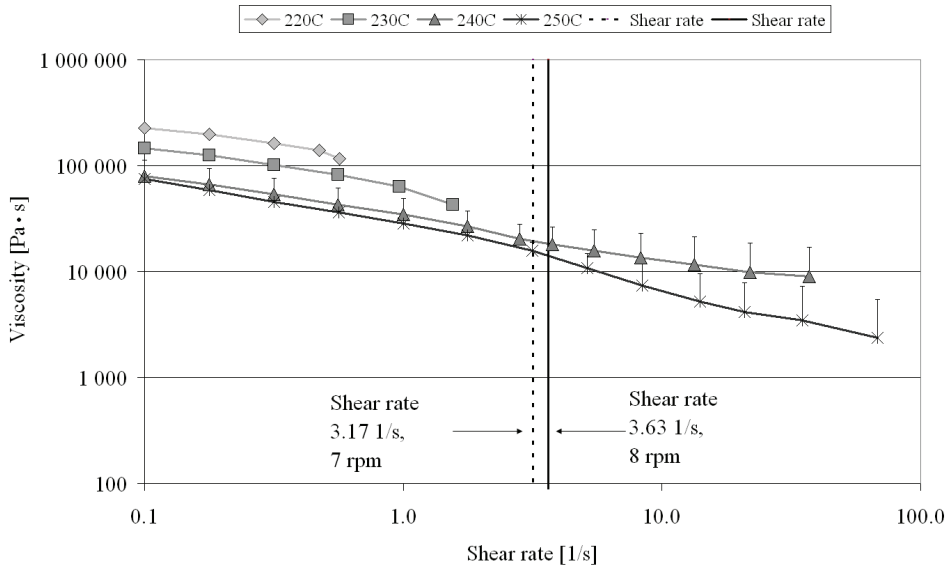

Figure 5. Viscosity at different temperatures of PLA48 on logarithmic scale, n=3.

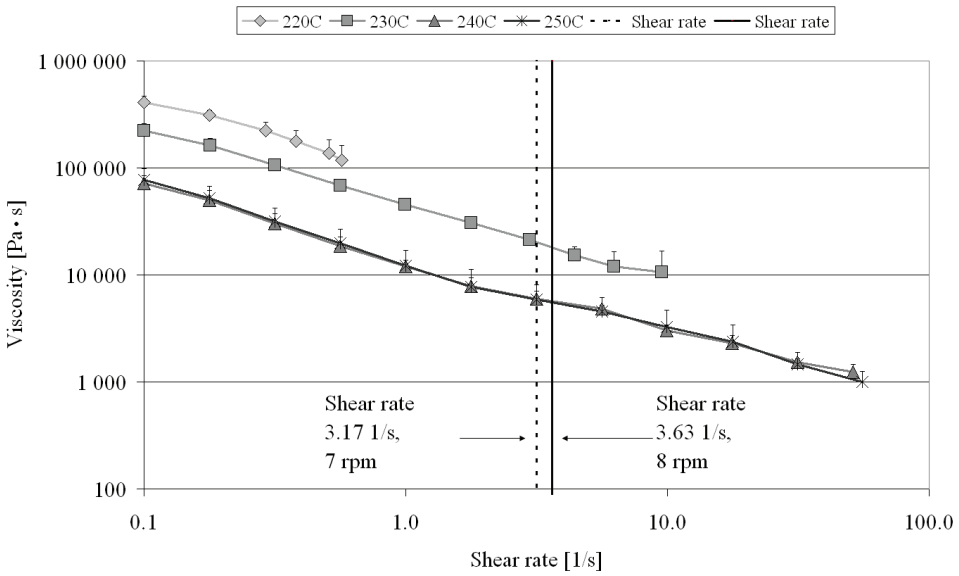

Figure 6. Viscosity at different temperatures of PLA63 on logarithmic scale, n=3.

With the flat plate approximation and assuming pure drag flow, the shear rate in the screw channel can be approximated by

$$\gamma = \frac{\pi D N}{h \times 60} \quad [19]$$

where:
γ = shear rate
N = screw revolution speed (rpm)
D = outer screw diameter
h = flight depth

The screw used in this study had the following dimensions: D = 11.9 mm, h = 1.375 mm (in the metering zone). With the screw revolutions (rpm) used in this study, it was possible to approximate shear rates: 3.17 1/s when N=7 (rpm) and 3.63 1/s when N=8 (rpm). Though the shear rate equation gives a mean, not an exact value, shear rates for melt-spinning all specimens can be used to approximate viscosities at test temperatures. Because the shear rate changes depending on the extruder screw section, it is reasonable to apply the equation in the metering zone of the screw. At the beginning of the screw, the non-molten material creates a much more complex situation, to which the equation does not apply.

3.4 Effects of hydrolytic degradation on molecular weight and strength retention

The effects of hydrolytic degradation on M_n and M_w are shown in Figure 7. The γ-irradiation levelled the differences between the molecular weights of melt-spun samples such that sample fibres had similar molecular weights at the beginning of the *in vitro* test series. Despite this similarity, the fibres differed significantly in their degradation behaviour. The most affected by the hydrolytic environment was F63, which degraded the most during melt spinning. During 24 weeks *in vitro*, the M_w loss of F63 was 84% whereas that of F48 was 61% and that of F22 only 10%. F63 lost most of its molecular weight (67%) in the first third of the *in vitro* period.

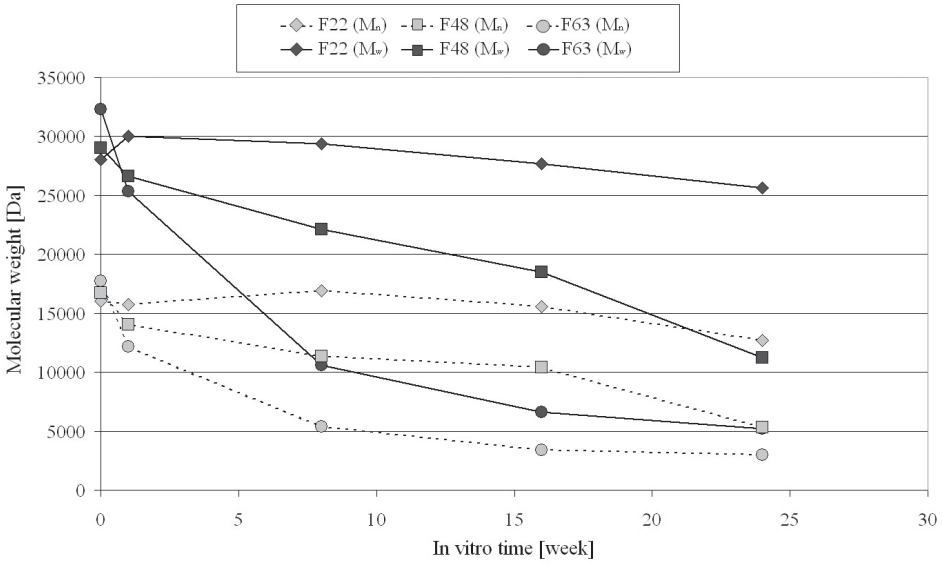

Figure 7. Effects of hydrolytic degradation on molecular weight, n=2.

Loss of tensile properties correlates well with loss of molecular weight (results of the tensile test given in Figure 8). F22 was the most stable, losing only 11% of its tensile strength over 24 weeks *in vitro*. F63 lost its tensile strength quite fast in the early weeks *in vitro*, and after 8 weeks the fibres could no more be tested for tensile strength because they had lost all their mechanical properties.

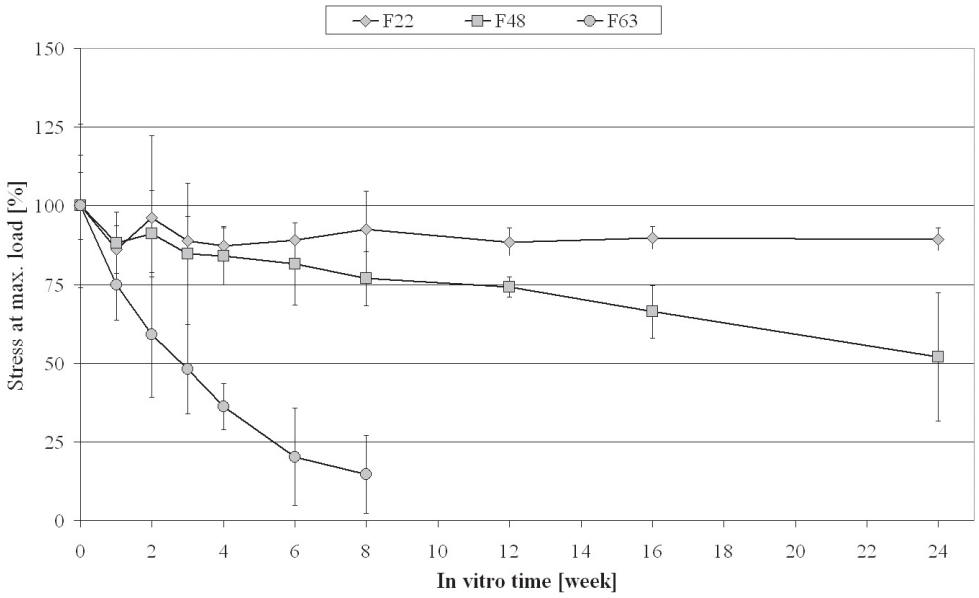

Figure 8. Effects of hydrolytic degradation on ultimate tensile strength, n=5.

4. Discussion

The P(L/D)LA 96/4 copolymers with different initial molecular weights showed different degradation characteristics during melt spinning so that the higher the initial molecular weight, the stronger the molecular degradation, with most degradation occurring in the length of the extruder barrel. In the extruder barrel, polymer chain degradation of PLA48 and PLA63 continued to the beginning of the meter zone, probably because of high shear stresses until the molecular weight was low enough to withstand the shearing of the screw. PLA22, which initially had a lower melt viscosity than PLA48 and PLA63, could withstand the shear stress and could also be melt-spun at lower temperatures than PLA48 and PLA63, and thus did not degrade in melt spinning. Earlier studies have reported a 50 % decrease in the i.v. of P(L/D)LA 96/4 with an i.v. of 4.21 dl/g in melt spinning [20], a 31 % decrease in the M_w of P(L/DL)LA 92/8 with an M_w of 16,400 Da [11], and a 68 % decrease in the viscometric molecular weight (M_v) of PLLA with an M_v of 330,000 Da [10].

Measurements made with the rotational rheometer testify to an interdependency between molecular weight and melt viscosity. Viscosities measured at shear rates used in the melt spinning of PLA48 and PLA63 were high compared to PLA22. In addition, viscosities decreased nearly linearly for PLA48 and PLA63, whereas PLA22 with its significantly lower viscosity showed typical shear-thinning behaviour, similar to that in [7]. The decrease of viscosity during the rotational rheometric analysis of PLA48 and PLA63 may have resulted from molecular chain degradation caused by interaction of high temperatures (240-250°C) and shear stress or from an edge fracture in the polymer melt during measurements inflicting an error into the analysis [21].

With the used melt-spinning parameters, the shear stress affecting the polymer in the first third of the extruder barrel length caused significant molecular degradation in PLA48 and PLA63. These polymers continued degrading molecularly until their molecular weights dropped so that the melt viscosity was probably low enough to halt the degradation caused by the shearing action of the screw in the extruder barrel. The melt-spinning of high-molecular-weight polylactides (PLA48 and PLA63) required significantly higher extruder temperatures than that of the low-molecular-weight polylactide (PLA22) to reach a low enough viscosity for melt-spinning to proceed. However, high extruder temperatures combined with high shear stress generated more lactide monomer on PLA48 (0.09 %) and PLA63 (1.9 %).

The varying effects of γ-irradiation on the fibres evened out the differences in their molecular weight after melt spinning. The radiation caused more molecular degradation in F48 and F63, which had higher molecular weights after melt spinning, than in F22. In [5], the decrease in the M_w of P(L/D)LA 96/4 in γ-irradiation (25 kGy) was reported as 73 %, and in [22] the decrease in the intrinsic viscosity of PLLA was 62 %. In both melt spinning and γ-irradiation (25 kGy), molecular degradation was reportedly 70 % in [20] and the decrease in i.v. ~80 % in [23] and 81 % in [24]. The variation between fibres used in this study and in the references [5,22] could be explained by the inaccuracy of the γ-irradiation process.

Melt-spun fibres showed different hydrolytic degradation behaviour *in vitro*, though tested fibres had nearly the same M_w and PDI before the *in vitro* test; the difference between the maximum and minimum in the M_w of melt-spun and γ-irradiated fibres was 1.7 % of that of the raw material. Similar behaviour has also been reported in [25], where the degradation rate of fibres melt-spun with different extruders showed significantly different degradation profiles regardless of their similar molecular weight and PDI before *in vitro* testing. Noteworthy in this study was that the lactide monomer content of the melt-spun fibres differed significantly with the monomer content ranging from <0.02 % to 1.9 %. In the 24-week *in vitro* study, the monomer content had a markedly increasing effect on the hydrolytic degradation rate, the drop in molecular weight (M_w) being 84 % for F63 (monomer content 1.9 %), 61 % for F48 (monomer content 0.09 %), and only 9 % for F22 (monomer content <0.02 %). The angle of the molecular weight slope is apparently linked with the lactide monomer content of the polymer so that the higher the monomer content, the steeper the slope of degradation. Earlier studies [26,27] have reported effects of residual monomer content on polylactide degradation but focused on demonstrating the importance of polymer purity on the performance of the material. However, in this study, lactide monomer was generated into purified polymer via thermal degradation in melt processing.

The 12-week *in vitro* strength retentions of the melt spun and γ-irradiated fibres were 88 % for F22 and 74 % for F48, which are better than or similar to those in [5] or [24], in which P(L/D)LA 96/4 fibres and yarns maintained 75 % and ~50 % , respectively, of their initial ultimate tensile strength during hydrolysation over 13 weeks. In this study, the molecular degradation rate of F48 was closest to the

fibres in [5] despite its lower initial molecular weight (M_w). Results similar to those for F22 and F63 on mechanical properties *in vitro* were achieved in [25], where fibres maintained ~80 % of their initial strength while their M_w dropped ~30 % during a 24-week *in vitro* period, or the fibres lost their mechanical properties after 8 weeks after their M_w had dropped ~75 %.

As generally understood, mechanical properties are related to the molecular weight of the polymer, but with thermally unstable and biodegradable fibres there are also other remarkable factors influencing, like monomer content. Strength retention *in vitro* can be controlled by controlling the degradation rate, which is likely to be related to the lactide monomer content of melt-processed polylactide. The higher the monomer content, the more rapidly molecular weight and mechanical properties decline.

5. Conclusions

The rheological properties of polylactide significantly affect its degradation in melt processing in terms of molecular weight and monomer generation, which markedly affect material properties *in vitro*. By studying the relationships between melt temperature and shear stress, we can better understand the degradation behaviour of a polymer in melt processing. In addition, the thermally generated lactide monomer may offer interesting possibilities to control the hydrolytic degradation rate of polylactide.

Acknowledgements

The authors appreciate the research funding received from the European Commission (Biosys: Intelligent Biomaterial Systems for Cardiovascular Tissue Repair, STRP 013633). We would also like to thank Eira Lehtinen and Sanna Siljander for their help during this work.

References:

1. Mäkelä P, Pohjonen T, Törmälä P, Waris T, Ashammakhi N. Strength retention properties of self-reinforced poly L-lactide (SR-PLLA) sutures compared with polyglyconate (Maxon®) and polydioxanone (PDS) sutures. An in vitro study. Biomaterials 2002; 23:2587-2592.
2. Saikku-Bäckström A, Tulamo R-M, Räihä JE, Kellomäki M, Toivonen T, Törmälä P, Rokkanen P. Intramedullary fixation of cortical bone osteotomies with absorbable self-reinforced fibrillated poly-96/4-lactide (SR-PLA96) rods in rabbits. Biomaterials 2001; 22:33-43.
3. Rokkanen PU, Böstman O, Hirvensalo E, Mäkelä EA, Partio EK, Pätiälä H, Vainionpää S, Kimmo Vihtonen, Törmälä P. Bioabsorbable fixation in orthopaedic surgery and traumatology. Biomaterials 2000; 21:2607-2613.
4. Kellomäki M, Niiranen H, Puumanen K, Ashammakhi N, Waris T, Törmälä P. Bioabsorbable scaffolds for guided bone regeneration and generation. Biomaterials 2000; 21:2495-2505.

5. Ellä V, Gomes M, Reis R, Törmälä P, Kellomäki M. Studies of P(L/D)LA 96/4 non-woven scaffolds and fibres; properties, wettability and cell spreading before and after intrusive treatment methods. J Mater Sci Mater Med 2007; 18:1253-1261.
6. Huttunen M, Ashammakhi N, Törmälä P, Kellomäki M. Fibre reinforced bioresorbable composites for spinal surgery. Acta Biomaterialia 2006; 2:575-587.
7. Schmack G, Tändler B, Optiz G, Vogel R, Komber H, Häußler L, Voigt D, Weinmann S, Heinemann M, Fritz H-. High-speed melt spinning of various grades of polylactides. J Appl Polym Sci 2004; 91:800-806.
8. Schmack G, Jehnichen D, Vogel R, Tändler B, Beyreuther R, Jacobsen S, Fritz H-. Biodegradable fibres spun from poly(lactide) generated by reactive extrusion. Journal of Biotechnology 2001; 86:151-160.
9. Gupta B, Revagade N, Anjum N, Atthoff B, Hilborn J. Preparation of poly(lactic acid) fiber by dry-jet-wet spinning. II. Effect of process parameters on fiber properties. J Appl Polym Sci 2006; 101:3774-3780.
10. Fambri L, Pegoretti A, Fenner R, Incardona SD, Migliaresi C. Biodegradable fibres of poly(L-lactic acid) produced by melt spinning. Polymer 1997; 38:79-85.
11. Schmack G, Tändler B, Vogel R, Beyreuther R, Jacobsen S, Fritz H-. Biodegradable fibers of poly(L-lactide) produced by high-speed melt spinning and spin drawing. J Appl Polym Sci 1999; 73:2785-2797.
12. Andriano KP, Pohjonen T, Törmälä P. Processing and characterization of absorbable polylactide polymers for use in surgical implants. Journal of Applied Biomaterials 1994; 5:133-140.
13. Penning JP, Dijkstra H, Pennings AJ. Preparation and properties of absorbable fibres from L-lactide copolymers. Polymer 1993; 34:942-951.
14. Fang Q, Hanna MA. Rheological properties of amorphous and semicrystalline polylactic acid polymers. Industrial Crops and Products 1999; 10:47-53.
15. Cam D, Marucci M. Influence of residual monomers and metals on poly (L-lactide) thermal stability. Polymer 1997; 38:1879-1884.
16. Kopinke F.-D, Remmler M, Mackenzie K, Möder M, Wachsen O. Thermal decomposition of biodegradable polyesters—II. Poly(lactic acid). Polymer Degradation and Stability 1996; 53:329-342.
17. Wachsen O, Platkowski K, Reichert K.-H. Thermal degradation of poly-L-lactide—studies on kinetics, modelling and melt stabilisation. Polymer Degradation and Stability 1997; 57:87-94.
18. Mall-Gleissle SE, Gleissle W, McKinley GH, Buggisch H. The normal stress behaviour of suspensions with viscoelastic matrix fluids. Rheologica Acta 2002; 41:61-76.
19. Giles, Harold F. Jr., Wagner, John R. Jr., Mount E, M. Extrusion - The Definitive Processing Guide and Handbook. William Andrew 2005. p. 79-81.
20. Kellomäki M, Puumanen K, Waris T, Törmälä P. *In vivo* degradation of composite membrane of P(ε-CL/L-LA) 50/50 film and P(L/D)LA 96/4 mesh. Materials for Medical Engineering 2000. p. 79-85.
21. Dealy JM. Melt Rheology and its Role in Plastics Processing Theory and Applications. Dordrecht: Kluwer Academic Publishers, 1999.

22. Nuutinen J, Clerc C, Virta T, Törmälä P. Effect of gamma, ethylene oxide, electron beam, and plasma sterilization on the behaviour of SR-PLLA fibres in vitro. Journal of Biomaterials Science. Polymer Edition 2002; 13:1325-1336.
23. Kellomäki M, Paasimaa S, Törmälä P. Pliable polylactide plates for guided bone regeneration: Manufacturing and in vitro. Proc Inst Mech Eng Part H J Eng Med 2000; 214:615-629.
24. Honkanen PB, Kellomäki M, Lehtimäki MY, Törmälä P, Mäkelä S, Lehto MUK. Bioreconstructive Joint Scaffold Implant Arthroplasty in Metacarpophalangeal Joints: Short-Term Results of a New Treatment Concept in Rheumatoid Arthritis Patients. Tissue Engineering 2003; 9:957-965.
25. Kellomäki M. Bioabsorbable and Bioactive Polymers and Composites for Tissue Engineering Applications. Tampere: TUT 2000. p. 68-69.
26. Kellomäki M, Pohjonen T, Törmälä P. Self reinforced polylactides. In: Arshady R, ed. Biodegradable Polymers London: Citus Books, 2003. 212.
27. Hyon S.-H, Jamshidi K, Ikada Y. Effects of residual monomer on the degradation of DL-lactide polymer. Polym Int 1998; 46:196-202.

Publication II

Paakinaho, K., Heino, H., Väisänen, J., Törmälä, T., Kellomäki, M.

Effects of lactide monomer on the hydrolytic degradation of poly(lactide-co-glycolide) 85L/15G

Journal of the Mechanical Behavior of biomedical Materials 4 (2011), pp. 1283-1290

Journal of the Mechanical Behavior of Biomedical Materials 4 (2011), pp. 1283-1290

Effects of lactide monomer on the hydrolytic degradation of poly(lactide-co-glycolide) 85L/15G

Paakinaho, K.[a,*], Heino, H.[a, b], Väisänen, J.[a], Törmälä, P. [b], Kellomäki, M.[a]

[a]*Department of Biomedical Engineering, Tampere University of Technology, Hermiankatu 12, P.O. Box 692, FI-33101 Tampere, Finland*

[b]*Bioretec Ltd, P.O. Box 135, 33721, Tampere, Finland*

**Corresponding author:* Kaarlo Paakinaho, kaarlo.paakinaho@tut.fi

Abstract

The hydrolytic degradation of oriented poly(L-lactide-co-glycolyde) 85L/15G (PLGA 85/15) sample materials with various amounts of lactide monomer was monitored *in vitro* at 37°C. The materials were manufactured from medical grade PLGA 85/15 by a two-step melt extrusion-die drawing process. Results showed that the hydrolytic degradation rate depended highly on the lactide monomer content, which in turn influenced the retention of mechanical properties, mass loss, crystallinity, and dimensional stability. Even small quantities of lactide monomer (0.05 – 0.20 wt-%) affected especially the retention of mechanical properties, which started to decline rapidly upon the inherent viscosity reaching 0.6-0.8 dl/g due to hydrolytic degradation. Based on our hydrolytic degradation data, we constructed a simplified mathematical model of degradation-related strength retention and recommend it as a functional quality control tool for melt-processed biodegradable medical devices manufactured from poly(L-lactide-co-glycolyde) 85L/15G.

1. Introduction

Used successfully since the 1980s [1], polylactide and its copolymers are currently the most common bioabsorbable polymers for medical devices. They are hydrolytically degradable polymers with significant advantages over non-absorbable materials for medical devices, because they need not be surgically removed as their degradation products are absorbed by the human body [2, 3, 4].

Melt processing methods such as extrusion or injection molding are commonly used to process polymers in the manufacture of bioabsorbable medical devices. At their best, these processes enable production of well functioning medical devices [2, 3, 5, 6, 7, 8] without harmful chemicals and allow addition of medically beneficial components such as osteoconductive ceramics [7, 9, 10, 11] or antibiotics [12] in multifunctional medical materials. Despite today's high quality of medical grade polylactides as raw material, a limiting factor in melt processing is these polyesters' molecular degradation due to their thermal instability. During processing, factors such as melt temperature and polymer molecular weight affect their degradation [13, 14, 15].

For use in medical devices, processed polylactide and its copolymers must be of high quality, functional, and predictable in their hydrolytic degradation. Regardless of how polylactide copolymers are processed and whether the device used is a bioabsorbable screw or a scaffold in tissue engineering, the end-products must perform as specified in the physiological environment. In addition to the commonly accepted factors of temperature, crystallinity, and polymer molecular weight, also residual [16-18] and thermally generated lactide monomer [13, 14] have been reported as affecting these materials' hydrolytic degradation. Thus it is essential to know the effects of melt processing on hydrolytic degradation.

Because melt processing-induced variations in hydrolytic degradation, such as degradation rate and morphological changes, may significantly affect the performance of bioabsorbable medical devices, the effect of degradation products formed during melt processing should be studied in detail to ensure high and sustainable quality of the processed materials. The objective of this study was to monitor and measure the effects of lactide monomer on the hydrolytic degradation of poly(lactide-co-glycolide) 85L/15G after melt extrusion and γ-irradiation.

2. Materials and Methods

2.1. Melt processing and die drawing

Seven extrusion trials were carried out using medical grade poly(L-lactide-co-glycolide) 85L/15G (PLGA 85/15) (LG 857 S, Boehringer Ingelheim Pharma GmbH & Co. KG, Ingelheim am Rhein, Germany) to produce biodegradable specimens with various grades of lactide monomer (Table 1). The inherent viscosity (i.v.) of the polymer raw material ranged from 5.5 to 6.1 dl/g, and the measured residual lactide monomer concentration was < 0.02 wt-%. Melt extrusions were performed using vacuum dried polymer granules by a co-rotating twin screw extruder (Mini ZE

20*11.5 D, Neste Oy, Porvoo Finland) under nitrogen atmosphere. Sample material was melt extruded into 3.1 ± 0.1 mm (extrusions 1-4) and 6.1 ± 0.1 mm (extrusion 5-7) round rods. In extrusions 1-4, low lactide monomer content was thermally produced in the samples, whereas in extrusions 5-7, L-lactide (L-lactide S, Boehringer Ingelheim Pharma GmbH & Co. KG, Ingelheim am Rhein, Germany) was added as a 4 wt-% premix to PLGA 85/15 granules before feeding them into the extruder to produce high monomer level specimens. The extruded rods were die-drawn into grooved shape according to the procedure described in [19] with a maximum diameter of 1.60 ± 0.04 mm (extrusion 1-4) and 3.4 ± 0.04 mm (extrusion 5-7). After die drawing, the samples were gamma irradiated for sterility with a radiation dose of a minimum of 25 kGy by Gamma-Service Produktbestrahlung GmbH, Radeberg, Germany.

Table 1. Extrusion batch material properties

Extrusion batch	Inherent viscosity (Raw material) [dl/g], n = 3	Inherent viscosity (Extruded) [dl/g], n= 3	Inherent viscosity (γ-irradiated) [dl/g], n= 3	Extrusion melt temperature [°C]	L-lactide content (Residual monomer, RM) [wt-%], n = 2	Melting enthalpy (γ-irradiated) [J/g], n =3
1. RM003*	5.5	3.9	1.3	210	0.03 ± 0.01	2.7 ± 0.8
2. RM005*	5.5	2.7	1.2	256	0.05 ± 0.01	6.2 ± 4.5
3. RM010*	5.5	2.4	1.1	260	0.10 ± 0.01	3.3 ± 2.1
4. RM020*	6.1	2.8	1.2	262	0.20 ± 0.01	3.1 ± 1.3
5. RM200**	6.1	3.7	1.6	210	2.0 ± 0.1	4.8 ± 1.8
6. RM300**	6.1	4.3	1.6	210	3.0 ± 0.1	n.a.
7. RM400**	6.1	4.4	1.6	210	4.0 ± 0.1	5.7 ± 0.9
RM% < 0.02, D=2.7 mm	6.5	4.0	1.5	210	< 0.02	1.2 ± 0.5
RM% < 0.02, D=3.2 mm	6.5	4.2	1.5	210	< 0.02	2.9 ± 1.9

* Lactide monomer - thermally generated
** Lactide monomer - added as a premix (4.0 wt-%)
Deviation for inherent viscosity analysis ± 0.05 dl/g (equipment derived deviation)
Sample series D = 2.7 mm and D = 3.2 mm with no measurable amount of lactide monomer are included as reference meterial

2.2. Material characterization

After extrusion, samples were measured for their lactide monomer content with a gas chromatograph (DC8000, CE Instruments, Rodano, Italy) and an FI-detector after chloroform dilution at a measuring resolution of 0.02 wt-% (Rambol Analytics Oy, Lahti, Finland). The decrease of i.v. during melt extrusion was measured by viscometric analysis (Lauda PSV1, Lauda-Königshofen, Germany) with Ubbelohde capillars (Schott-Instrument, Mainz, Germany) in chloroform at 25°C.

2.3. Hydrolysis degradation studies

To study hydrolytic degradation and its effect on the material properties *in vitro*, the samples were placed in 37°C Sörensen buffer solution, and their degradation was monitored by viscometric analysis up to 52 weeks and with shear strength tests, three-point bending tests, (Lloyd 2000S, Lloyd Instruments Ltd., Fareman, Hampshire, UK), and mass loss measurements up to 26 weeks.

Shear strength and bending tests were performed in an aqueous environment at 37°C. The percentage mass loss was calculated from the following equation:

mass loss [% from initial] = 100% - [(initial weight – tested dry weight) / initial weight] × 100%.

Changes in the buffer solution pH were monitored weekly, and the pH was maintained in the range of 7.4 ± 0.2. Degradation-mediated crystallization, measured as change in melting enthalpy, was monitored with a differential scanning calorimeter (DSC) (DSC Q1000, TA Instruments, New Castle, Delaware, USA). Analyses were performed with 5 to 10 mg vacuum dried samples in a temperature range from 10 to 200°C with a heating rate of 20°C/min. In the analysis the sum of the enthalpies of cold crystallization and melting was used. Structural and dimensional changes in the oriented polymer matrix were monitored by measuring the samples' maximum length and diameter and by using a scanning electron microscope (SEM) (Jeol JSM-T1000, Tokyo, Japan) with selected samples. SEM samples were frozen in liquid nitrogen and broken along their longitudinal axis, and the fracture surface was used for SEM imaging. Release of lactide monomer from the polymer matrix in the 37°C aqueous environment was measured from samples containing 2.0 to 4.0 wt-% of lactide monomer.

3. Results

3.1. Melt extrusion and γ-irradiation

Table 1 shows the results on the production of melt-extruded PLGA 85/15 specimens with various amounts of lactide monomer, generated either thermally or by melt-mixing. The melt temperatures applied correlate well with the monomer content; the higher the melt temperature, the higher the amount of lactide monomer and the more significant the drop in inherent viscosity. Premixing lactide monomer with PLGA 85/15 granules resulted in higher post-processing-inherent viscosities over thermally generating lactide monomer, due to lower melt temperatures. The relative decreases in inherent viscosities due to γ-irradiation were 67% (RM003), 57% (RM005), 53% (RM010), 59% (RM020), 58% (RM200), 63% (RM300), and 64% (RM400). In addition, γ-irradiation evened out the post-processing i.v. values of the sample materials such that the difference between their maximum (RM400, 4.4 dl/g) and minimum (RM010, 2.4 dl/g) dropped by 78 % (RM400, 1.58 dl/g and RM010, 1.14 dl/g).

3.2. Effects of lactide monomer on molecular degradation, mechanical properties, and mass loss in vitro

The decrease in molecular-weight-dependent inherent viscosities at 37°C *in vitro* of melt processed and γ-irradiated sample materials, shown in Figure 1, testifies to a significant effect of lactide monomer on the degradation rate of PLGA 85/15. For all sample materials, the decrease in i.v. appeared linear as far as the critical 0.4-0.2 dl/g, after which the degradation rate slowed down

significantly, leveling at 0.1 dl/g for up to 52 weeks. The effect of lactide monomer on the degradation rate of PLGA 85/15 is clearly evident in comparing low-monomer (RM003-RM020) and high-monomer samples (RM200-RM400). However, even small amounts of lactide monomer (e.g., 0.20 wt-%) affected the degradation rate: specimens with a low monomer content (RM003-RM020) took 6 to 14 weeks to reach 0.8 dl/g and 10 to 18 weeks to reach 0.6 dl/g, depending on their lactide monomer content and initial inherent viscosity (see Figure 2 for the linear section of the i.v. curves and linear regression curves). The linear parts of the curves were calculated by using data points up to 0.6 dl/g plus the following two data points. Samples RM300 and RM400 show a similar degradation rate regardless of a significant difference in their monomer contents.

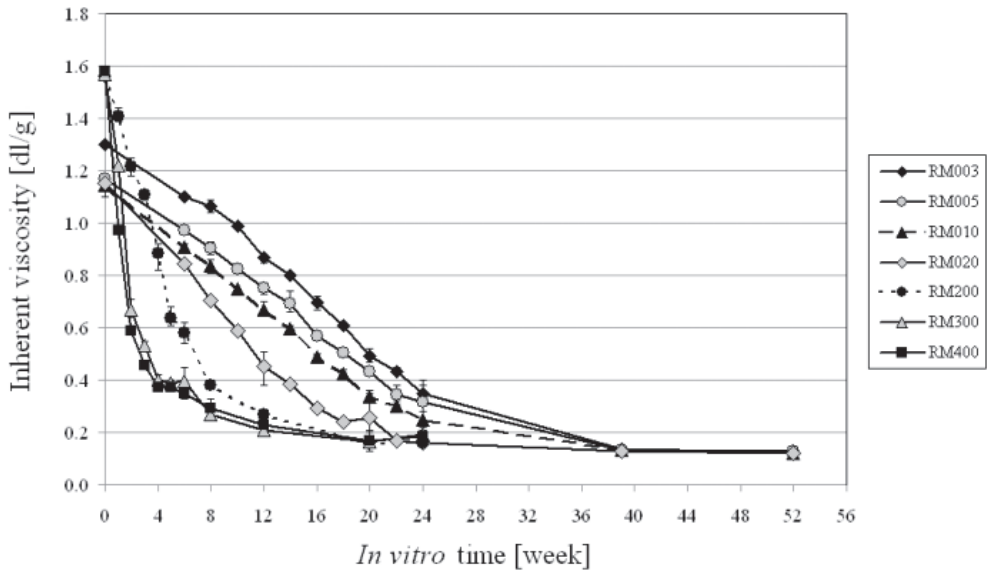

Figure 1. Hydrolytic-degradation-induced decrease in inherent viscosities of PLGA 85/15 with various lactide monomer contents at 37°C *in vitro* (n=3)

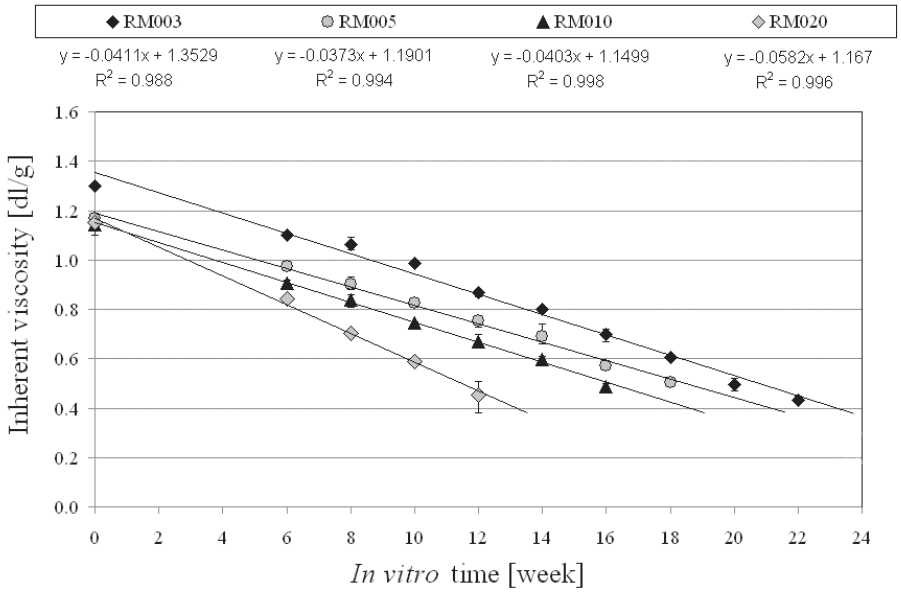

Figure 2. Linear sections of hydrolytic-degradation-induced decrease in inherent viscosities of PLGA 85/15 with various amounts of thermally generated, process-induced lactide monomer with linear regression curves, related equations, and R^2-values (n=3)

Tests of the mechanical properties of shear strength and bending were markedly affected by even small amounts (≤0.20 wt-%) of lactide monomer (Figure 3). The shear strength of the samples was only slightly affected by hydrolytic degradation before reaching the critical zone, after which it plunged. Both the thermally generated materials and those containing melt-mixed lactide monomer degraded in this manner. The time for maintaining over 80 % of initial shear strength was 16 weeks for RM003, 14 weeks for RM005, 12 weeks for RM010, 8 weeks for RM020, 6 weeks for RM200, 2 weeks for RM300, and only one week for RM400.

Samples tested by bending showed similar behavior as those tested by shear: after their molecular-degradation-rate-dependent length of a stabile level, their maximum bending load dropped substantially (Figure 4). Retention of the maximum bending load was similar to the lactide-monomer-dependent retention of shear strength at 37°C *in vitro*. In addition to the loss of mechanical properties, the bending test showed also the decrease of ductility at a critical level of degradation after which the samples were broken down during the test instead of ductile bending.

Mass loss *in vitro*, measured as percentage difference between initial dry weights and dry weights of degraded samples followed the same order in mass reduction as the drop in inherent viscosities. The mass loss initiated between the i.v. values of 0.38 - 0.43 dl/g and occurred after 22 weeks for RM003, 20 weeks for RM005, 18 weeks for RM010, and 14 weeks for RM020. During the 26-week test, samples with thermally generated lactide monomer lost 2 to 25 % of their dry weight, depending of their lactide monomer content.

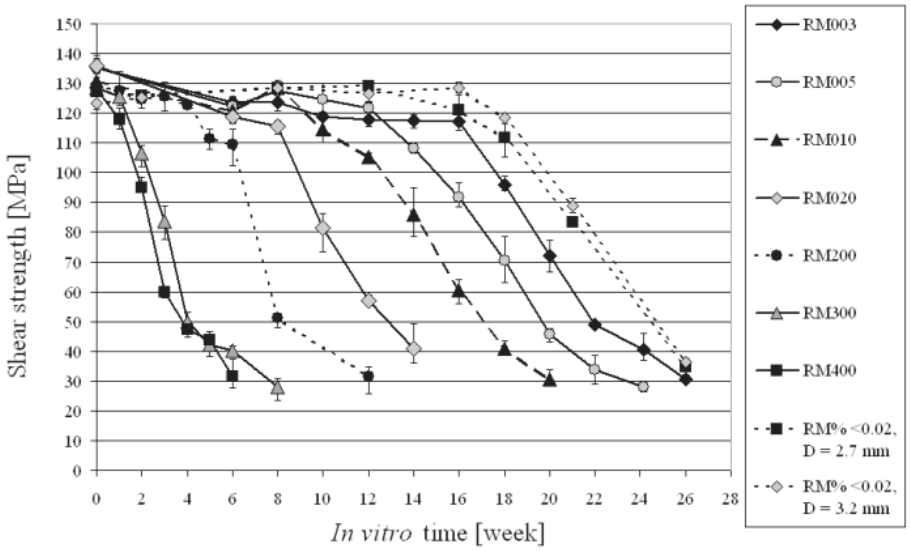

Figure 3. Effect of lactide monomer on shear strength retention of PLGA 85/15 with various lactide monomer contents (n=3). Sample series of 2.7 mm and 3.2 mm are included in the figure as reference material with < 0.02 wt-% of measured lactide monomer.

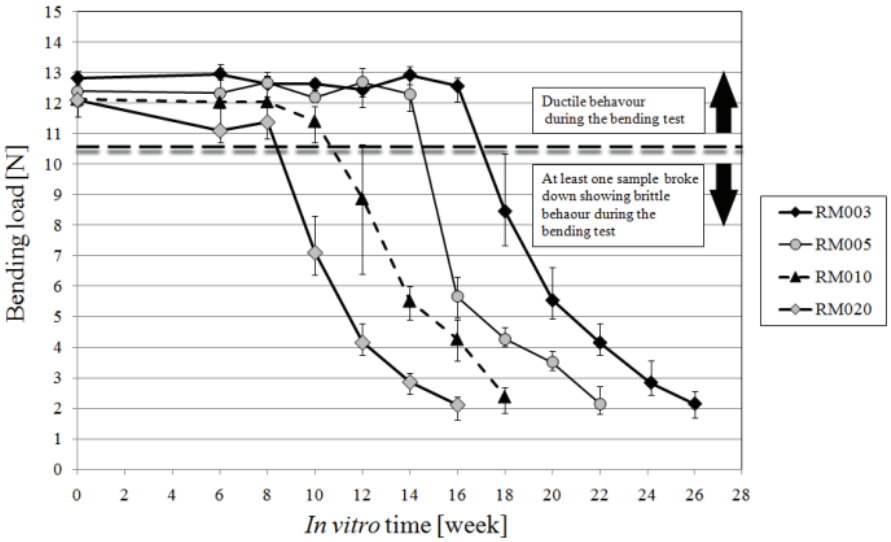

Figure 4. Effect of hydrolytic degradation on maximum bending load of PLGA 85/15 with various lactide monomer contents (n=3)

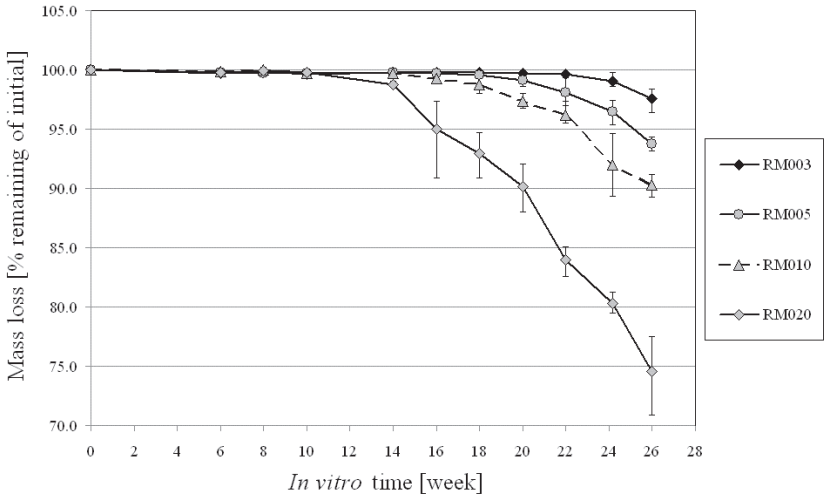

Figure 5. Mass loss of PLGA 85/15 with various lactide monomer contents *in vitro* (n=3)

3.3. Effects of hydrolytic degradation on thermal properties

The effect of the degradation rate on changes in crystallinity, measured as increase in melting enthalpy, is shown in Figure 6. The melting enthalpy of the crystal phase of the polymer structure increased against degradation time and depended on the degradation rate of the polymer samples. Samples with 2 and 4 wt-% of lactide monomer, melt processed from the premix, showed significantly faster relative crystallization of their polymer structure than those with a monomer content of 0.03 to 0.20 wt-%.

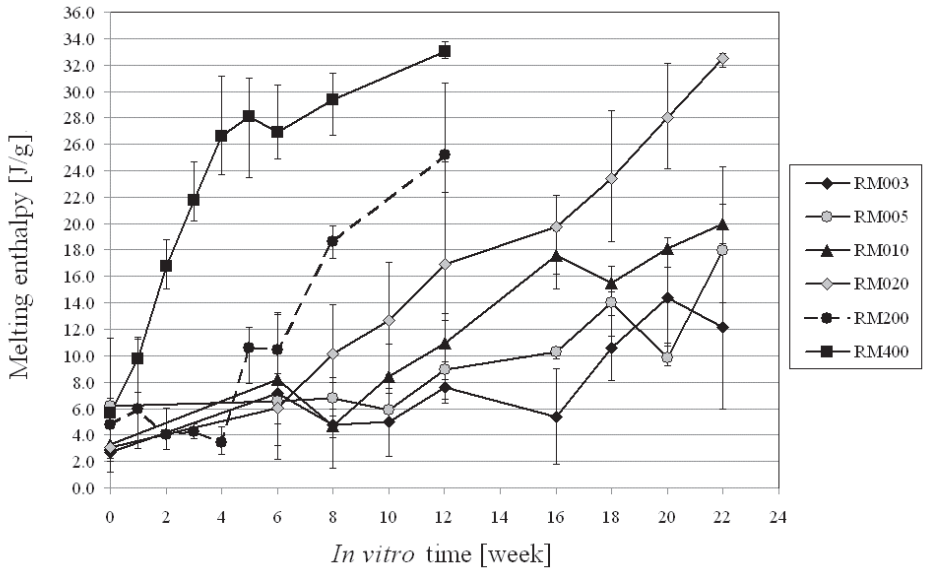

Figure 6. Melting enthalpy of PLGA 85/15 with various lactide monomer contents *in vitro* (n=3), presented as the sum of cold crystallization and melting enthalpies

3.4. Effect of hydrolytic degradation on the dimensional stability and microstructure of oriented PLGA 85/15

Figures 7 and 8 show dimensional changes measured as radial expansion of the samples' diameter and longitudinal contraction 37°C *in vitro*. The speed and extent of the radial expansion and longitudinal contraction correlated with the lactide monomer content and were thus linked with the degradation rate. Samples with high monomer content, from 2 to 4 wt-%, showed more significant dimensional instability than those with a monomer content between 0.03 and 0.20 wt-%. However, after 8 weeks *in vitro*, samples with a monomer content of 0.20 wt-% showed significant radial expansion. Samples with monomer contents of 3 and 4 wt-% reached their maximum radial expansion (5 %), after which their diameter started to decrease due to substantial degradation, and after 8 weeks the diameter and length of samples with 2-4 wt-% of monomer could no longer be measured because of material fragmentation.

The scanning electron microscopy images in Figure 9 show microstructural changes in oriented PLGA85/15 with lactide monomer contents of 0.03 wt-% (RM003) and 0.20 wt-% (RM020). The initial lengthwise oriented solid structure, seen in the 0-week samples, begins to transform to porous structure shown in (RM020, 22 wks). The SEM images (RM003, 22 wks) and (RM020, 14 wks) show a structure with detectable mass loss, whereas in (RM020, 22 wks) mass loss is already well underway.

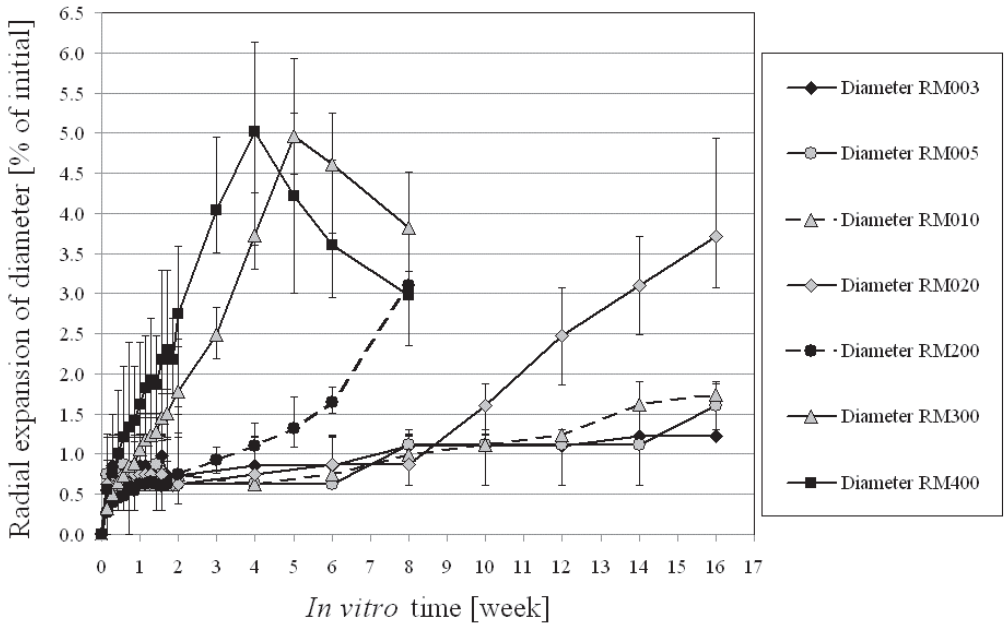

Figure 7. Radial expansion of the diameter of PLGA 85/15 (n=5 for RM003-RM020, n=10 for RM200-RM400)

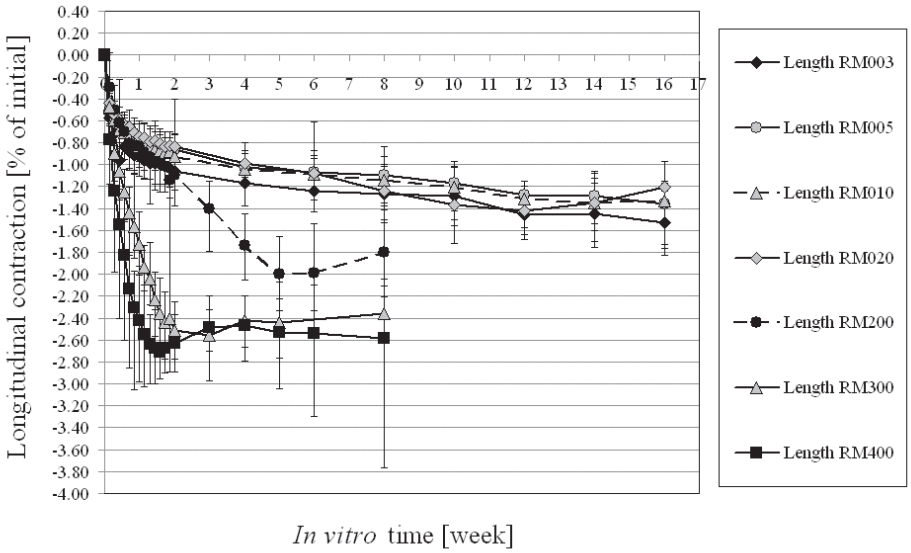

Figure 8. Longitudinal contraction of PLGA 85/15 (n=5 for RM003-RM020, n=10 for RM200-RM400), initial length 40±1 mm

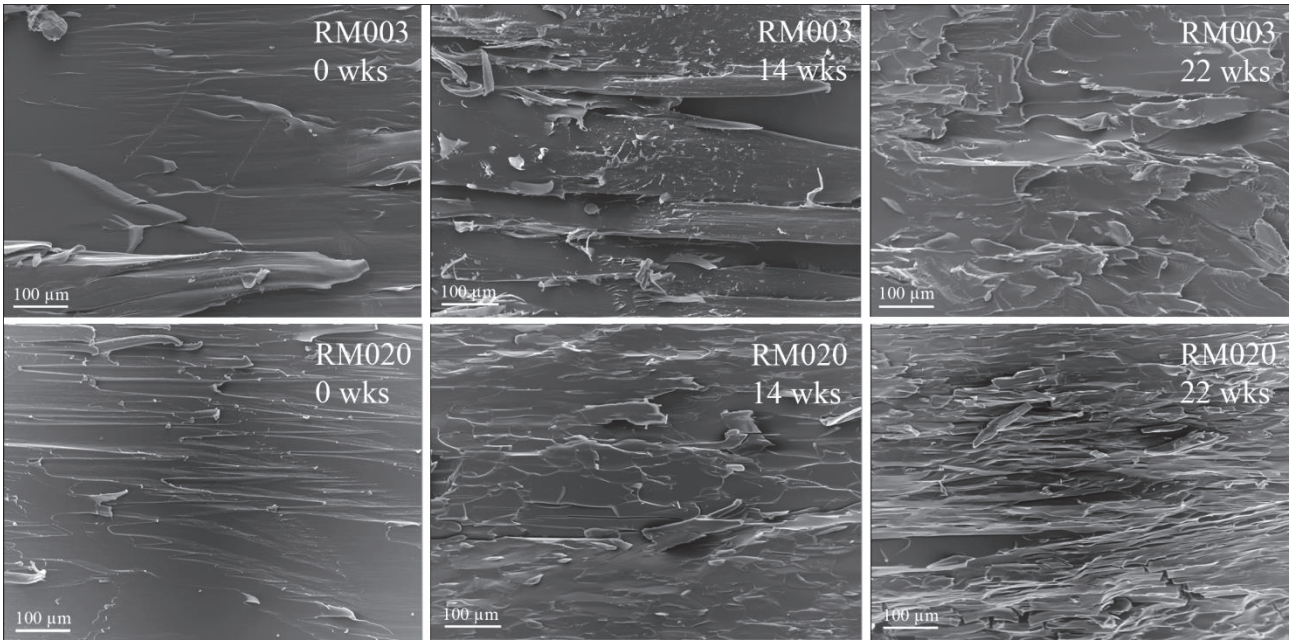

Figure 9. SEM images of PLGA 85/15 with a lactide monomer content of 0.03 wt-% (RM003) and 0.20 wt-% (RM020) after 0, 14, and 22 weeks

3.5. Release of lactide monomer

Release of lactide monomer was monitored in high-monomer specimens (RM200, RM300 and RM400), which were melt-processed from the premix of L-lactide and PLGA 85/15. The samples' initially high monomer content rapidly released from their polymer matrices, and after four weeks

no lactide monomer was measured in samples initially containing 3-4 wt-% of it. Samples that initially had 2 wt-% of monomer had only 6 % of it remaining after four weeks *in vitro.*

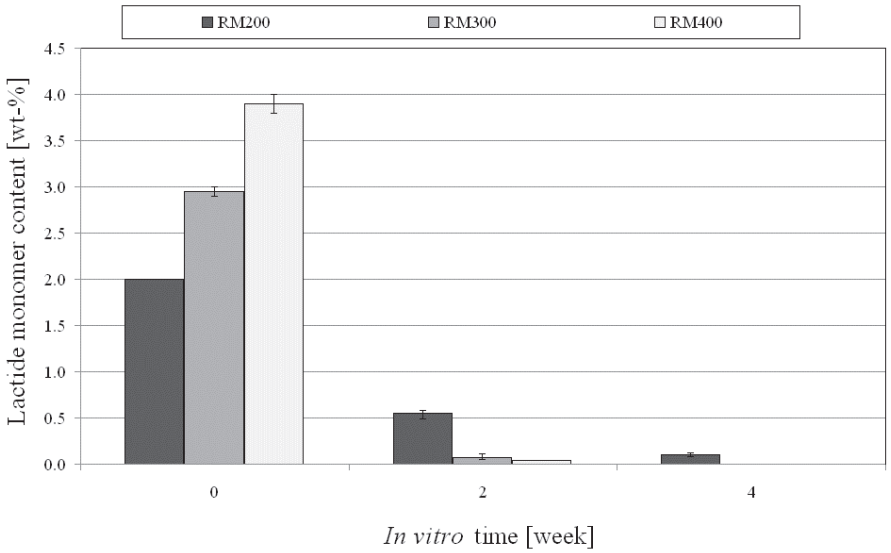

Figure 10. Change in lactide monomer content at 37°C *in vitro*

4. Discussion

Hydrolytic degradation of polylactide and its copolymers is a sum of complex interrelated events consisting of decreasing molecular weight, morphological changes, and mass loss. In hydrolytic conditions, at 37°C *in vitro*, these phenomena are significantly affected by molecular degradation during melt processing. Not only does it significantly lower molecular weight, but it also affects the thermal generation of lactide monomer, which again markedly affects the hydrolytic degradation rate at 37°C *in vitro* [14, 13]. The γ-irradiation used for the sterilization of the sample materials has been reported not to affect the lactide monomer content of polylactide copolymers, whether the materials have contained lactide monomer or not prior to the γ-irradiation [13].

In this study, the hydrolytic degradation at 37°C *in vitro* depended highly on the samples' lactide monomer content and remained linear up to a critical level and then slowed down. This was likely due to hydrolysis of the amorphous phase of the oriented semicrystalline polymer, which degraded to a level at which molecular chain mobility in the oriented amorphous phase was sufficient enough to allow cleavage-induced crystallization of the polymer chains. In addition, more confined amorphous regions, generated by the hydrolytic degradation, have been proposed not to be as readily degradable as the polymer chains in the amorphous gaps of the semicrystalline polymer, because the highly crystalline regions can possibly limit the penetration of water molecules into these amorphous regions [20]. The fraction of crystalline material increased as the amorphous regions degraded and diluted out of the polymer matrix causing the degradation to proceed more slowly as only more ordered crystalline regions remained [26]. As in [13], the degradation of melt-

extruded materials was faster in thicker samples. Though the degradation rates differed only slightly between RM005, RM010, and RM020, which all had the same initial i.v., degradation had significant long-term effects. For example, these polymers' inherent viscosity dropped to 0.6 dl/g in 16, 14, and 10 weeks, respectively. Both thermally generated and melt-blended monomer affected the degradation rate of PLGA 85/15. The molecular degradation rate was proportional to the samples' post-processing monomer content despite the elution of lactide monomer from the polymer matrix into the surrounding medium during the first weeks. Thus the initial lactide monomer content in the polymer matrix most likely catalyzed the chain scission at 37°C *in vitro*, resulting in the formation of acidic end groups, which further enhanced the rate of hydrolysis [21, 22].

Melt processing had a strong impact on the retention of mechanical properties. The shear strength remained at a stable level minimum of 80 % of its initial value up to the critical stage of molecular degradation, after which it declined rapidly. This drop-zone in mechanical properties was related to the measured i.v. such that the shear strength began to decline rapidly when the sample i.v. reached 0.8 - 0.6 dl/g. This shows that even small quantities (0.05-0.20 wt-%) of lactide monomer catalyzed molecular degradation and further loss of mechanical properties in PLGA 85/15 at 37°C *in vitro*. The mechanical properties, measured as maximum bending load, declined especially rapidly after the critical stage of molecular degradation because of degradation-induced crystallization in the oriented polymer matrix, which in turn transformed the oriented polymer from ductile to brittle. This morphological change to a more crystalline structure was simultaneous with the degradation and most likely due to the degradation of the amorphous phase, which crystallized because of increased molecular mobility, increasing thus proportionally the volume of the polymer crystal phase [20, 23]

The degradation-induced morphological change altered the structure of and created cracks in the oriented PLGA 85/15 matrix (Figure 9), supporting thus the inference in [9] that degradation morphology is related to the purity of the material and especially to its monomer content, not only as residual in the raw material [17, 18], but also as process-induced [13, 14]. Like degradation, crystallization, and structural change, also mass loss followed the degradation rate. Similar mass loss profiles for this copolymer (PLGA 85/15) have been reported in [24] in which the mass losses were comparable to RM003 and RM020.

During hydrolysis, oriented PLGA 85/15 underwent small dimensional transformations towards its original non-oriented shape. The simultaneous radial expansion of its diameter and longitudinal contraction were both related mainly to the degradation rate. A high lactide monomer content (2.0 - 4.0 wt-%) stimulated the transformation of oriented PLGA 85/15 significantly more than small amounts (0.03 - 0.20 wt-%). The small shape recovery at 37°C *in vitro* at an early phase, before significant decrease of i.v., was likely due to the water-molecule-driven plasticization of the amorphous phase of the polymer [25], which in turn enabled the small molecular movement of the oriented polymer chains towards the non-oriented state. With continued degradation, initially

oriented polymer chains in the amorphous phase may have relaxed into energetically more favorable conformations, pulling the adjacent crystal lamella closer together and thus generating a small shape transformation [20, 26].

Based on our hydrolytic degradation data, we are proposing simplified model for degradation-related strength retention. Because the hydrolytic degradation of PLGA 85/15 is markedly affected by its lactide monomer content and because the mechanical properties of oriented PLGA 85/15 significantly decline in the i.v. range of 0.8-0.6 dl/g, in a hydrolytic environment at 37°C strength retention can be predicted according to the model shown in Figure 11. The model assumes that the polymer loses its shear strength shear strength at below 80 % of the initial value. In this study, the last time points indicating shear strength of at least 80 % of the initial value are marked in Figure 11. The two curves show calculated values, based on the regression curves in Figure 2, at the time point when degradation has progressed to 0.6 dl/g and 0.8 dl/g *in vitro* at 37°C with various lactide monomer contents. Only the data on thermally generated lactide monomer samples was analyzed, because the monomer was probably more homogeneously distributed in the polymer matrix. In Figure 13 a mathematical equation defining the surface has been fitted based on the measurement results with surface fitting toolbox in Matlab. Since the R^2-value is 0.99 the equation represents the degradation phenomena well, however to be noted that equation is suitable within the range of lactide contents and in vitro times used on the measurements, as shown also in Figure 13. These models enable us to estimate the strength retention time for PLGA 85/15 with various lactide monomer contents and show that even small amounts of lactide monomer significantly affect the strength retention of PLGA 85/15. Consequently, the models are useful in predicting and controlling hydrolytic degradation *in vivo* and in setting up quality control in manufacturing bioabsorbable medical devices by melt processing.

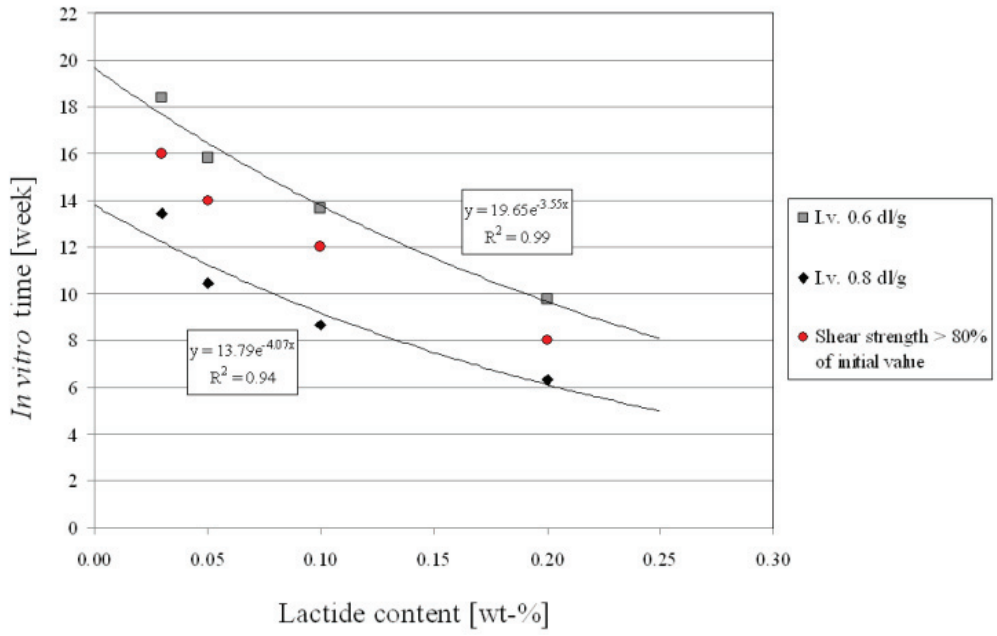

Figure 11. Simplified model of strength retention of PLGA 85/15 with various amounts of lactide monomer showing maximum (i.v. 0.6 dl/g) and minimum (i.v. 0.8 dl/g) limiting values for strength retention and fitted curves with equations [Lactide content ≤ 0.20 wt-%]; measured true values for strength retention time are shown with red bullets

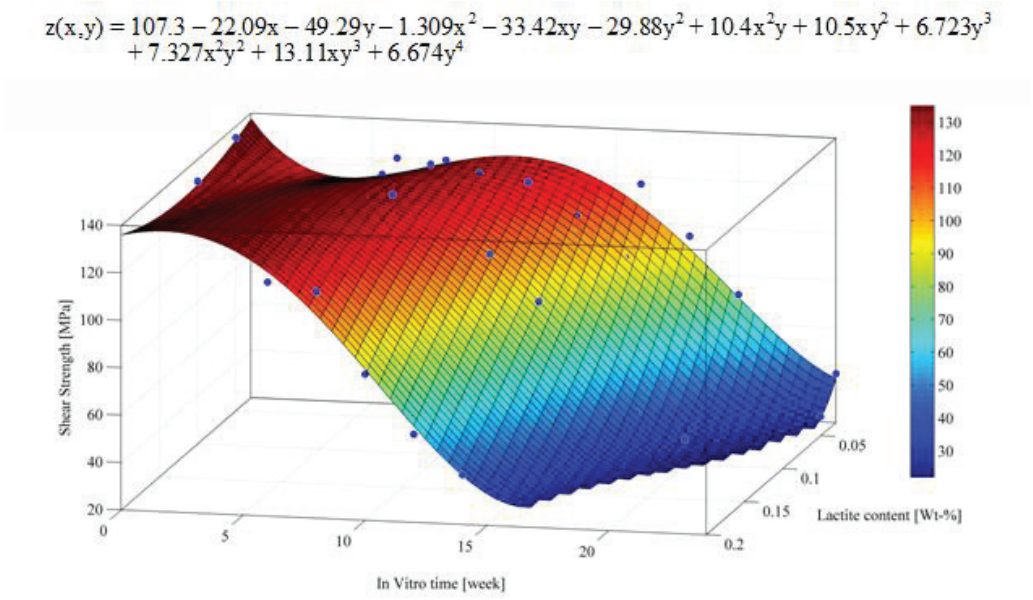

Figure 12. Mathematical model and equation for strength retention (z) of PLGA 85/15 at 37°C *in vitro* with various lactide monomer contents (x) as a function of *in vitro* time (y). R^2=0.99

5. Conclusions

As shown in this study, even with high quality raw materials, the performance of the end product in a hydrolytic environment at 37°C may vary significantly depending on how the product was melt-processed. Lactide monomer, whether thermally generated or melt-mixed, significantly affects the degradation rate of PLGA 85/15. Even small amounts of pre-hydrolysis lactide monomer affect in the long term especially the product's mechanical properties. Oriented PLGA 85/15 maintains its mechanical properties up to a specific i.v. range and then loses them rapidly; the time to this drop-zone depends on the polymer's lactide monomer content. This finding not only enables quality control of bioabsorbable medical devices, but also programming the degradation time for this lactide copolymer, and perhaps for other lactide copolymers as well.

Acknowledgements

We thank the Graduate School of the Processing of Polymers and Polymer-Based Multimaterials, financed by Finland's Ministry of Education, and Kaija Honkavaara and Milla Törmälä, who assisted us in the laboratory during the study.

References:

1. Rokkanen, P., Böstman, O., Vainionpää, S., Vihtonen, K., Törmälä, P., Laiho, J., Kilpikari, J., Tamminmäki, M., 1985. Biodegradable implants in fracture fixation: Early results of the treatment of fractures of the ankle. The Lancet 325,1422-1424.
2. Rokkanen, P.U., Böstman, O., Hirvensalo, E., Mäkelä, E.A., Partio, E.K., Pätiälä, H., Vainionpää, S., Vihtonen, K., Törmälä, P., 2000. Bioabsorbable fixation in orthopaedic surgery and traumatology. Biomaterials 21, 2607-2613.
3. Landes, C., Ballon, A., Roth, C., 2006. Maxillary and Mandibular Osteosyntheses with PLGA and P(L/DL)LA Implants: A 5-year inpatient biocompatibility and degradation experience. Plast. Reconstr. Surg. 117, 2347-2360.
4. Hollinger, J., Battistone, G., 1986. Biodegradable bone repair materials. Synthetic polymers and ceramics. Clin. Orthop. Rel. R. 207, 290-305.
5. Törmälä, P., 1992. Biodegradable self-reinforced composite materials; Manufacturing structure and mechanical properties. Clin. Mater. 10, 29-34.
6. Ashammakhi, N., Gonzalez, A.M., Törmälä, P., Jackson, I.T., 2004. New resorbable bone fixation. Biomaterials in craniomaxillofacial surgery: Present and future. Eur. J. Plast. Surg. 26, 383-390.
7. Kellomäki, M., Niiranen, H., Puumanen, K., Ashammakhi, N., Waris, T., Törmälä, P., 2000. Bioabsorbable scaffolds for guided bone regeneration and generation. Biomaterials 21, 2495-2505.
8. Tiainen, J., Soini, Y., Törmälä, P., Waris, T., Ashammakhi, N., 2004. Self-reinforced polylactide/polyglycolide 80/20 screws take more than 1 1/2 years to resorb in rabbit cranial bone. J. Biomed. Mater. Res. - A Part B 70, 49-55.

9. Niiranen, H., Pyhältö, T., Rokkanen, P., Kellomäki, M., Törmälä, P., 2004. In vitro and in vivo behavior of self-reinforced bioabsorbable polymer and self-reinforced bioabsorbable polymer/bioactive glass composites. J. Biomed. Mater. Res. Part A 69, 699-708.
10. Niemelä T., 2005. Effect of β-tricalcium phosphate addition on the in vitro degradation of self-reinforced poly-L,D-lactide. Polym. Degrad. Stabil. 89, 492-500.
11. Haaparanta, A-M., Haimi, S., Ellä, V., Hopper, N., Miettinen, S., Suuronen, R., Kellomäki, M., 2010. Porous polylactide/β-tricalcium phosphate composite scaffolds for tissue engineering applications. J. Tissue Eng. Regen. Med. 4, 366-373.
12. Veiranto, M., Törmälä, P., Suokas, E., 2002. In vitro mechanical and drug release properties of bioabsorbable ciprofloxacin containing and neat self-reinforced P(L/DL)LA 70/30 fixation screws. J. Mater. Sci. - Mater. M. 13,1259-1263.
13. Ellä, V., Nikkola, L., Kellomäki, M., 2011. Process-induced monomer on a medical-grade polymer and its effect on short-term hydrolytic degradation. J. Appl. Polym. Sci. 119, 2996-3003.
14. Paakinaho, K., Ellä, V., Syrjälä, S., Kellomäki, M., 2009. Melt spinning of poly(L/D)lactide 96/4: Effects of molecular weight and melt processing on hydrolytic degradation. Polym. Degrad. Stabil. 94, 438-442.
15. von Oepen, R., Michaeli, W., 1992. Injection moulding of biodegradable implants. Clin. Mater. 10, 21-28.
16. Hyon, S-H., Jamshidi, K., Ikada, Y., 1998. Effects of residual monomer on the degradation of DL-lactide polymer. Polym. Int. 46,196-202.
17. Kellomäki, M., Pohjonen, T., Törmälä, P., 2003. Self reinforced polylactides, in: Arshady R, Biodegradable Polymers. Citus Books, London, p. 212.
18. Zhang, X., Wyss, U.P., Pichora, D., Goosen, M.F.A., 1994. An investigation of poly(lactic acid) degradation. J. Bioact. Compat. Pol. 9, 80-100.
19. Allinniemi, T., Heino, H., Törmälä, P., 2007. US2007/0299449 A1.
20. Zong, X., Wang, Z., Hsiao, B.S., Chu, B., Zhou, J.J., Jamiolkowski, D.D., Muse, E., Dormier, E., 1999. Structure and morphology changes in absorbable poly(glycolide) and poly(glycolide-co-lactide) during in vitro degradation. Macromolecules 32, 8107-8114.
21. Edlund, U., Albertsson, A-C., 2003. Polyesters based on diacid monomers. Adv. Drug. Deliver. Rev. 55, 585-609.
22. Tsuji, H., Ikada, Y., 2000. Properties and morphology of poly(L-lactide) 4. Effects of structural parameters on long-term hydrolysis of poly(L-lactide) in phosphate-buffered solution. Polym. Degrad. Stab. 67, 179-189.
23. Li, S., Vert, M., 1994. Morphological changes resulting from the hydrolytic degradation of stereocopolymers derived from L- and DL-lactides. Macromolecules 27, 3107-3110.
24. Ramchandani, M., Pankaskie, M., Robinson, D., 1997. The influence of manufacturing procedure on the degradation of poly(lactide-co-glycolide) 85:15 and 50:50 implants. J. Control. Release 43, 161-173.
25. Blasi, P., D'Souza, S.S., Selmin, F., DeLuca, P.P., 2005. Plasticizing effect of water on poly(lactide-co-glycolide). J. Control. Release 108, 1-9.

26. King, E., Cameron, R.E., 1997. Effect of hydrolytic degradation on the microstructure of poly(glycolic acid): An x-ray scattering and ultraviolet spectrophotometry study of wet samples ultraviolet. J. Appl. Polym. Sci. 66, 1681-1690.

Publication III

Paakinaho, K., Heino, H., Pelto, M., Hannula, M., Törmälä, P., Kellomäki, M.

Programmed water-induced shape-memory of bioabsorbable poly(D,L-lactide): activation and properties in physiological temperature

Journal of Material Science: Materials in Medicine 23 (2012), pp. 613-621

Journal of Material Science: Materials in Medicine 23 (2012), pp. 613-621

Programmed Water-Induced Shape-Memory of Bioabsorbable Poly(D,L-lactide); Activation and Properties in Physiological Temperature

Paakinaho, K.[a*], Heino, H.[a, b], Pelto, M.[a], Hannula, M.[a], Törmälä, P.[b], Kellomäki, M.[a]

[a] *Department of Biomedical Engineering, Tampere University of Technology, Hermiankatu 12, P.O. Box 692, FI-33101 Tampere, Finland*
[b] *Bioretec Ltd, P.O. Box 135, 33721, Tampere, Finland*

*Corresponding author: Kaarlo Paakinaho, kaarlo.paakinaho@tut.fi

Keywords: shape-memory, polylactide, programming, degradation

Abstract

This study reports of the novel water-induced shape-memory of bioabsorbable poly(D,L-lactide). We have developed an orientation-based programming process that generates an ability for poly(D,L-lactide) to transform its shape at 37°C in an aqueous environment without external energy and to adapt to a predefined stress level by stress generation or relaxation. In this orientation-programming process, polymer material is deformed and oriented at an elevated temperature and subsequently cooled down while retaining its deformed shape, tension, and polymer chain entanglements. At body temperature and in an aqueous environment, the shape-memory is activated by the plasticizing effect of water molecules diffused into the polymer matrix causing an entropy-driven directed relaxation of oriented and preloaded polymer chains. This plasticizing effect is clearly seen as a decrease of the onset glass transition temperature by 10-13°C. We found that γ-irradiation used for sterilizing the orientation-programmed materials strongly affected the shape-recovery rate, but not the recovery ratio. Both non-γ-irradiated and γ-irradiated sample materials showed excellent shape-recovery ratios during a ten-week test period: 94% and 97%, respectively. The orientation-programmed materials generated a predefined load in a 37°C aqueous environment when their shape-recovery was restricted, but when external tension was applied to them, they adapted to the predefined level by stress relaxation. Our results show that functionality in terms of shape-memory can be generated in bioabsorbable polymers without tailoring the polymer chain structure thus shortening the time from development of technology to its utilization in medical devices.

1. Introduction

Shape-memory polymers constitute a unique group of materials with a predefined shape transformation capability. This advanced material property enables active and controlled movement and deformation of medical devices, and further the development and implementation of new surgical techniques [1-3]. Active shape transforming implants could be advantageous in minimally invasive and craniofacial surgery. They could be inserted through a small incision into the body and transformed to their permanent shape at the implantation site or used as fully implantable tissue augmentation devices [3, 4].

The shape-memory of these polymers is based on molecular-level programming whereby a stimuli-sensitive temporary shape is created. Shape-recovery from a temporary shape is initiated by a material-specific stimulus, e.g., heat or light [5-7]. So far, the most frequently reported methods in developing medical devices with shape-memory properties take advantage of the thermally induced shape-memory effect [3, 5, 6, 8, 9]. It is based on triggering the deformed temporary shape by raising the temperature of the material above the transition temperature, at which the polymer chain mobility is significantly increased. These polymers are typically either chemically cross-linked polymers, in which the cross-links determine the permanent shape, or physically cross-linked block copolymers with hard and soft segments, the hard segments determining the permanent shape. [3]

In medical applications direct actuation of the thermally-induced shape-memory is not always desirable since excessive heating may be harmful for the surrounding tissues. An efficient approach for this issue is water-induced shape-memory, which is based on an indirect activation of the thermally induced shape-memory by the plasticizing effect of water. This type of shape transformation is initiated at a significantly lower temperature in aqueous environment than when dry, due to water-molecule-driven decrease of the polymer's transition temperature. Shape-memory properties, which can be programmed similar to thermally induced shape-memory, but activated at significantly lower temperatures have been reported on polyurethanes [10,11] and tailored amorphous polymer networks based on lactide and glycolide segments [12]. In addition to the tailored polymers a small scale water-induced shape memory effect has been reported with amorphous poly(DL-lactide) in controlled drug release systems and in oriented poly(lactide-co-glycolide) 85L/15G [13, 14].

In developing functional materials for medical applications the problem is the long time-span from polymer synthesis to applying it clinically as a device. Rather than synthesizing completely new materials we have studied and developed shape-memory properties for bioabsorbable polymers already approved for medical applications with advanced processing methods. This study reports and discusses of the novel water-induced shape-memory properties of poly(D,L-lactide) and a programming process, in which the orientating force affects the generated force during the shape recovery of oriented poly(D,L-lactide). This new combination of functions, shape-memory and stress generation capability, is designated here as the mechanically active shape-memory.

2. Materials and methods

2.1. Polymer processing and orientation-programming

The polymer used in this study was medical grade poly(D,L-lactide) (PDLLA, Boeringer Ingelheim, R207 S) with an inherent viscosity of 1.6 dl/g and a measured residual monomer content of 0.02 wt-%. A co-rotating twin-screw extruder (Mini ZE 20*11.5 D, Neste Oy, Porvoo Finland) was used to melt-extrude the raw material to 6.6 ± 0.2-mm round rods which were deformed into grooved shape, similar to Allinniemi et al. [15], with a maximum diameter of 3.35 ± 0.1 mm in a process called orientation-programming. This continuous programming process is based on heating and deforming the polymer in temperatures above the glass transition temperature (T_g), but below the melting temperature, and subsequently cooling the deformed and uniaxially oriented polymer while maintaining the predefined tension within the entangled polymer chains (Figure 1). The drawing force during the orientation-programming process was between 80-120 N coinciding the tensional stress of 10-16 MPa. γ-irradiation was used as a sterilization method with a minimum radiation dose of 25 kGy by Gamma-Service Produktbestrahlung GmbH, Radeberg, Germany.

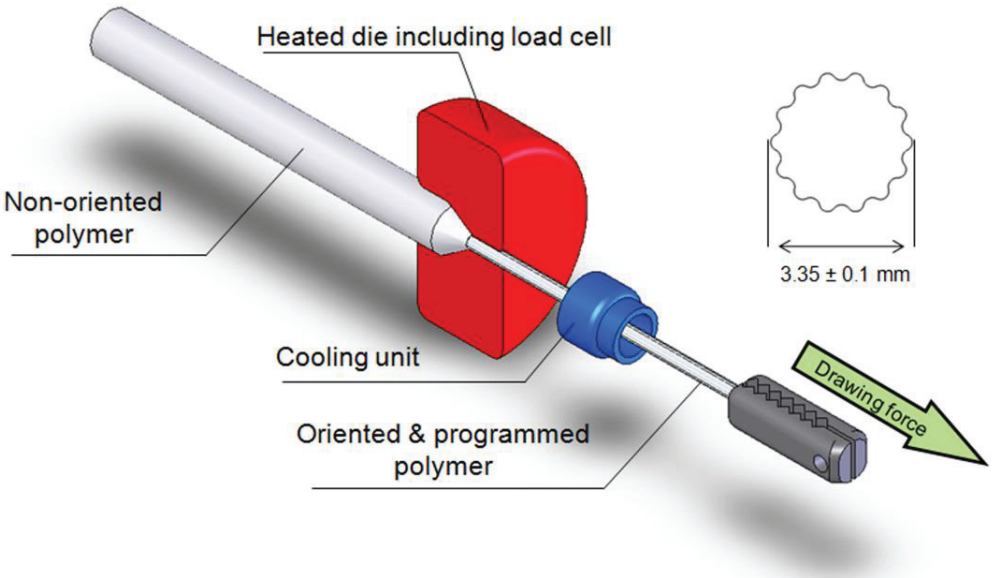

Figure 1. Principle of the orientation-programming process and the cross-section of an orientation-programmed grooved shaped polymer rod with diameter and tolerances

2.2. Shape- and structural transformation and water absorption in vitro

To measure the shape transformation rate and extent in a simulated physiological environment, the samples were placed in 37 ± 1°C Sörensen buffer solution, with a buffer solution volume/sample weight ratio greater than 30:1 (ml/g), and their radial expansion and longitudinal contraction were measured as maximum diameter

and length over 10 weeks *in vitro*. The buffer solution pH was monitored weekly and kept within the range of 7.4 ± 0.2. The transformation of the oriented structure was monitored also with a scanning electron microscope (Jeol JSM-T1000, Jeol Ltd., Tokyo, Japan). The water absorption was determined by weighing wet samples after carefully removing excess water from the sample surface and by comparing wet sample weights to initial dry ones. Shape transformation and water absorption measurements *in vitro* were performed on both non-γ-irradiated and γ- irradiated samples with ten parallel samples. In addition to samples tested at 37± 1°C *in vitro*, sample materials were also tested at room temperature (21 ± 1°C) *in vitro* (n=3) and dry at 37 ± 1°C (n=3).

2.3. Stress generation and stress relaxation

The stress generation and stress relaxation behavior of both non-γ-irradiated and γ-irradiated samples was monitored in 37 ± 1°C Sörensen buffer solution. The equipment in stress generation and stress relaxation tests comprised a temperature-controlled water bath with a temperature sensor (1.5 mm K-type thermocouple, Nokeval, Nokia, Finland), a process automation controller (National Instruments, Fieldpoint 2015, Austin, Texas, USA), a transducer (Gefran 40B 96, Gefran S.p.A, Provaglio d'Iseo, Italy), and a load cell (Gefran OC 50/500N, Gefran S.p.A, Provaglio d'Iseo, Italy). Samples were attached to the load cell with a gauge length of 20 ± 1 mm, and the system was adjusted such that free shape transformation was restrained. Force generation was monitored at time periods 1, 3, and 10 weeks. In addition, stress generation tests were combined with stress relaxation: after one week an external force of 200 N was applied to γ-irradiated sample and 250 N to non-γ-irradiated sample. The lower external force used for γ-irradiated samples was due to their lower initial mechanical properties over non-γ-irradiated samples. After one week of stress relaxation, the force level was dropped manually to zero and force generation was monitored. Stress generation and stress relaxation were cycled over a ten-week period for non-γ-irradiated samples and over a five-week period for γ-irradiated samples. Measuring system and principle are presented in Figure 2.

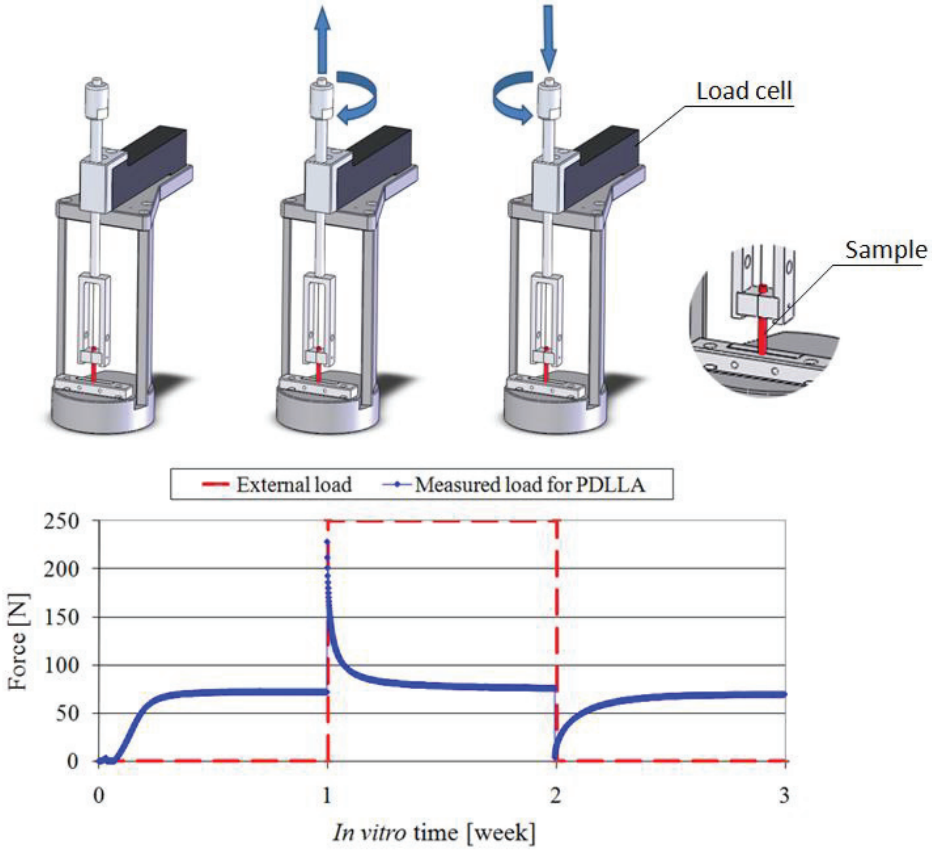

Figure 2. Measuring system and method for cycled stress generation and stress relaxation at 37°C *in vitro*

2.4. Thermal analysis

Thermal properties were studied with a temperature-modulated differential scanning calorimeter (MDSC) (DSC Q1000, TA Instruments, New Castle, Delaware, USA). Analyses were performed on six parallel 5 to 10-mg samples in hermetically sealed pans with a temperature range of 5 to 80°C, an amplitude of 0.16 s, a modulation period time of 40 s, and a heating rate of 1°C/min. Excess moisture was carefully removed from sample surfaces before placing the samples in hermetically sealed pans. The onset glass transition temperature (T_g-onset) of both dry and wet non-γ-irradiated and γ-irradiated samples was analyzed and monitored as a function of time at 37 ± 1°C *in vitro*.

2.5. Molecular degradation and strength retention in vitro

To study degradation *in vitro*, samples were placed in 37 ± 1°C Sörensen buffer solution, and degradation was monitored with three parallel samples in shear strength tests (MTS Insight 30, MTS Systems Corporation, Eden Prairie, MN USA) in an aqueous environment at 37 ± 1°C, and with inherent viscosity (i.v.) measurements in viscometric analysis (Lauda PSV1, Lauda-Königshofen, Germany) with Ubbelohde capillars (Schott-

Instrument, Mainz, Germany) in choloform at 25°C. To restrain shape transformation *in vitro* during the 16-week test, samples tested for shear strength were placed in buffer solution inside custom-made hex-cylinders with water channels on each face of the hexagon. A sample of length 30 mm was placed inside three 10-mm hex-cylinders with a central cavity diameter of 3.44 mm. Shear tests were performed with samples placed inside the hex-cylinders by fixing the lateral hex-cylinder to a holder and shearing the sample by pulling the middlemost cylinder upwards (basic shear strength test principle with hex-cylinders is shown in Figure 3). Lactide monomer content was measured from samples after melt-processing using gas chromatography (DC8000, CE Instruments, Rodano, Italy) and an FI-detector after chloroform dilution (Rambol Analytics Oy, Lahti, Finland). The measuring resolution was 0.02 wt-%, and a mean of three parallel measurements were used to determine the monomer content.

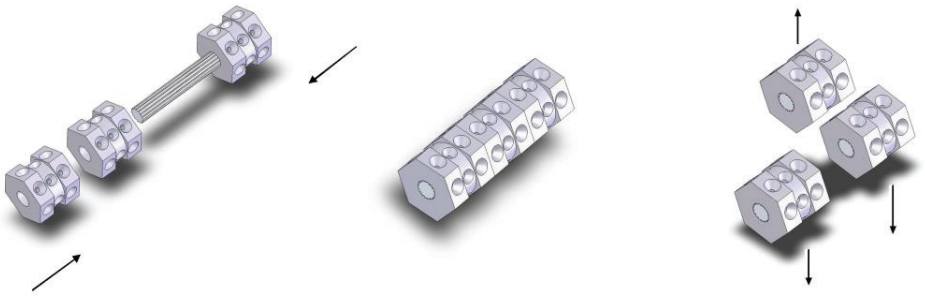

Figure 3. Schematic of a shear test with hex-cylinders

3. Results

3.1. Shape recovery and water absorption

The shape recovery of orientation-programmed PDLLA, both non-γ-irradiated (i.v. 1.5 dl/g) and γ-irradiated (i.v. 0.9 dl/g), started in the 37°C buffer solution within 24 hours (Figures 4 and 5). During the ten-week *in vitro* test, shape recovery ratios were 94 % for non-γ-irradiated samples and 97 % for γ-irradiated samples, measured as a function of radial expansion. During the 10 weeks *in vitro*, both samples showed a longitudinal contraction of 74 %. γ-irradiation increased markedly the shape recovery rate but had no significant effect on their shape recovery ratio. A 90% limit in shape recovery, measured as radial expansion, was reached in four weeks with γ-irradiated samples and in eight weeks with non-γ-irradiated samples. The orientation-programmed grooved shape was transformed back towards the initial non-oriented round shape and no grooves were found when the shape-recovery was in the range of 50 to 60 %. Samples tested dry at 37°C or at 21°C *in vitro* showed no

appreciable shape recovery over the ten-week test with a longitudinal contraction of maximum 1 % and a radial expansion of maximum 0.5 % for both samples showing that the shape-memory effect of PDLLA requires both 37°C temperature and the aqueous environment.

Scanning electron microscope images (Figure 6) show changes in the initially oriented structure *in vitro* at 37°C. The start of a shape-recovery-derived deorientation is clearly visible after five days, and after three weeks, the fully oriented structure had transformed into alternating-oriented and non-oriented zones.
Both non- and γ-irradiated samples absorbed small amounts (0.7 - 0.9 wt-%) of water when immersed in buffer solution (Figure 7). Most of the water was absorbed during the first two days, after which the polymers' water content stabilized. The water content of non-γ-irradiated samples remained stable for the whole 10-week period, whereas the water absorption of γ-irradiated samples started slowly to increase after five weeks *in vitro*.

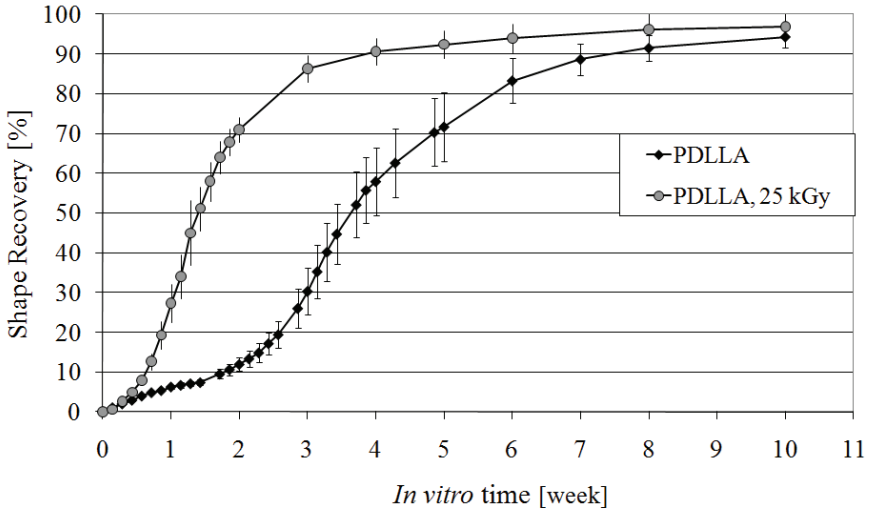

Figure 4. Average values and standard deviations of shape recovery measured as radial expansion of PDLLA at 37°C *in vitro*, n=10

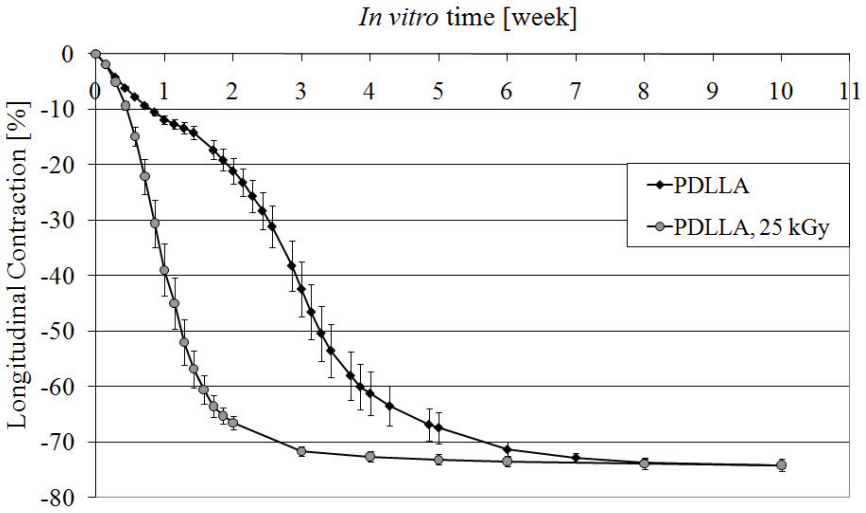

Figure 5. Average values and standard deviations of shape recovery measured as longitudinal contraction of PDLLA at 37°C *in vitro*, n=10

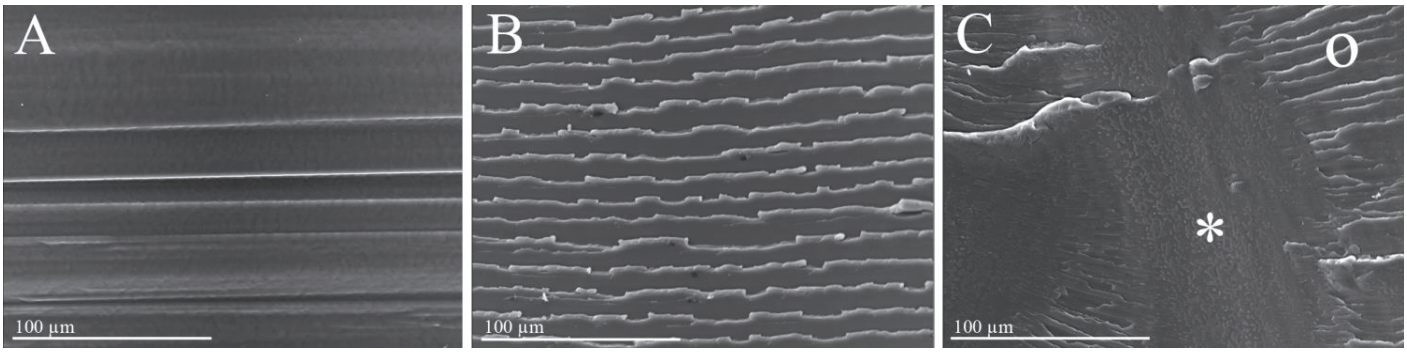

Figure 6. Scanning electron microscope images of longitudinal fracture surface of γ-irradiated PDLLA; initial orientated structure (A), 5 d *in vitro* (B), and 21 d *in vitro* (C); oriented structure visible as horizontal lines in all images and as bands of oriented (o) and deoriented (*) zones after 21 d *in vitro*.

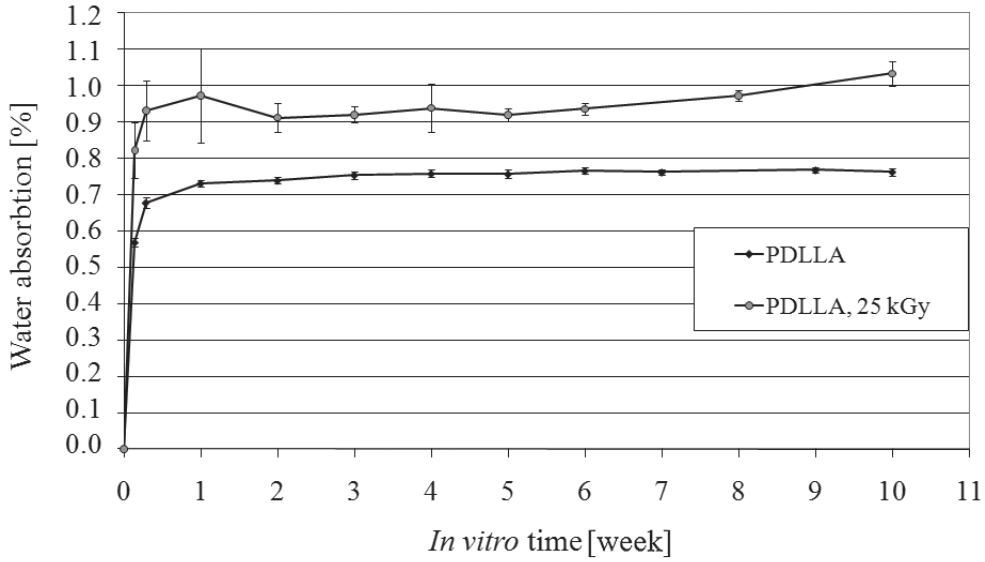

Figure 7. Weight increase due to water absorbed into polymer matrix *in vitro*, n=10

3.2 Stress generation and stress relaxation in vitro

The results of the stress generation tests on PDLLA are shown in Figure 8. After submerging the samples in a 37°C aqueous environment, stress generation occurred at the earliest in 30 minutes and at the latest in 15 hours. After programming, polymers could generate a stress level of approximately 10 MPa in their 37°C aqueous environment, which accorded with the tensile stress applied in the orientation-programming process (10-15 MPa). γ-irradiation had a significant effect on their stress generating capability: the maximum generated stress for γ-irradiated samples was 7 to 8 MPa, and the polymer could not maintain a steady contracting stress as in non-γ-irradiated PDLLA. During the 10 weeks *in vitro*, the measured stress dropped by 96 % in the γ-irradiated sample but only by 19 % in the non-γ-irradiated sample.

Orientation-programmed PDLLA showed novel properties in the cycled stress generation and stress relaxation test: it displayed a tendency to recall the original and programmed tension despite the external loading (Figure 9). In the cycled stress generation and relaxation test, the polymer was able to generate a contracting force, which accorded with that used in the orientation-programming, but when the material was subjected to an external tensional force greater than one used the orientation-programming, it stress relaxed back to the programmed level. After the relaxation cycle (1 week) and removal of all load and generated stress such that no load could be measured, the programmed material tended to contract and generate a stress that again accorded with that used in the orientation-programming.

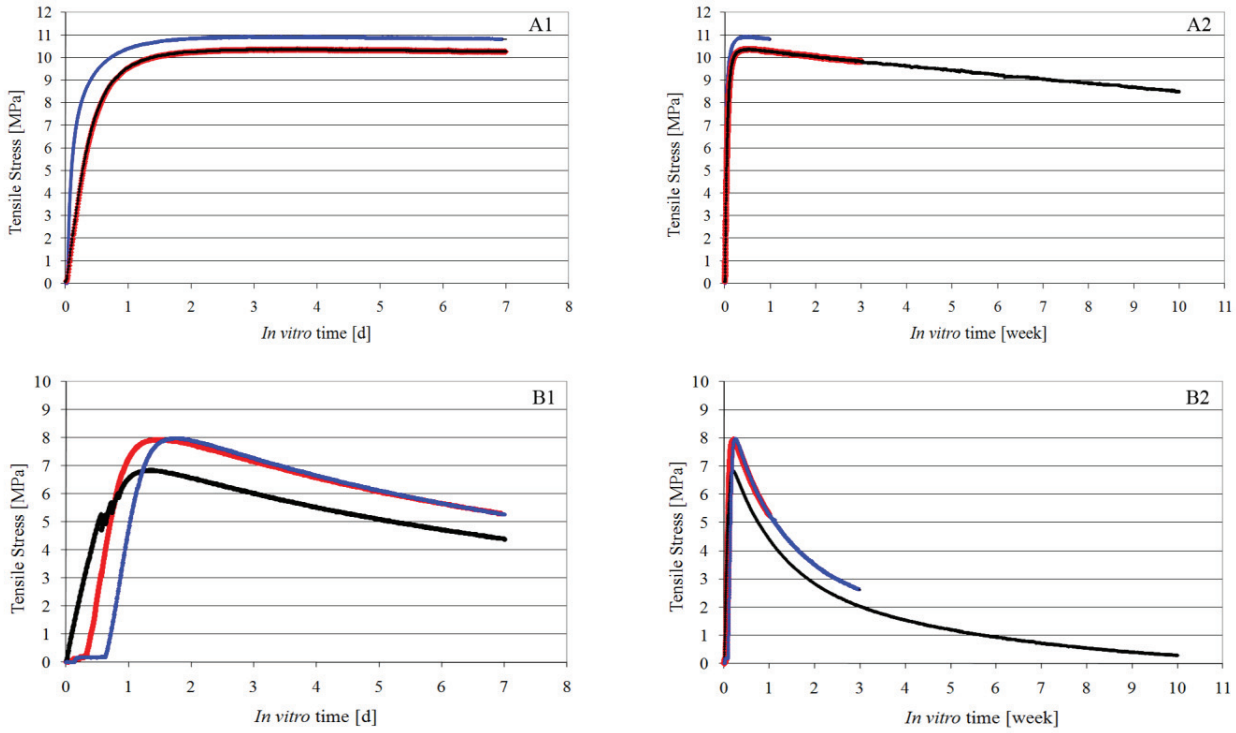

Figure 8: Generation of tensile stress due to restrained shape transformation of PDLLA (A) and γ-irradiated PDLLA (B); short-term force generation (A1, B1) at left, long-term (A2, B2) at right

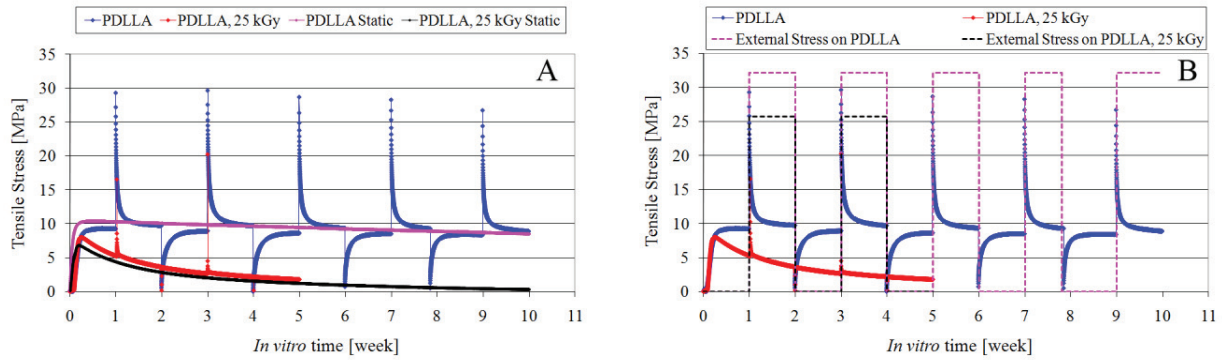

Figure 9: Cycled stress generation and stress relaxation of PDLLA compared to a static, non-cycled, stress generation test (A), combined stress generation and stress relaxation of PDLLA and applied external stress (B)

3.3. Thermal analysis

A small amount of absorbed water in the polymer matrix had a pronounced effect on the thermal properties of the oriented PDLLA sample materials. The initial T_g -onset of dry polymers, 57°C for non-γ-irradiated and 55°C for γ-irradiated samples, dropped dramatically already after 24 hours *in vitro* to 46°C and 42°C, respectively (results of changes in the onset value of T_g *in vitro* at 37°C, analyzed wet, as well as the start of the T_g range of the same samples as deviation from the T_g-curve baseline are shown in Table 1). Though the T_g-onset is over 40°C, a 2% deviation of the baseline, indicating the start of the T_g range, can be seen after 24 hours below 37°C with γ-irradiated samples. Figure 10 shows representative MDSC heat flow curves of dry and wet PDLLA samples after 24 hours *in vitro* at 37°C. The T_g region shows a large enthalpy relaxation peak for both dry samples, but already after 24 hours at 37°C the peak has markedly changed and T_g has dropped from 57°C to 46°C with non-γ-irradiated samples and from 55°C to 42°C with γ-irradiated samples.

Table 1. T_g-onset and MDSC-curve baseline deviations (2-5 %) indicating the start of the T_g range at various incubation time points, n=6

	PDLLA					PDLLA 25 kGy				
In vitro time [d]	Tg-onset [°C]	2% dev. [°C]	3% dev. [°C]	4% dev. [°C]	5% dev. [°C]	*In vitro* time [d]	Tg-onset [°C]	2% dev. [°C]	3% dev. [°C]	4% dev. [°C]	5% dev. [°C]
0	56.6 ± 0.8	50.6 ± 3.8	51.8 ± 3.7	52.6 ± 3.1	53.8 ± 0.4	0	55.3 ± 0.3	48.0 ± 2.1	52.1 ± 0.3	52.3 ± 0.3	52.5 ± 0.3
1	45.8 ± 0.4	40.3 ± 0.9	41.3 ± 0.6	42.0 ± 0.6	42.4 ± 0.6	1	42.2 ± 0.8	36.7 ± 1.7	37.9 ± 1.4	38.7 ± 1.2	39.3 ± 1.0
3	45.0 ± 0.4	38.7 ± 2.9	39.9 ± 2.2	40.8 ± 1.4	41.5 ± 1.0	3	40.8 ± 0.7	35.2 ± 2.7	36.4 ± 3.2	38.0 ± 1.7	38.8 ± 1.5
7	44.2 ± 0.4	37.9 ± 2.1	39.3 ± 1.2	40.5 ± 0.8	41.0 ± 0.8						

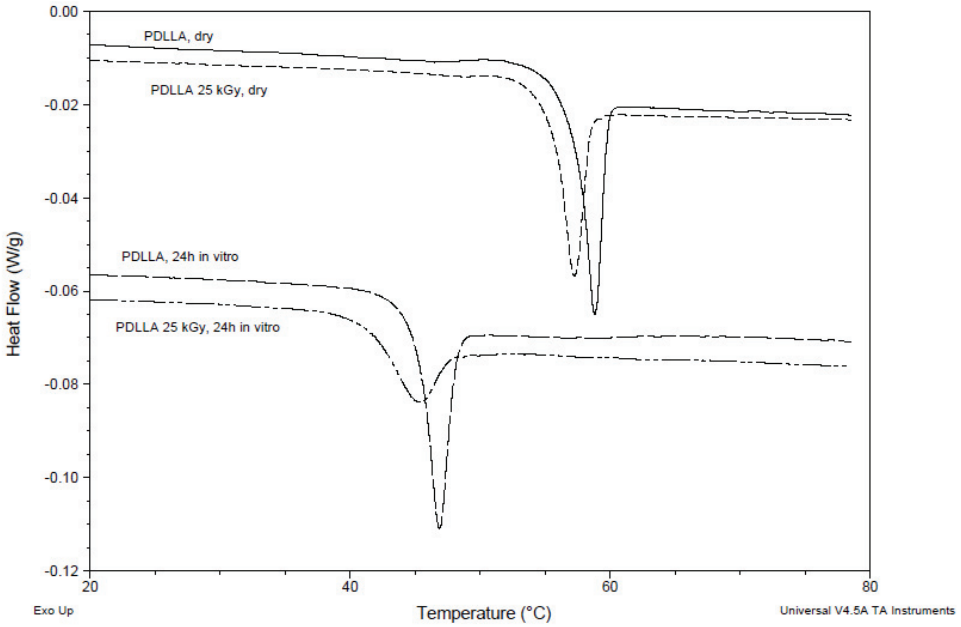

Figure 10. Representative MDSC-curves of dry and wet samples incubated 24 hours *in vitro* at 37°C, showing decrease in T_g and a marked change in enthalpy relaxation peak of γ-irradiated PDLLA after 24 h of incubation

3.4. Molecular degradation and strength retention in vitro

The i.v. of the melt-extruded PDLLA was 1.5 dl/g and the measured lactide monomer concentration <0.02 wt-%. After subsequent 25 kGy γ-irradiation, the i.v. dropped to 0.9 dl/g. The hydrolytic degradation measured as decrease in i.v. of orientation-programmed and γ-irradiated PDLLA appeared linear (Figure 11), and during the 16-week test it dropped to 0.5 dl/g. The degradation of non-γ-irradiated samples was monitored for four weeks (selected main activity time), over which the i.v. declined from 1.5 dl/g to 1.4 dl/g.

The initial shear strength of orientation-programmed and γ-irradiated PDLLA was 85 MPa with its mechanical properties deteriorating as its hydrolytic degradation progressed. The sharp drop in shear strength during the first two weeks was due to shape transformation in the initially grooved samples, which expanded into a tube-like inner cavity of the hex-cyliders used in the shear test. This small shape transformation changed the orientation ratio of the sample materials and thus affected their shear strength.

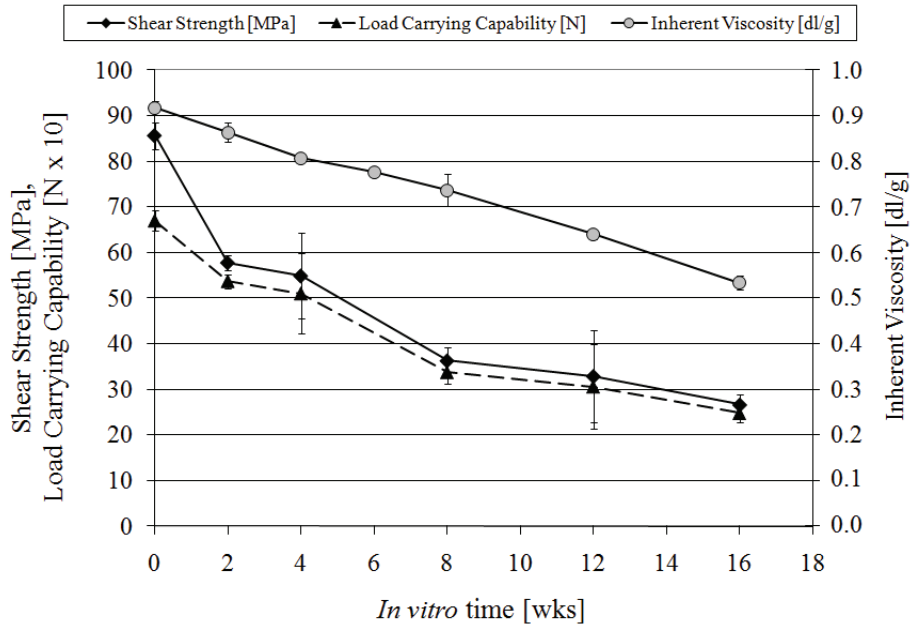

Figure 11. Strength retention of γ-irradiated PDLLA and decrease in inherent viscosity due to hydrolytic degradation at 37°C *in vitro* (n=3); shown are average values and standard deviations

4. Discussion

In the orientation-programming process, PDLLA polymer chains are heated and strained, and a tensional stress is applied to the polymer, which is then cooled down while maintaining the deformation, tension, and polymer chain entanglements. These entanglements act as the physical cross-links determining the permanent shape. The polymer chains are forced from their initially non-organized amorphous molecular structure into an oriented, more organized and less preferred state, thus decreasing entropy as the number of possible molecular conformations decreases [13, 1]. The entropically unfavourable conformations and macroscopic state are maintained at 37°C when the polymer is dry, because the molecular motions are limited due to the T_g-onset of dry PDLLA (55-57°C).

After immersion in aqueous environment a small amount of diffused water molecules in the polymer matrix cause a significant decrease of T_g of the polylactide copolymer [12,13,17-20], in this study 12-15°C. Steendam and Hancock have reported that amorphous glassy materials exhibit significant entropy-driven molecular mobility below their T_g, which involves relaxation of small molecular groups with sufficient mobility [13, 19, 21]. In addition the time-scale of the largest molecular movements, below or near the intended ambient temperature (physiological temperature), can be greatly reduced by lowering the glass transition temperature by plasticizing molecules diffusing into the amorphous polymer matrix. Although the analysed T_g-onset is above physiological temperature, the molecular movement are possible, because glass transition is not a single temperature, but occurs in a range in which the polymer changes from glassy to rubbery. As shown in Table 1,

after 24 hours a 2% deviation from the baseline of the MDSC curve occurs below 37°C with γ-irradiated PDLLA, marking the start of the glass transition zone just below the physiological temperature and enabling a slow shape-recovery towards the non-oriented state. This can be seen macroscopically as shape transformation of orientation-programmed PDLLA.

As shown in this study, γ-irratiation, which is used to sterilize bioabsorbable medical devices, had accelerated the shape-recovery rate of orientation-programmed PDLLA. While the γ-irradiation decreased the i.v., T_g, it possibly generated low-molecular-weight-oriented polymer chains capable of molecular movement in a low energetic state into the material. Due to the low i.v., γ-irradiated PDLLA could also absorb more plasticizing water into its polymer matrix than non-γ-irradiated PDLLA, thus increasing the number of molecules possibly interacting with the polar chain groups, disrupting the weak molecular interactions of adjacent polymer chains, and removing barriers to bond rotation and chain mobility [17]. It is unlikely that γ-irradiation caused crosslinking of the polymer chains in PDLLA, because the initial polymer is linear and the possibly reactive groups are located at the ends of the polymer. No increase of molecular weight, measured as i.v., was observed after γ-irradiation.

Though non-γ-irradiated PDLLA samples with a higher i.v. showed a significantly slower shape-recovery rate than γ-irradiated samples, their shape-recovery ratio at week ten *in vitro* was the same. Such behaviour is in contrast to compressed particles reported by Steendam, but is probably due to differences related to processing [19]. In a physiological environment, the shape transformation of orientation-programmed PDLLA was slow compared to the thermally-stimulated shape-memory polymers, which were directly heated over their transition temperature [3, 16] and whose shape transformation occurred in seconds or minutes. However, orientation-programmed PDLLA needed no external energy to start its shape-recovery, but was activated by the simulated physiological environment. This type of shape-memory in bioabsorbable polymers could be used to increase the functionality of simple and easy-to-use medical devices.

Orientation-programmed PDLLA could generate a predefined level of stress measured as compression *in vitro* at 37°C when shape transformation was restricted. The stress generated *in vitro* was of the same level than that used in the orientation-programming, indicating that the programming load could be stored in the polymer and then mobilized in a 37°C aqueous environment. γ-irradiation had a significant effect on the stress generation capability: it lowered the maximum generated stress and caused the polymer to stress relax due to the tension it had first generated. This was probably due to chain slippage in the lower-molecular-weight polymer chains, which had fewer possible chain entanglements (physical crosslinks) than non-γ-irradiated PDLLA with a higher molecular weight. Another factor may be that the initial T_g of γ-irradiated PDLLA was lower than that of non-γ-irradiated PDLLA, enabling thus more molecular movement and chain slippage. The initial stress generated by non-γ-irradiated PDLLA also decreased, though the small dip was related more to the rate of degradation, causing eventually similar chain slippage, than to γ-irradiated PDLLA, which had initial i.v. at lower level. Intriguing here is that the actual loading in orientation-programming determines the stress level, or more precisely, the stress profile, to which orientation-programmed PDLLA tends adapt despite the external forces

affecting it. This phenomenon can be seen in Figure 9, which shows test data on orientated and thus pre-stressed PDLLA being intentionally subjected to an external stress or the stress being removed.

Melt-extruded and orientation-programmed and γ-irradiated PDLLA showed good mechanical properties and a linear hydrolytic degradation profile at 37°C *in vitro*. Over the first two weeks *in vitro*, its shear strength was more affected than its measured load carrying capability due to the initial radial expansion of its initially grooved shape, which made the rods round inside the hex-cylinders and thus changed the orientation ratio of the tested samples and affected their calculated value. Because lactide monomer, whether residual or thermally-generated, has been reported markedly to affect the degradation rate [14, 22-24] and to possess an antiplasticizing effect when diffusing out of the PDLLA matrix [13], the results of this study give reliable data on its hydrolytic degradation behavior. The orientation-programming not only yields novel shape transformation properties, but also simultaneously acts as a reinforcing method whereby polylactide copolymers [25] can be processed into strong and ductile biodegradable medical materials.

5. Conclusions

Shape-memory, triggered in a 37°C aqueous environment, can be generated into amorphous PDLLA by advanced processing methods without chemical modifications of the polymer. The orientation-programming generates a novel oriented and entangled structure for PDLLA which is transformed back towards the non-oriented state at physiological temperature due to the plasticizing effect of a small amount of diffused water (1 wt-%). This type of novel function can be generated in a single step programming process and the technology can be easily applied to medical devices to increase their functionality.

Acknowledgements

We appreciate the research collaboration with Bioretec Ltd. and the funding from Tekes and POPROK Graduate School. We would also like to thank Kaija Honkavaara and Milla Törmälä for their help during this work.

References:

1. Metcalfe A, Desfaits A, Salazkin I, Yahia L, Sokolowski WM, Raymond J. Cold hibernated elastic memory foams for endovascular interventions. Biomaterials 2003;24:491-497.
2. Yakacki CM, Shandas R, Lanning C, Rech B, Eckstein A, Gall K. Unconstrained recovery characterization of shape-memory polymer networks for cardiovascular applications. Biomaterials 2007;28:2255-2263.
3. Lendlein A, Langer R. Biodegradable, Elastic shape-memory polymers for potential biomedical applications. Science 2002;296:1673-1676.

4. Guimaraes-Ferreira J, Gewalli F, David L, Maltese G, Heino H, Lauritzen C. Calvarial bone distraction with a contractile bioresorbable polymer. Plastic and Reconstructive Surgery 2002;104:1325-1331.
5. Zheng X, Zhou S, Li X, Weng J. Shape memory properties of poly(D,L-lactide)/hydroxyapatite composites. Biomaterials 2006;27:4288-4295.
6. Lendlein A, Schmidt A, Langer R. AB-Polymer networks based on oligo(ε-caprolactone) segments showing shape-memory properties. Proceedings of the National Academy of Sciences of the United States of America 2001;98:842.
7. Lendlein A, Jiang H, Junger O, Langer R. Light-induced shape-memory polymers. Nature 2005;434:879-882.
8. Langer R, Tirrell DA. Designing materials for biology and medicine. Nature 2004;428:487-492.
9. Min C, Cui W, Bei J, Wang S. Biodegradable shape-memory polymer - Polylactide-co-poly(glycolide-co-caprolactone) multiblock copolymer. Polymers for Advanced Technologies 2005;16:608-615.
10. Huang WM, Yang B, An L, Li C, Chan YS. Water-driven programmable polyurethane shape memory polymer: Demonstration and mechanism. Applied Physic Letters 2005;86:114105.
11. Yang B, Huang WM, Li C, Li L. Effects of moisture on the thermomechanical properties of a polyurethane shape memory polymer. Polymer 2006;47:1348-1356.
12. Pierce BF, Bellin K, Behl M, Lendlein A. Demonstrating the influence of water on the shape-memory polymer networks based on poly[(rac-lactide)-co-glycolide] segments *in vitro*. International Journal of Artificial Organs 2011;34:172-179.
13. Steendam R. Amylodextrin and poly(DL-lactide) oral controlled release matrix tablets; concepts for understanding their release mechanisms. 2005.
14. Paakinaho K, Heino H, Väisänen J, Törmälä P, Kellomäki M. Effects of lactide monomer on the hydrolytic degradation of poly(lactide-co-glycolide) 85L/15G. Journal of the Mechanical Behavior of Biomedical Materials 2011; 4:1283-1290
15. Allinniemi T, Heino H, Törmälä P, 2007. US2007/0299449 A1.
16. Wischke C, Lendlein A. Shape-memory polymers as drug carriers-a multifunctional system. Pharmaceutical Research 2010;27:527-529.
17. Blasi P, D'Souza SS, Selmin F, DeLuca PP. Plasticizing effect of water on poly(lactide-co-glycolide). Journal of Controlled Release 2005;108:1-9.
18. Siemann U. The influence of water on the glass transition of poly(DL-lactic acid). Thermochimica Acta 1985;85:513-516.
19. Steendam R, van Steenbergen MJ, Hennink WE, Frijlink HW, Lerk CF. Effect of molecular weight and glass transition on relaxation and release behaviour of poly(DL-lactic acid) tablets. Journal of Controlled Release 2001;70:71-82.
20. Passerini N, Craig DQM. An investigation into the effects of residual water on the glass transition temperature of polylactide microspheres using modulated temperature DSC. Journal of Controlled Release, 2001;73:111-115.
21. Hancock BC, Shamblin SL, Zografi G. Molecular Mobility of Amorphous Pharmaceutical Solids Below Their Glass Transition Temperatures. Pharmaceutical Research 1995;12:799-806.

22. Kellomäki M, Pohjonen T, Törmälä P. Self reinforced polylactides. In: Arshady R, editor. Biodegradable PolymersLondon: Citus Books, 2003. p. 212.
23. Paakinaho K, Ellä V, Syrjälä S, Kellomäki M. Melt spinning of poly(l/d)lactide 96/4: Effects of molecular weight and melt processing on hydrolytic degradation. Polymer Degradation and Stability 2009;94:438-442.
24. Hyon S-H, Jamshidi K, Ikada Y. Effects of residual monomer on the degradation of DL-lactide polymer. Polymer International 1998;46:196-202.
25. Törmälä P. Biodegradable self-reinforced composite materials; Manufacturing structure and mechanical properties. Clinical Materials 1992;10:29-34.

Publication IV

Paakinaho, K., Hukka, T.I., Kastinen, T., Kellomäki, M.

Demonstrating the Mechanism and Efficacy of Water-Induced Shape-Memory and the Influence of Water on the Thermal Properties of Oriented Poly(D,L-lactide)

Accepted for publication: Journal of Applied Polymer Science 2013

Tampereen teknillinen yliopisto
PL 527
33101 Tampere

Tampere University of Technology
P.O.B. 527
FI-33101 Tampere, Finland

ISBN 978-952-15-3100-2
ISSN 1459-2045